ISSN 2096-7071 (Print)
ISSN 2096-3101 (Online)
CN 10-1629/R1

CHINA CDC WEEKLY

Vol. 7 No. 37 Sept. 12, 2025

中国疾病预防控制中心周报

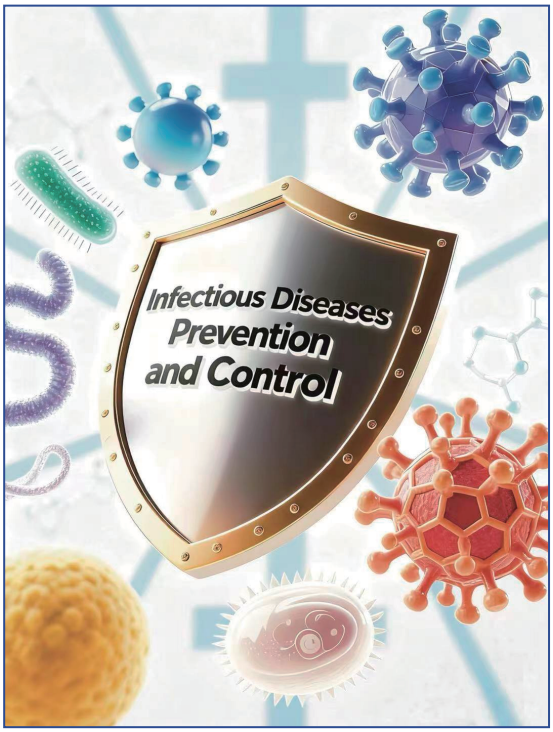

ISSN 2096-7071

China CDC Weekly

Cover Image: adapted from Doubao image generation.

Commentary

Confronting the Antimicrobial Resistance Crisis in China: Emerging Superbugs, Genomic Surveillance, and Innovative Countermeasures

Qian Tong[1,2]; Liping Zeng[3]; Yixin Ge[4]; Jia Jia[1,#]

ABSTRACT

The antimicrobial resistance (AMR) crisis in China has escalated into a critical public health threat. Extensive antibiotic use in both clinical and agricultural settings has created strong selective pressures, promoting the emergence of resistant strains and accelerating their dissemination. This increasing threat is exemplified by the rapid spread of multidrug-resistant bacteria. Consequently, genomic surveillance of these pathogens and the development of effective countermeasures are urgently needed. In this paper, we highlight three critical dimensions of the AMR challenge in China, which include the recent emergence of resistant bacteria, genomic surveillance efforts, and progress in the development of novel antimicrobial agents. By synthesizing recent research on the evolutionary dynamics of drug-resistant pathogens in China and outlining innovative antimicrobial strategies, this study provides insights to guide evidence-based antimicrobial stewardship programs.

Update of the World Health Organization (WHO) Bacterial Priority Pathogen List (BPPL)

Currently, antimicrobial resistance (AMR) is one of the top ten public health threats that not only impacts human public health but also substantially influences animal and environmental health (*1*). According to a systematic analysis of the past 3 decades (1990–2021) of global bacterial AMR, it is estimated that 4.71 million deaths associated with bacterial AMR occurred in 2021, including 1.14 million deaths attributable to bacterial AMR (*2*). In response to this threat, the WHO released the BPPL, which emphasized the prioritization of AMR countermeasures by 2024, highlighting the urgent need to develop novel therapeutics targeting increasingly resistant pathogens (*3*). This updated list covers 24 antibiotic-resistant pathogens spanning 15 bacterial families, categorizing them into critical, high-, and medium-priority groups, reflecting their global impact. These multidrug-resistant (MDR) pathogens are associated with high morbidity and mortality rates, and therefore, referred to as "superbugs" and are considered a serious threat to global health (*4*). Based on the bacterial resistance profile and public health impact, the critical antibiotic-resistant ESKAPE pathogens (*Enterococcus faecium*, *Staphylococcus aureus*, *Klebsiella pneumoniae*, *Acinetobacter baumannii*, *Pseudomonas aeruginosa,* and *Enterobacter* spp.) had predominantly high scores in the 2024 WHO BPPL list, underscoring their considerable threat to global health (*5*). Among Gram-negative bacteria, carbapenem-resistant *K. pneumoniae* (CRKP, top-ranked), third-generation cephalosporin-resistant *E. coli*, and carbapenem-resistant *A. baumannii* (CRAB) were among the top three. Carbapenem-resistant *P. aeruginosa* (CRPA) and *Enterobacter* spp. were ranked above 60% of the total score. Among the Gram-positive bacteria, vancomycin-resistant *E. faecium* (VREfm) and methicillin-resistant *S. aureus* (MRSA) were ranked the highest (*5*).

Critical Challenge of AMR in China

Given the global threat of AMR, China has implemented a comprehensive range of strategies in alignment with its National Plan on AMR, achieving considerable progress in containment efforts. However, the prevalence of antibiotic-resistant bacteria in clinical settings remains a notable concern (*6*–*7*). Based on the CHINET surveillance data of clinical ESKAPE pathogens isolated from approximately 70 hospitals across China over the past decade, although the proportion of ESKAPE strains has remained stable annually (Figure 1A), their absolute numbers showed an increasing trend, in parallel with the overall increase

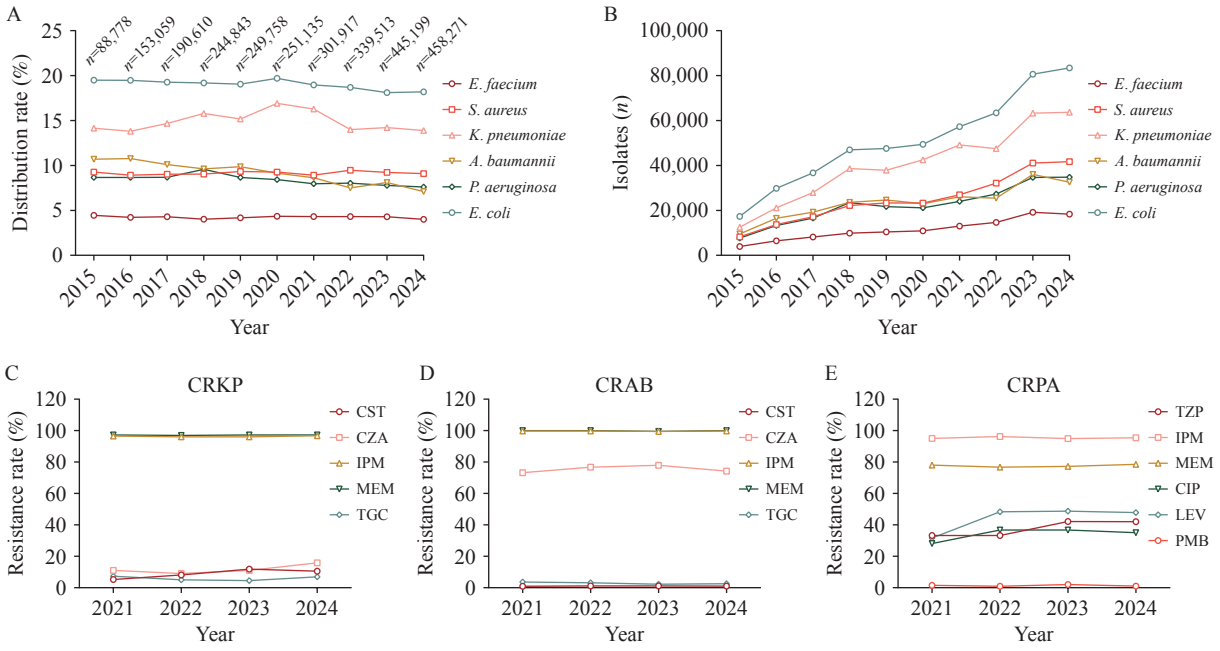

FIGURE 1. Trends and antibiotic resistance profile of ESKAPE pathogen clinical isolates in China. (A) Distribution of ESKAPE pathogens from 2015 to 2024; (B) Number of ESKAPE pathogens clinical isolates from 2015 to 2024; (C) Resistance profile of CRKP clinical isolates from 2021 to 2024; (D) Resistance profile of CRAB clinical isolates from 2021 to 2024; (E) Resistance profile of CRPA clinical isolates from 2021 to 2024.
Note: The above data were obtained from CHINET. In panel A, the total number of clinical isolates per year is presented. Abbreviation: CRAB=carbapenem-resistant *Acinetobacter baumannii*; CST=colistin; CZA=ceftazidime-avibactam; IPM=imipenem; MEM=meropenem; TGC=tigecycline; SCF=cefoperazone-sulbactam; TZP=piperacillin-tazobactam; CIP=ciprofloxacin; LEV=levofloxacin; PMB=polymyxin B; ESKAPE=*Enterococcus faecium*, *Staphylococcus aureus*, *Klebsiella pneumoniae*, *Acinetobacter baumannii*, *Pseudomonas aeruginosa*, *Enterobacter* spp.

in clinical isolates (Figure 1B). According to the resistance rate data in China, the prevalence of VREfm showed an upward trend from 2019 to 2022 (*8*). The higher prevalence of MRSA among children has garnered considerable attention despite a decline from 2005 to 2022 (*8*). As shown in the CHINET data, resistance rates of CRKP, CRAB, and CRPA to carbapenems (imipenem and meropenem) were markedly elevated, exceeding 80% and approaching 100% over the past 4 years (Figure 1C–E). Although the resistance rate of CRKP slightly increased in response to ceftazidime-avibactam, it gained momentum against both colistin and tigecycline, the two main antibiotics used to treat carbapenem-resistant bacteria (Figure 1C). The resistance rate of CRAB remained relatively stable but exhibited a high level of resistance to cefoperazone-sulbactam, a widely employed antimicrobial compound in salvage combination regimens, with a rate exceeding 60% (Figure 1D). The prevalence of CRPA was associated with a notable increase in levofloxacin resistance (from 31.6% in 2021 to 47.9% in 2024) and a growing resistance to piperacillin-tazobactam and ciprofloxacin (Figure 1E).

The shifting genomic landscape of ESKAPE pathogens poses considerable challenges to public health and clinical medicine owing to the continuous evolution of antibiotic-resistant bacterial clones (*9*). For example, the prevalence of the VREfm ST80 strain carrying a new type *vanA*-bearing plasmid is steadily increasing in Guangdong, China (*10*). Moreover, the genetic diversity of MRSA has been expanding, with the ST59 strain having high potential virulence and emerging as the predominant lineage at 35.6%, surpassing the previously dominant ST239 strain (*11–12*). The dominant clone of hypervirulent CRKP (Hv-CRKP) ST11 reportedly displays the complexity of MDR, along with genetic heterogeneity in virulence factor profiles, and is considered a health concern owing to its dual threat of high virulence and drug resistance in China (*13–14*). The widely drug-resistant *A. baumannii* and *P. aeruginosa* pose a serious risk to public health, especially in hospital settings, where they can lead to various infections. The widespread clonal ST208 strain, frequently associated with carbapenem resistance genes, is the predominant strain of the

extensively drug-resistant *A. baumannii* (XDRAB), isolated from the intensive care unit (ICU) of a hospital in Jinhua, Zhejiang Province (*15*). Song *et al.* reported T3SS-mediated simultaneous secretion of ExoS and ExoU in high-risk *P. aeruginosa,* which has emerged as a new subset of hypervirulent strains in China (*16*). Therefore, the complex diversity of emerging ESKAPE highlights the urgent need for careful surveillance of these high-risk strains.

Genomic Surveillance of Drug-Resistant Bacteria in China

To address this challenge, surveillance and mechanistic investigations of bacterial resistance play a crucial role in detecting and tracking the spread of resistant bacteria. Innovations in genome/metagenomic sequencing and analysis technologies could revolutionize AMR surveillance (*17*). The use of whole-genome sequencing (WGS) of pathogens for AMR surveillance has grown considerably compared with phenotypic surveillance of AMR (*18*). The construction and interpretation of phylogenetic trees derived from WGS facilitate the identification of transmission events and understanding the dynamics of outbreaks. Using WGS and comparative genome analysis, a multicenter molecular epidemiological survey reported that the high-risk ST11 KL64 CRKP serotype demonstrated substantial expansion potential and survival advantages in China between 2011 and 2021 (*19*). WGS data can also be used to detect new genomic features, such as AMR genes and virulence genes involved in AMR. A recent multicenter genomics study applied WGS to identify the genomic characteristics and phylogenetic relatedness of CRKP colonization and infection in ICU patients in Anhui Province, China, highlighting the need for coordinated efforts between healthcare facilities and networks to aid CRKP management (*20*). Moreover, WGS has empowered clinical researchers to identify and monitor AMR while enabling the detection of virulence factors and mobile genetic elements, such as plasmids, which are crucial for understanding the adaptability, pathogenicity, and dissemination of AMR bacteria (*18*,*21*). For instance, an additional example of a small $bla_{\text{KPC-2}}$-bearing plasmid essential for the emergence and spread of KPC-2 CRKP from a hospital in Zhejiang, China, was identified upon WGS analysis of a rare CRKP ST437 isolate (*22*). Furthermore, Liu *et al.* conducted genetic typing analysis of 90 non-redundant Hv-CRKP isolates from patients and revealed that Hv-CRKP transferability relies on the dominant ST11-K64 clone (*23*). By analyzing the WGS results of plasmids from 12 representative CRKP isolates, the authors uncovered the clonal spread and clinical evolution of Hv-CRKP within Zhejiang hospitals, involving binary vehicles and 2 fusion plasmid types that facilitate the co-transfer of *rmpA* hypervirulence and KPC-2 carbapenem resistance (*23*). Likewise, Huang *et al.* performed a clinical genomic analysis and reported the diversity and dynamics of $bla_{\text{KPC-2}}$-producing CRPA, providing novel insights into the heterogeneity among CRPA and plasmid-mediated transmission of $bla_{\text{KPC-2}}$ in clinical settings in China (*24*). Collectively, these studies emphasize the importance of WGS in providing additional insights, thus enhancing epidemiological data and transmission control of AMR pathogens (Figure 2).

Development of Multitarget Antimicrobial Agents

An effective approach to circumvent existing antibiotic resistance warrants the discovery of new chemical classes, particularly in the fields of natural-product-derived and synthetic small molecules, as well as novel targets and modes of action (*25*). Compared with single-target drugs, multitarget drugs can simultaneously regulate multiple targets to reduce resistance caused by single-target mutations or expression changes, and have become an effective strategy to combat bacterial resistance (*26*). A growing body of evidence has shown promise in this regard (Figure 2). For example, Li et al. synthesized a series of novel monobactam derivatives and demonstrated their efficacy against β-lactamase-producing MDR *E. coli* and *K. pneumoniae*, with the dual inhibition on PBP3 and class A and C β-lactamases (*27*). Jia *et al.* reevaluated chrysomycin A, a novel natural product, which is highly active against MRSA persisters by inhibiting multiple novel targets involved in the biosynthetic pathways of cell wall peptidoglycan and lysine precursors (*28*). Similarly, multitarget antimicrobial agents quaternized with antimicrobial peptide mimics have been shown to kill MRSA by interacting with lipoteichoic acid and peptidoglycan, causing membrane damage through depolarization, and disrupting cellular redox homeostasis by binding to lactate dehydrogenase (*29*). Multitarget antibacterial medications are a novel strategy to combat bacterial

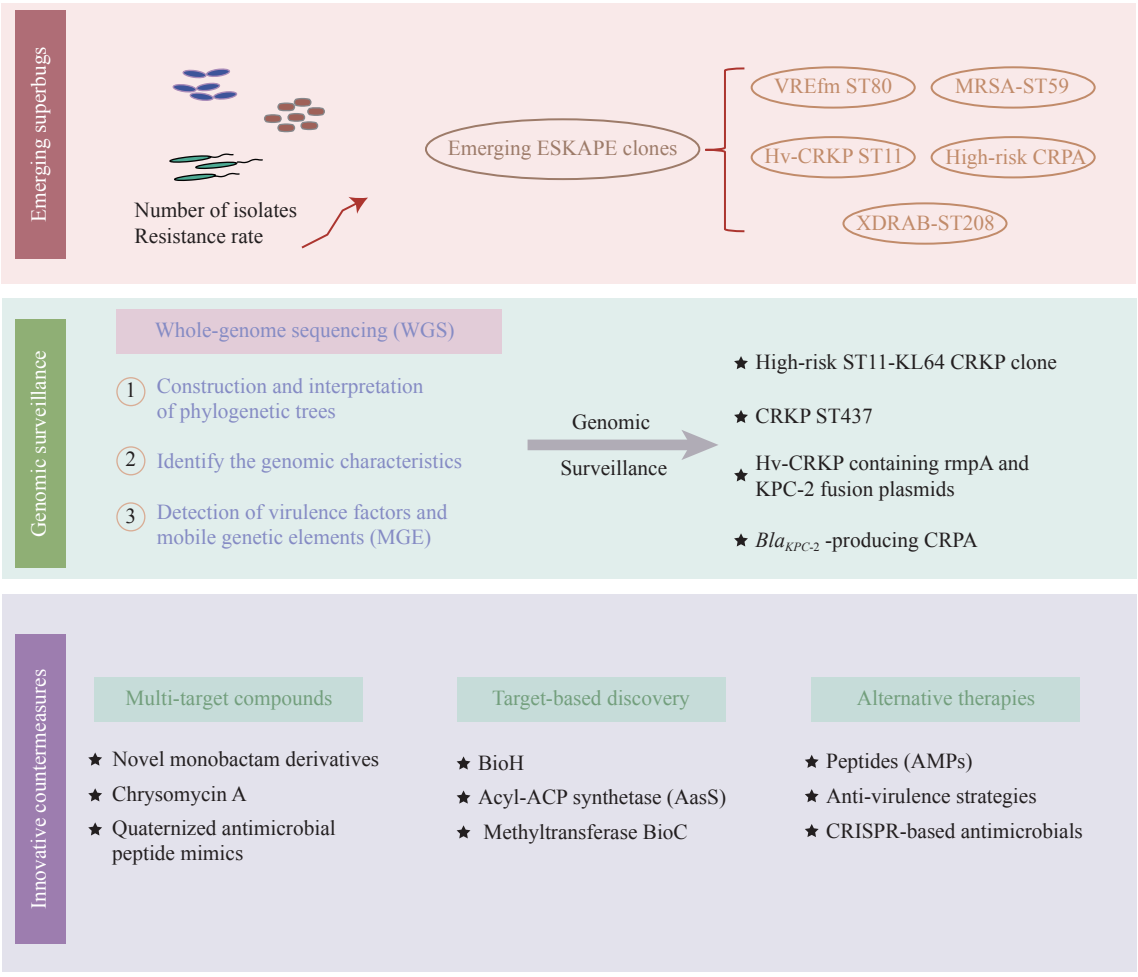

FIGURE 2. Structural schematic of the antimicrobial resistance crisis and countermeasures in China.
Abbreviation: AMPs=antimicrobial peptides; CRPA=carbapenem-resistant *Pseudomonas aeruginosa*; ESKAPE=*Enterococcus faecium*, *Staphylococcus aureus*, *Klebsiella pneumoniae*, *Acinetobacter baumannii*, *Pseudomonas aeruginosa*, *Enterobacter* spp; MGE=mobile genetic elements; WGS=whole-genome sequencing; CRKP=carbapenem-resistant *Klebsiella pneumoniae*.

resistance, and the rational discovery of multitarget drugs may usher in a new golden era for antibiotic discovery.

Validation of Target-Based Antibacterial Agents

To develop novel antibiotics, target-based strategies must meet the criteria to combat MDR infections. Numerous antibiotic discovery programs have switched to target-based methods to identify substances capable of blocking specific bacterial targets (i.e., essential enzymes or proteins). For instance, the component enzymes of fatty acid or biotin (fatty acid derivatives) synthetic pathways are considered sources of novel antibacterial targets and hold promise for tackling antibiotic-resistant bacteria, such as BioA (*30*) and BioH (*31*). Shi et al. discovered that BioH is essential for *P. aeruginosa* virulence and validated a therapeutic target for reducing CRPA viability, highlighting the potential of inhibiting biotin synthesis following anti-CRPA therapy (*32*). Huang *et al.* elucidated the inhibitory mechanism between the acyl adenylate mimic C10-AMS and acyl-ACP synthetase (AasS), which provided a molecular basis for targeting AasS by the C10-AMS inhibitor, thus enabling the re-sensitization of fatty acid synthesis II-targeted antimicrobials (*33*). Intriguingly, the bacterial methyltransferase BioC, which initiates biotin synthesis, has been identified as a virulence factor of *K. pneumoniae*, representing an attractive anti-ESKAPE druggable pathway (*34*).

Exploration of Alternative Therapies Against Drug-Resistant Bacteria

As bacteria become resistant to conventional antibiotics, alternative therapies have been explored in recent years, including antimicrobial peptides (AMPs), anti-virulence strategies, CRISPR-based antimicrobials, and other methods (*35*). The discovery of novel AMPs is expanding the arsenal of antibacterial drugs. For example, fluorescent 2-phenyl-1 *H*-phenanthro[9,10-*d*] imidazole-antimicrobial peptide mimic conjugates have been found to rapidly kill MRSA by disrupting membrane integrity, triggering reactive oxygen species accumulation, causing protein damage, and exhibiting low susceptibility to bacterial resistance (*36*). Antimicrobial biofilms are expected to efficiently inhibit drug-resistant bacteria. Recently, phenazine-inspired antibiotics were found to be highly active against resistant bacteria, including MRSA, MRSE, and VREfm, by inhibiting biofilm formation (*37*). A novel gene editing-based antimicrobial strategy was developed using the CRISPR-Cas system to specifically target vital bacterial or resistance genes. The CRISPR-Cas system reportedly targets and eliminates carbapenem-resistant plasmids, thereby restoring antibiotic susceptibility (*38*). This approach, although still in the experimental stages, offers a potential solution to the challenge of antibiotic-resistant bacteria without the need for novel therapies. Furthermore, the combination of AI and deep learning techniques has the potential to transform drug discovery by accelerating the discovery of novel antibiotic candidates and refining treatment plans based on predictive models of resistance patterns (*39*).

Although a growing number of antibacterial drugs are under investigation, challenges remain in the development of antimicrobials against drug-resistant pathogens. Currently, approximately 32 new antibacterial compounds are in the clinical trial phase of development, and less than 25% of the drugs in the clinical development pipeline represent a novel class or act through a novel mechanism. Unfortunately, all lack the potential to be effective against major WHO threat pathogens or Gram-negative ESKAPE (*40*). Hence, developing new antibiotics to combat drug-resistant bacteria remains a challenge.

Future Efforts to Combat Drug-Resistant Bacteria

The growing threat of antibiotic resistance warrants a strong and resourceful response based on technological and scientific innovations. Therefore, to preserve antimicrobial efficacy and control resistance transmission, greater efforts should be invested in the discovery and development of novel antimicrobial strategies and in improving comprehensive surveillance systems using next-generation sequencing for source-tracking AMR pathogens. In particular, genomic surveillance involving comprehensive resistance, virulence, and plasmid gene content profiling will enable real-time customization of AMR interventions and address barriers impeding widespread implementation. More importantly, the One Health approach emphasizes the intertwined health of humans, animals, and the environment in disease prevention and control; hence, the control and surveillance of AMR pathogens needs to be considered in all three sectors (*1*). Coordinated actions across these sectors, such as shared data platforms, joint surveillance programs, and integrated intervention strategies, are pivotal to effectively prevent cross-species transmission and to safeguard public and environmental health in the future (*41*).

Conflicts of interest: No conflicts of interest.

Funding: Supported by the National Natural Science Foundation of China (32470188).

doi: 10.46234/ccdcw2025.197

[#] Corresponding author: Jia Jia, jiajia25@tongji.edu.cn.

[1] Deparment of Immunology and Pathogen Biology, Research Centre for Infection and Immunity, School of Medicine, Tongji University, Shanghai, China; [2] Laboratory Medicine Center, Department of Transfusion Medicine, Zhejiang Provincial People's Hospital, Affiliated People's Hospital, Hangzhou Medical College, Hangzhou City, Zhejiang Province, China; [3] Department of Pathogen Biology, Jiangsu Key Laboratory of Pathogen Biology, Nanjing Medical University, Nanjing City, Jiangsu Province, China; [4] Huadong Research Institute for Medicine and Biotechniques, Nanjing City, Jiangsu Province, China.

Submitted: April 07, 2025
Accepted: August 21, 2025
Issued: September 12, 2025

REFERENCES

1. Udaondo Z, Huertas MJ. Fighting the enemy: one health approach against microbial resistance. Microb Biotechnol 2020;13(4):888 – 91. https://doi.org/10.1111/1751-7915.13587.
2. GBD 2021 Antimicrobial Resistance Collaborators. Global burden of bacterial antimicrobial resistance 1990-2021: a systematic analysis with forecasts to 2050. Lancet 2024;404(10459):1199 – 226. https://doi.org/10.1016/S0140-6736(24)01867-1.

3. Ma YY, Chen P, Mo Y, Xiao YH. WHO revised bacterial priority pathogens list to encourage global actions to combat AMR. hLife 2024;2(12):607 – 10. https://doi.org/10.1016/j.hlife.2024.10.003.
4. Painuli S, Semwal P, Sharma R, Akash S. Superbugs or multidrug resistant microbes: a new threat to the society. Health Sci Rep 2023;6 (8):e1480. https://doi.org/10.1002/hsr2.1480.
5. Sati H, Carrara E, Savoldi A, Hansen P, Garlasco J, Campagnaro E, et al. The WHO Bacterial Priority Pathogens List 2024: a prioritisation study to guide research, development, and public health strategies against antimicrobial resistance. Lancet Infect Dis 2025;25(9):1033 – 43. https://doi.org/10.1016/S1473-3099(25)00118-5.
6. Ding L, Hu FP. China's new national action plan to combat antimicrobial resistance (2022-25). J Antimicrob Chemother 2023;78 (2):558 – 60. https://doi.org/10.1093/jac/dkac435.
7. Xiao YH, Nishijima T. Status and challenges of global antimicrobial resistance control: a dialogue between Professors Yonghong Xiao and Takeshi Nishijima. hLife 2024;2(2):47 – 9. https://doi.org/10.1016/j.hlife.2023.11.004.
8. Qin XH, Ding L, Hao M, Li P, Hu FP, Wang MG. Antimicrobial resistance of clinical bacterial isolates in China: current status and trends. JAC Antimicrob Resist 2024;6(2):dlae052. https://doi.org/10.1093/jacamr/dlae052.
9. Luo QX, Lu P, Chen YB, Shen P, Zheng BW, Ji JR, et al. ESKAPE in China: epidemiology and characteristics of antibiotic resistance. Emerg Microbes Infect 2024;13(1):2317915. https://doi.org/10.1080/22221751.2024.2317915.
10. Shen C, Luo L, Zhou HY, Xiao YL, Zeng JX, Zhang LL, et al. Emergence and ongoing outbreak of ST80 vancomycin-resistant *Enterococcus faecium* in Guangdong province, China from 2021 to 2023: a multicenter, time-series and genomic epidemiological study. Emerg Microbes Infect 2024;13(1):2361030. https://doi.org/10.1080/22221751.2024.2361030.
11. Chen HB, Yin YY, van Dorp L, Shaw LP, Gao H, Acman M, et al. Drivers of methicillin-resistant *Staphylococcus aureus* (MRSA) lineage replacement in China. Genome Med 2021;13(1):171. https://doi.org/10.1186/s13073-021-00992-x.
12. Zhou WX, Jin Y, Chen P, Ge Q, Dong X, Chen YB, et al. Reshaping the battlefield: a decade of clonal wars among *Staphylococcus aureus* in China. Drug Resist Updat 2025;78:101178. https://doi.org/10.1016/j.drup.2024.101178.
13. Li P, Liang QQ, Liu WG, Zheng BW, Liu LZ, Wang W, et al. Convergence of carbapenem resistance and hypervirulence in a highly-transmissible ST11 clone of *K. pneumoniae*: an epidemiological, genomic and functional study.. Virulence 2021;12(1):377 – 88. https://doi.org/10.1080/21505594.2020.1867468.
14. Chen T, Ying LY, Xiong LY, Wang XT, Lu P, Wang Y, et al. Understanding carbapenem-resistant hypervirulent *Klebsiella pneumoniae*: key virulence factors and evolutionary convergence. hLife 2024;2(12):611 – 24. https://doi.org/10.1016/j.hlife.2024.06.005.
15. Shi JC, Mao XT, Sun FT, Cheng JH, Shao LY, Shan X, et al. Epidemiological characteristics and antimicrobial resistance of extensively drug-resistant *Acinetobacter baumannii* in ICU wards. Microbiol Spectr 2025;13(4):e02619 – 24. https://doi.org/10.1128/spectrum.02619-24.
16. Song YQ, Mu YQ, Wong NK, Yue Z, Li J, Yuan M, et al. Emergence of hypervirulent *Pseudomonas aeruginosa* pathotypically armed with co-expressed T3SS effectors ExoS and ExoU. hLife 2023;1(1):44 – 56. https://doi.org/10.1016/j.hlife.2023.02.001.
17. Wheeler NE, Price V, Cunningham-Oakes E, Tsang KK, Nunn JG, Midega JT, et al. Innovations in genomic antimicrobial resistance surveillance. Lancet Microbe 2023;4(12):e1063 – 70. https://doi.org/10.1016/S2666-5247(23)00285-9.
18. Weinmaier T, Conzemius R, Bergman Y, Lewis S, Jacobs EB, Tamma PD, et al. Validation and application of long-read whole-genome sequencing for antimicrobial resistance gene detection and antimicrobial susceptibility testing. Antimicrob Agents Chemother 2023;67(1): e01072 – 22. https://doi.org/10.1128/aac.01072-22.
19. Wang Q, Wang RB, Wang SY, Zhang AR, Duan QY, Sun SJ, et al. Expansion and transmission dynamics of high risk carbapenem-resistant *Klebsiella pneumoniae* subclones in China: an epidemiological, spatial, genomic analysis. Drug Resist Updat 2024;74:101083. https://doi.org/10.1016/j.drup.2024.101083.
20. Wu YL, Chu WW, Hu XQ, Lyu YY, Tai JH, Li RJ, et al. Genomic characteristics and phylogenetic analyses of colonization and infection with carbapenem-resistant *Klebsiella pneumoniae* in multicenter intensive care units: a cohort study. Microbiol Spectr 2025;13(4): e01584 – 24. https://doi.org/10.1128/spectrum.01584-24.
21. Cipriani G, Helmersen K, Mazzon RR, Wagner G, Aamot HV, Ferreira FA. Evaluation of whole-genome sequencing protocols for detection of antimicrobial resistance, virulence factors and mobile genetic elements in antimicrobial-resistant bacteria. J Med Microbiol 2025;74(3): 001990. https://doi.org/10.1099/jmm.0.001990.
22. Chen QW, Liu LZ, Hu XF, Jia X, Gong XW, Feng YJ, et al. A small KPC-2-producing plasmid in *Klebsiella pneumoniae*: implications for diversified vehicles of carbapenem resistance. Microbiol Spectr 2022;10 (3):e02688 – 21. https://doi.org/10.1128/spectrum.02688-21.
23. Liu LZ, Lou NJ, Liang QQ, Xiao W, Teng GQ, Ma JG, et al. Chasing the landscape for intrahospital transmission and evolution of hypervirulent carbapenem-resistant *Klebsiella pneumoniae*. Sci Bull (Beijing) 2023;68(23):3027 – 47. https://doi.org/10.1016/j.scib.2023.10.038.
24. Huang M, Liu LZ, Li XX, Shi Y, Zhang HM, Lu T, et al. Heterogeneity and clinical genomics of bla_{KPC-2}-producing, carbapenem-resistant *Pseudomonas aeruginosa*. hLife 2024;2(6):314 – 9. https://doi.org/10.1016/j.hlife.2024.04.001.
25. Sun SW, Chen XYZ. Mechanism-guided strategies for combating antibiotic resistance. World J Microbiol Biotechnol 2024;40(10):295. https://doi.org/10.1007/s11274-024-04106-8.
26. Feng J, Zheng YL, Ma WQ, Ihsan A, Hao HH, Cheng GY, et al. Multitarget antibacterial drugs: an effective strategy to combat bacterial resistance. Pharmacol Ther 2023;252:108550. https://doi.org/10.1016/j.pharmthera.2023.108550.
27. Li ZW, Guo ZH, Lu X, Ma XC, Wang XK, Zhang R, et al. Evolution and development of potent monobactam sulfonate candidate IMBZ18g as a dual inhibitor against MDR Gram-negative bacteria producing ESBLs. Acta Pharm Sin B 2023;13(7):3067 – 79. https://doi.org/10.1016/j.apsb.2023.03.002.
28. Jia J, Zheng MX, Zhang CW, Li BL, Lu C, Bai YF, et al. Killing of *Staphylococcus aureus* persisters by a multitarget natural product chrysomycin A. Sci Adv 2023;9(31):eadg5995. https://doi.org/10.1126/sciadv.adg5995.
29. Liu JY, Cao YG, Xu CG, Li RC, Xiong YY, Wei Y, et al. Quaternized antimicrobial peptide mimics based on harmane as potent anti-MRSA agents by multi-target mechanism covering cell wall, cell membrane and intracellular targets. Eur J Med Chem 2024;276:116657. https://doi.org/10.1016/j.ejmech.2024.116657.
30. Liu F, Dawadi S, Maize KM, Dai R, Park SW, Schnappinger D, et al. Structure-based optimization of pyridoxal 5'-phosphate-dependent transaminase enzyme (BioA) inhibitors that target biotin biosynthesis in *Mycobacterium tuberculosis*. J Med Chem 2017;60(13):5507 – 20. https://doi.org/10.1021/acs.jmedchem.7b00189.
31. Xu YC, Yang J, Li WH, Song SJ, Shi Y, Wu LH, et al. Three enigmatic BioH isoenzymes are programmed in the early stage of mycobacterial biotin synthesis, an attractive anti-TB drug target. PLoS Pathog 2022;18(7):e1010615. https://doi.org/10.1371/journal.ppat.1010615.
32. Shi Y, Cao QD, Sun J, Hu XF, Su Z, Xu YC, et al. The opportunistic pathogen *Pseudomonas aeruginosa* exploits bacterial biotin synthesis pathway to benefit its infectivity. PLoS Pathog 2023;19(1):e1011110. https://doi.org/10.1371/journal.ppat.1011110.
33. Huang HM, Chang SH, Cui T, Huang M, Qu JX, Zhang HM, et al. An inhibitory mechanism of AasS, an exogenous fatty acid scavenger: implications for re-sensitization of FAS II antimicrobials. PLoS Pathog 2024;20(7):e1012376. https://doi.org/10.1371/journal.ppat.1012376.
34. Su Z, Zhang WZ, Shi Y, Cui T, Xu YC, Yang RS, et al. A bacterial methyltransferase that initiates biotin synthesis, an attractive anti-ESKAPE druggable pathway. Sci Adv 2024;10(51):eadp3954. https://

doi.org/10.1126/sciadv.adp3954.
35. MacNair CR, Rutherford ST, Tan MW. Alternative therapeutic strategies to treat antibiotic-resistant pathogens. Nat Rev Microbiol 2024;22(5):262 – 75. https://doi.org/10.1038/s41579-023-00993-0.
36. Xu T, Yan XT, Kang AY, Yang LH, Li XH, Tian Y, et al. Development of membrane-targeting fluorescent 2-phenyl-1*H*-phenanthro[9,10-*d*] imidazole-antimicrobial peptide mimic conjugates against methicillin-resistant *Staphylococcus aureus*. J Med Chem 2024;67(11):9302 – 17. https://doi.org/10.1021/acs.jmedchem.4c00436.
37. Sousa CA, Ribeiro M, Vale F, Simões M. Phenazines: natural products for microbial growth control. hLife 2024;2(3):100 – 12. https://doi.org/10.1016/j.hlife.2023.11.005.
38. Rafiq MS, Shabbir MA, Raza A, Irshad S, Asghar A, Maan MK, et al. CRISPR-Cas system: a new dawn to combat antibiotic resistance. BioDrugs 2024;38(3):387 – 404. https://doi.org/10.1007/s40259-024-00656-3.
39. Li Y, Cui XY, Yang XY, Liu GQ, Zhang J. Artificial intelligence in predicting pathogenic microorganisms' antimicrobial resistance: challenges, progress, and prospects. Front Cell Infect Microbiol 2024;14:1482186. https://doi.org/10.3389/fcimb.2024.1482186.
40. Beyer P, Paulin S. The antibacterial research and development pipeline needs urgent solutions. ACS Infect Dis 2020;6(6):1289 – 91. https://doi.org/10.1021/acsinfecdis.0c00044.
41. Gao GF, Hoffmann JA, Walzer C, Lu JH. Global public health crisis response: a roundtable discussion with Professor George Fu Gao, Professor Jules A Hoffmann, Professor Chris Walzer and Professor Jiahai Lu. hLife 2023;1(2):63 – 70. https://doi.org/10.1016/j.hlife.2023.10.001.

Vital Surveillances

Genomic Surveillance and Phylogenetic Analysis of Monkeypox Virus Sampled from Clinical Monkeypox Cases and Sewage — Sichuan Province, China, 2023

Ranran Cao[1]; Chengxia Liu[1]; Ying Shi[2]; Can Luo[1]; Xin Chen[3]; Li Liu[1]; Chaohua Xu[1]; Ming Pan[1]; Changcheng Wu[4,#]; Li Zhang[1,#]; Wenjie Tan[4,#]

ABSTRACT

Introduction: Monkeypox (Mpox) has reemerged globally, with thousands of confirmed cases reported in China. However, limited data exist on the genomic variations and transmission patterns of monkeypox virus (MPXV) in southwestern China.

Methods: Clinical samples from Mpox cases and sewage samples from wastewater treatment plants were collected from Sichuan Province for whole-genome sequencing and MPXV analysis.

Results: In the second half of 2023, 96 clinical samples from Mpox patients were collected, yielding 58 full-length viral genomes. All sequenced viruses belonged to the Western African clade (IIb), comprising three C.1 and fifty-five C.1.1 sequences. This study determined that Mpox cases in Sichuan originated from both importation and subsequent local transmission, with evidence of at least six distinct transmission clusters. Additionally, 26 sewage samples were collected, and 3 complete MPXV genomes were constructed. Analysis of viral genomes from sewage samples demonstrated a 95% concordance in high-frequency mutation sites with those observed in clinical cases, suggesting that sewage surveillance effectively captures diagnosed cases and serves as a robust complement to conventional monitoring. The integration of newly sequenced genomes with published data revealed an increased mutation rate in MPXV, along with fluctuating patterns of expansion and contraction of the effective viral population size.

Conclusion: This study provides preliminary insights into MPXV transmission dynamics and genomic evolution in Sichuan and demonstrates the utility of sewage monitoring in tracking viral diversity.

Monkeypox (Mpox) is a zoonotic disease caused by infection with Monkeypox virus (MPXV), characterized by clinical symptoms including fever, rash, and lymphadenopathy (*1*). Since the first reported case of Mpox in the Democratic Republic of Congo in 1970 (*2*), it has primarily circulated in African countries. However, the number of Mpox cases has been increasing in Europe (*3*) and the Americas (*4*), and has attracted global attention since 2022. By January 2025, 130 countries had reported Mpox cases, with approximately 127,960 cases and 281 deaths (WHO). Recently, MPXV strains from Central Africa (including clades Ia and Ib) began to appear (*5*), prompting the WHO to reclassify Mpox as a Public Health Emergency of International Concern (PHEIC). In September 2022, China reported the first imported case of Mpox (*6*–*7*), with no further reports thereafter. However, in June 2023, Beijing provincial-level administrative division (PLAD) reported the first local case of Mpox, followed by reports from several other provinces such as Beijing, Guangdong (*8*), Zhejiang, and Jiangsu PLADs (*9*), leading to local transmission with a cumulative number of cases exceeding 1,000 (*10*).

The rapid global spread of MPXV may be attributed to factors such as the accelerated virus evolution rate (*11*) and changes in transmission routes (*12*); however, the genetic evolution characteristics and evolutionary trajectory of MPXV remain unclear. Therefore, continuous research on the variation and evolution of MPXV and its role in the transmission process is crucial for tracking the sources of infection, predicting transmission patterns, and monitoring epidemic warnings. However, there have been no reports of the long-term monitoring of Mpox transmission and virus evolution patterns within the scope of a province in China. Moreover, reports on the simultaneous monitoring of MPXV in Mpox cases and sewage samples are limited. The performance of sewage sample-based monitoring in detecting variants and

mutations requires further investigation. Chengdu, the capital city of Sichuan Province, has a resident population of 21.4 million, making it the fourth largest city in the country. Despite consistently ranking high in the reported Mpox cases nationally, there have been relatively few reports on the genomic characteristics of locally circulating strains.

In this study, researchers conducted whole-genome sequencing of MPXV from confirmed Mpox cases and sewage samples from Sichuan, China. These findings expand China's genomic surveillance dataset of MPXV and enhance national understanding of Mpox transmission dynamics, evolutionary patterns, and containment strategies: offering critical insights for both national and global public health efforts.

METHODS

Sample Collection and Pretreatment

The definition of confirmed cases refers to the "Monkeypox Prevention and Control Plan" from China's Center for Disease Control and Prevention. A total of 96 clinical samples, including throat swabs and vesicle fluid swabs, were collected from confirmed cases of Mpox in Sichuan Province (Supplementary Table S1, available at https://weekly.chinacdc.cn/). These samples were transported to the laboratory of the Sichuan Provincial Center for Disease Control and Prevention (SCDC) and stored at −80 °C. Sewage samples (300 mL) were collected weekly from the Ninth Regenerated Water Plant in Chengdu City, Sichuan Province (a living sewage treatment facility in the core area of Chengdu City with an area of about 200 km^2) and transported to the SCDC laboratory. According to the "Method for enrichment and nucleic acid detection of SARS-CoV-2 in sewage" (WS/T 799-2022), the polyethylene glycol precipitation method was used to concentrate 105 mL of sewage to 0.6 mL for subsequent nucleic acid extraction.

Nucleic Acid Extraction and PCR Diagnosis

To determine the total viral nucleic acid content in clinical samples of Mpox cases, a magnetic bead virus DNA/RNA extraction kit (Xi'an Tianlong Technology Co., Ltd.) was used, and the extracted nucleic acid was stored at −80 °C according to the operating instructions of the GeneRotex 96 Nucleic Acid Extractor (Xi'an Tianlong Technology Co., Ltd.). To determine the total viral nucleic acid content in sewage samples, the Shuoshi nucleic acid extraction kit (Jiangsu Shuoshi Biological Technology Co., Ltd.) was used, and the extracted nucleic acid was stored at −80°C following the operating instructions. The MPXV nucleic acid detection reagent (Jiangsu Shuoshi Biological Technology Co., Ltd.) was used to detect nucleic acids in the sewage samples using a SLAN-96S fully automatic PCR medical analysis system (Shanghai Hongshi Medical Technology Co., Ltd.).

Whole Genome Amplification and Sequencing

All samples meeting the criteria of monkeypox virus nucleic acid detection with Ct values ≤32 were subjected to subsequent viral genome sequencing. Detailed experimental procedures for MPXV genome amplification, library construction, and sequencing were as described in this study's authors' recent studies (*7*,*13*). Briefly, the MPXV whole-genome sequencing kit (Hangzhou Baiyi Technology Co., Ltd.) was used to specifically amplify the whole genome of MPXV in clinical samples of cases and sewage samples. The amplification products were purified using the AMPure XP purification kit (Beckman Coulter, USA). Subsequently, sequencing was performed on the Illumina Nextseq2000, QNome-3841, and Oxford Nanopore GridION platforms. The sequencing platform had no significant impact on the accuracy of the monkeypox virus genomic variant identification (*7*). Therefore, only one sequencing platform was used for the genomic sequencing of each sample.

Genome Assembly

The viral genomes were assembled and analyzed using the MPXV genome analysis workbench developed by Hangzhou Baiyi Technology Co., Ltd. Initially, primers were eliminated using Porechop (v0.2.4) and Fastp (v0.23.2) (*14*). The clean reads were aligned to MPXV-M5312_HM12_Rivers (NC_063383.1) using Minimap2 (v2.24-r1122) (*15*). For second- and third-generation sequencing data, the minimum depth thresholds were set at 10× and 40×, respectively. Variants were identified using Freebayes (v1.3.2) (*16*), with low-quality variations filtered using bcftools (v1.15.1) (*17*). The definitive consensus sequence was then derived based on high-confidence mutations (allele frequency ≥50%) employing the bcftools consensus command. Alignment visualization was performed using IGV (v2.12). To minimize false-

positive mutations caused by low-quality sequencing data, this study retained 49 high-quality datasets from Mpox cases and 3 from sewage samples, each with at least 80% genome coverage at 10× sequencing depth, for mutation profile analysis.

Phylogenetic Analysis

The quality and lineage of the assembled genome were evaluated using NextClade with the pre-built clade IIb dataset (*18*). Genome sequences from representative clades (or lineages) were downloaded from the GISAID database and subjected to multiple alignments with the reference genome (GenBank: NC_063383.1) using NextClade. The meta-information on the sequences used is provided in Supplementary Tables S1 and S2. To avoid including false-positive mutations introduced by sequencing errors, only the region from 1,500 to 190,000 bp was retained for further analysis, as previously described (*7*,*11*). A phylogenetic tree was constructed using IQtree2 (v2.3.6) with the GTR+F+I+G4 model, and the bootstrap value was set to 1,000 (*19*). Time calibration of the phylogenetic tree (i.e., tMRCA estimation) and population size inference were conducted using TreeTime (v0.11.4) (parameters: --reroot oldest --covariation --coalescent skyline) (*20*). Briefly, TreeTime estimates the mutation rate through linear regression of root-to-tip genetic distances against sampling time. Sequences with abnormally high mutation counts (classified as outliers) were excluded. A time-calibrated phylogenetic tree was generated using the branch2time function, while a skyline plot (reflecting effective population size changes) was constructed based on the coalescent theory. A haplotype network of the complete MPXV genome was generated using fastHaN with the modified_tcs algorithm (*21*).

RESULTS

Genome Sequencing of MPXV from Clinical Samples and Sewage Samples in Sichuan

Between June and October 2023, Sichuan Province reported 129 confirmed Mpox cases, including 120 in Chengdu, 6 in Leshan, and 1 each in Yibin, Neijiang, and Mianyang, none of whom had a recent travel history. Demographic data revealed that 99.2% of the patients were male (128/129), with ages ranging from 15 to 52 years (median=31.5), consistent with national trends (*10*). Clinical samples from 96 confirmed cases (94 in Chengdu, 1 each in Yibin and Mianyang) were collected, and most cases were identified between July and August (Supplementary Table S1 and Figure 1A). The ninth wastewater treatment plant in Chengdu, serving an urban area of 200 km^2, provided 26 influent samples that were collected twice a week from July to September 2023. All clinical and PCR-positive sewage samples (n=67) were subjected to amplicon sequencing, with 59 originating from mpox cases and 8 from sewage samples. Five MPOX case datasets and five sewage sample datasets with low coverage ratios (<80%) of the viral genome were filtered.

Genomic Characteristics and Phylogenetic Analysis of MPXV from Sichuan

The MPXV genome from mpox cases includes 46 high-quality sequences (defined by Nextclade as "good" or "mediocre" via the qc.overallStatus metric) and 9 low-quality ones. Three genome sequences were recovered from the sewage samples, with two having high-quality scores and one having low-quality scores. All newly sequenced genomes were assigned to the C.1 lineage (also known as B.1.3.1) and its sub-lineage, C.1.1, which belongs to the West African clade (Clade IIb). These newly assembled sequences were deposited in GenBank under the accession numbers C_AA103396.1 to C_AA103462.1 (Supplementary Table S1). Among the 58 sequences, 55 were classified as the C.1.1 lineage, which exhibited a distinct mutation (C149963T; OPG176:S52L). Integration of the newly sequenced genomes with published genomes revealed that the MPXV genomes in Sichuan clustered into multiple distinct groups (Figure 1B). Most sequences were grouped according to their respective lineages, except for one of the poor-quality sequences, which was possibly caused by sequencing errors. Furthermore, intercountry transmission events have been identified in China, Japan, the Republic of Korea, Portugal, the United States, and other countries.

Haplotype network diagrams offer an intuitive method for visualizing transmission relationships during both coronavirus disease 2019 (COVID-19) (*22*) and Mpox (*9*). To investigate potential MPXV import and local transmission in Sichuan, this study constructed a haplotype network using newly sequenced high-quality genomes and 351 evolutionarily closely related genomes downloaded

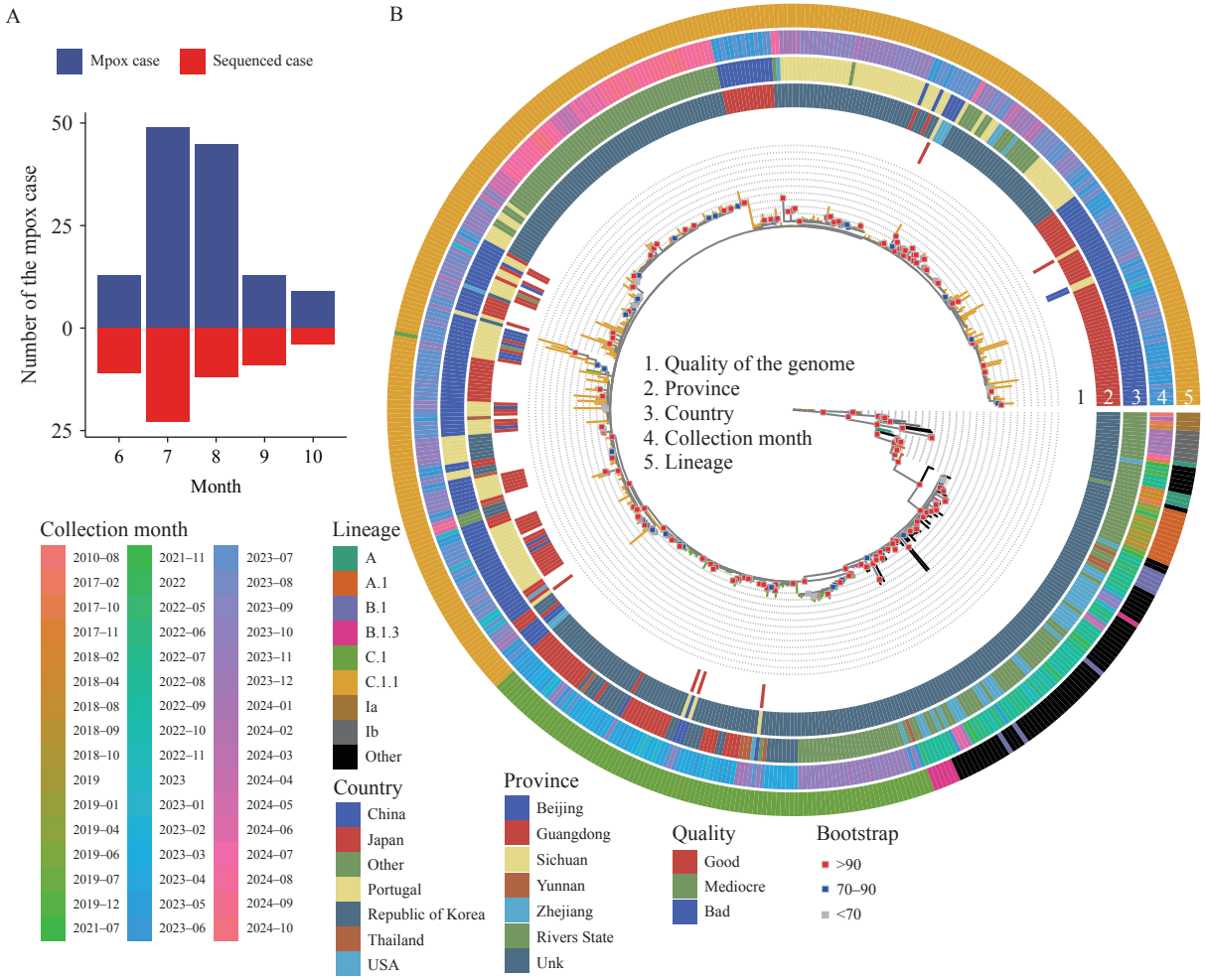

FIGURE 1. Genomic characteristics of MPXV from Mpox in Sichuan. (A) Number of confirmed Mpox cases and sequenced MPXV genomes; (B) Phylogenetic tree of the sequenced MPXV genomes and randomly selected published ones.
Note: Tips are color-coded according to their respective lineages. For clarity, bootstrap support values for branches are categorized into three confidence intervals (<70, 70–90, and >90), represented by gray, blue, and red rectangular shapes, respectively. Five concentric rings, numbered 1 to 5 from the innermost to outermost, indicate: 1) quality of newly sequenced viral genomes from Mpox cases; 2) geographic origins of sequences; 3) country-level origins; 4) collection dates; and 5) lineages. Rivers State is part of Nigeria; genomic sequences lacking province- or state-level administrative division information are labeled as "Unk" (Unknown). To enhance the clarity, we simplified the lineage categories by highlighting only the Ia/Ib/A/A.1/B.1/B.1.3/C.* lineages, while the remaining ones were categorized as “Other”.
Abbreviation: MPXV=Monkeypox virus; Mpox=monkeypox.

from public databases. The newly sequenced genomes clustered into at least six groups within the network (Figure 2), suggesting multiple importation events and simultaneous local co-circulation in Sichuan. The largest cluster comprised 31 sequences and was closely related to the genomes reported in Beijing, Guangdong, and Yunnan PLADs in China and Portugal. The three smallest groups consisted of only a single Sichuan case, indicating the occasional importation of MPXV. Due to effective public health advocacy and monitoring measures, these clusters did not expand further.

Mpox Outbreaks in Sichuan Province Resulted from Multiple Importation Events

To investigate the evolutionary dynamics of MPXVs in Sichuan, this study temporally calibrated a phylogenetic tree using sample collection dates. Most clusters exhibited time to the most recent common ancestor (tMRCA) estimates between March and July 2023. Notably, a distinct cluster of cases (n=25) emerged exclusively in Sichuan from July to October 2023 (Figure 3A), demonstrating rapid localized

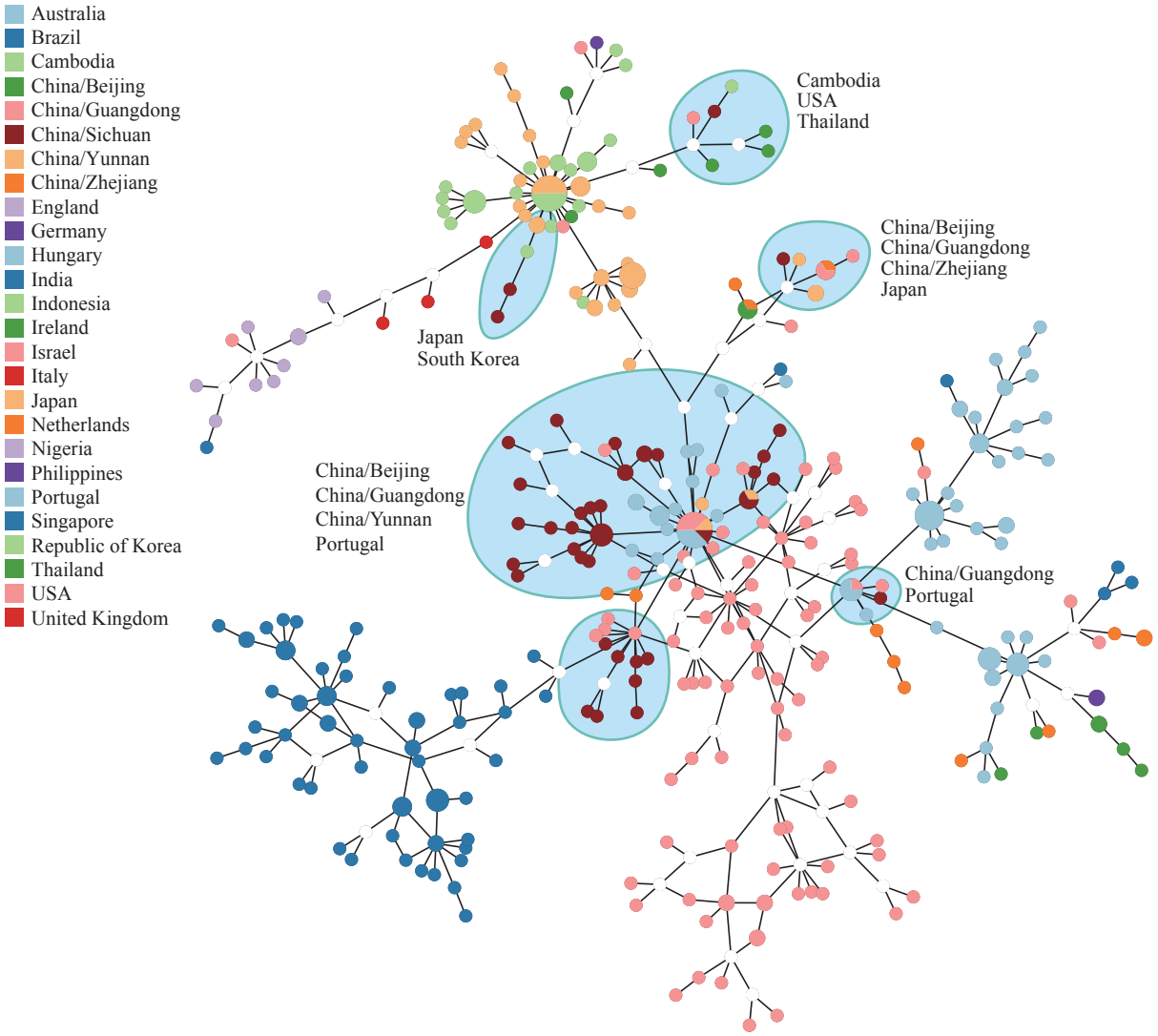

FIGURE 2. Haplotype network of the MPXV from Mpox in Sichuan.
Note: Haplotype network illustrates newly sequenced MPXV genomes from confirmed mpox cases in the Sichuan Province and representative genomes from other lineages. Six major transmission hubs (identified and highlighted in light blue) demonstrated clustering patterns. Node sizes were normalized according to the number of sequences. The sources of the closely related sequences within each hub are listed as references.
Abbreviation: MPXV=Monkeypox virus.

transmission. This study estimated the MPXV evolutionary rate by analyzing the temporal relationship between accumulated mutations and sampling dates, yielding a mutation rate of 5.23± 0.5×10^{-5} substitutions/site/year (Figure 3B), consistent with previous findings (*11*). The effective population size of MPXV showed a marked expansion beginning in early 2023, peaking in June 2023, followed by a sharp decline, consistent with the reported case numbers (Figure 3C). These findings underscore the efficacy of the recent mpox containment measures.

Sewage Samples Reflected the Mutational Spectrum of the MPXV Carried by Mpox Cases

Direct clinical sample collection faces ethical and logistic challenges, including patient privacy concerns. The utility of sewage sample-based surveillance systems for recovering viral genome fragments has been demonstrated in prior pathogen monitoring efforts, such as norovirus and SARS-CoV-2 tracking, which facilitate the detection of emerging mutations. A recent study reported successful retrieval of the full-length

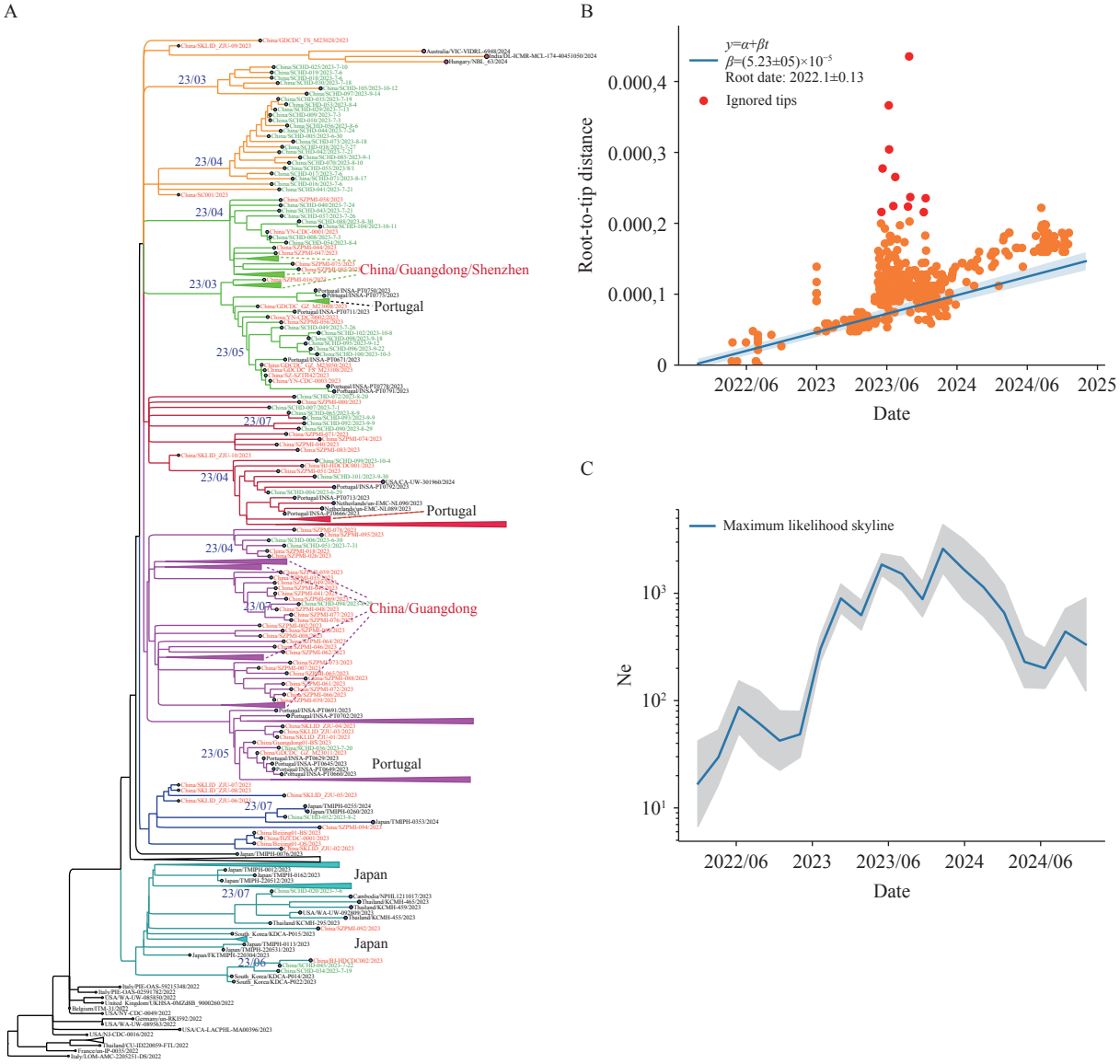

FIGURE 3. Phylodynamics of the 2023 Mpox Outbreak in Sichuan. (A) Time-calibrated phylogenetic tree of newly sequenced MPXV genomes; (B) Linear regression of root-to-tip divergence against sampling dates; (C) Temporal fluctuations in the effective population size (*Ne*) of MPXV.
Note: In panel A, MPXV genome sequences from Sichuan and those from other provinces/regions in China are labeled in green and red, respectively. A subset of sequences from Portugal, Japan, and other regions was collapsed. The time to the most recent common ancestor (tMRCA) of the newly sequenced MPXV and their closest relatives is annotated on the corresponding branch. In panel B, sequences with ambiguous quality or uncertain collection dates are color-coded in red.
Abbreviation: MPXV=Monkeypox virus; Mpox=monkeypox.

MPXV genome from sewage samples (*23*). In this study, 26 sewage samples were collected, 8 of which tested positive for MPXV. Following viral particle enrichment and genome amplification, sequencing achieved a high coverage of the MPXV genome in the three samples. All sewage-derived viral genomes belonged to MPXV C.1.1 lineage, which matched the viral strains identified in locally transmitted cases. Comparative analysis of high-frequency mutations between sewage-derived and clinical samples revealed that sewage detection encompassed all mutation sites observed in local infections, supporting the utility of sewage monitoring for tracking the evolution of MPXV (Figure 4A). However, distinct mutations were uniquely identified in both clinical cases and sewage samples (Figure 4B–C), underscoring the need for an integrated surveillance approach that combines clinical and environmental data to comprehensively assess the

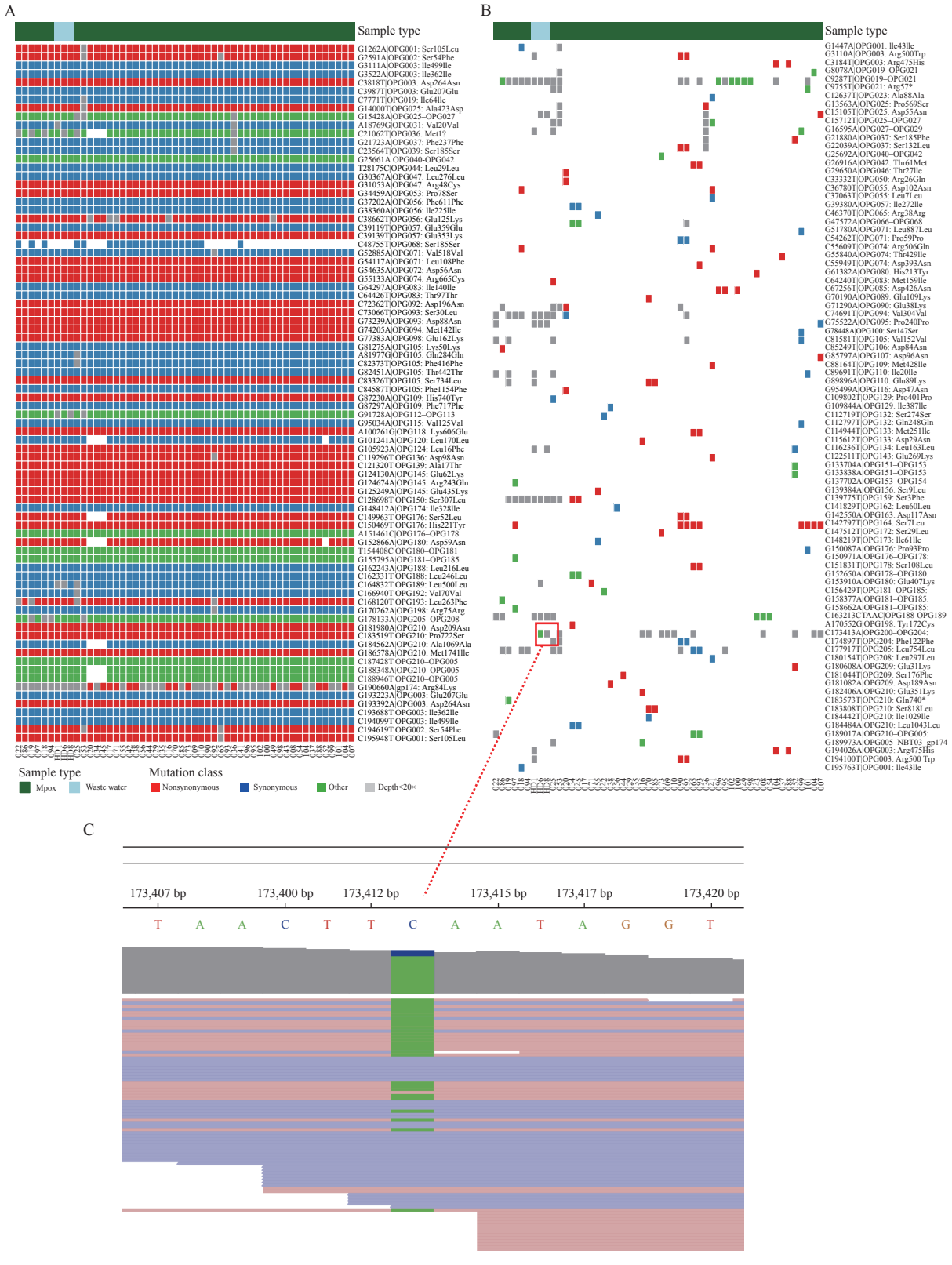

FIGURE 4. Mutation profiles of MPXV from Mpox cases and sewage samples. (A) Profiles of high and low-frequency; (B) Mutation in the collected samples; (C) Distinct mutations identified in sewage sample HD01.
Note: Detailed information on the Mpox and sewage samples is provided in Supplementary Table S1.
Abbreviation: MPXV=Monkeypox virus.

genetic diversity of MPXV.

DISCUSSION

This study collected clinical and sewage samples from Sichuan Province, China in 2023, and conducted whole-genome sequencing of MPXV. Based on the phylogenetic analysis, the transmission characteristics and mutation trends of MPXV in this region were studied. Genomic analysis of MPXV samples from various regions in China, notably Sichuan, indicated that the strains responsible for local infections belonged to either subtype C.1 or C.1.1, consistent with previous reports (*9*,*24*). The newly sequenced genome did not reveal any notable high-frequency amino acid mutations in genes targeting drugs or vaccines, indicating the likelihood of effective control. Concerning the *F3L* gene, a key target for Mpox detection in China, no significant mutations were detected in the newly sequenced sequences, confirming the efficacy of existing detection primers in identifying the present cases of Mpox infection in China. In Sichuan, there is a dual-level interaction involving Mpox cases at both the national and provincial levels, underscoring the intricate nature of transmission and infection within the local population. Significant variations existed in the number of Mpox cases among the six clusters categorized by the haplotype network. Further analysis of the characteristics of each transmission cluster, based on on-site epidemiological investigation results will aid in the formulation of scientifically effective prevention and control strategies. Notably, most patients did not provide information regarding their activity trajectories or close contacts due to privacy protection concerns. Consequently, the transmission relationships inferred from the viral genome sequencing analysis could not be cross-validated against the actual infection processes in these cases. Phylogenetic tree and haplotype network analyses revealed that the genomic sequences of the Sichuan cases showed high similarity with sequences uploaded from countries/regions including Japan, Portugal, the United States, the Republic of Korea, the Netherlands, and Thailand. This suggests the potential import of Mpox cases from these regions into Sichuan. Notably, viral sequences from other Chinese provinces also clustered within the same 5/6 viral clades (Figure 2), indicating possible domestic transmission origins for the Sichuan cases. Owing to the challenges in conducting field epidemiological investigations, the precise origins of these viral clusters cannot be definitively determined based solely on available genomic sequencing data.

Molecular evolutionary trend analysis showed that the evolutionary rate of MPXV in the West African evolutionary branch was significantly higher than that of the known double-stranded DNA viruses (*25*). Mutations that accumulate in the monkeypox virus after spreading across the population are largely attributable to host APOBEC3 editing (*3*). Wu et al. found that genetic mutations in early local cases of monkeypox virus infection in China followed this trend (*9*). This study examined variations in the effective population size of the MPXV C.1 and its sublineages from June 2022 to the present. The results show a significant shift in the expansion and contraction of the effective population. The transition occurred mainly in the first half of 2024, which is consistent with the trends in the number of Mpox cases in China and other countries or regions during the same period. The decline in MPXV population size was primarily attributable to effective prevention and control measures. These include vaccination campaigns, antiviral treatments, expedited diagnosis, and reduced direct contact with infected individuals through isolation protocols and social distancing policies. Nevertheless, the present count of confirmed monkeypox cases exceeds the pre-2022 levels, and the recent interspecies transmission of Clade I MPXV in Africa underscores the ongoing critical need for monkeypox prevention and control measures (*26*). The high-frequency mutations (n=82) consisted of 37 non-synonymous, 34 synonymous, and 11 intergenic events. A start codon loss mutation (C21062T) was observed in the *OPG036* gene in all C.1.1 genomes. However, whether this mutation disrupts the translation of OPG036 remains unclear. The observed ratio of *N* to S substitutions was significantly lower than the expected ratio (37/34 *vs.* 126,244/39,292; P=9.11×10^{-6}; Fisher's Exact Test), indicating that the MPXV genome experiences purifying selection, consistent with findings from our recent study (*7*).

Due to the particularity of the transmission route of Mpox, there is a low proportion of proactive patients seeking medical treatment. Hence, conventional monitoring methods may not entirely depict the comprehensive scenario of an Mpox epidemic. An environmental monitoring system that specifically targets domestic sewage has been implemented globally to offer epidemiological insights into different pathogens at the population level, thus serving as a valuable supplement to individual case monitoring

(*23*,*26*–*27*). The WHO released interim guidelines in 2024, indicating that sewage and environmental monitoring can provide more information for the prevention and control of Mpox (*28*). The Mpox cases in Sichuan Province primarily originated from Chengdu. Sewage samples were collected for testing from the inflow of a major municipal water reclamation plant located in the central area of Chengdu City. These findings revealed a high level of consistency between the MPXV mutations identified in sewage samples and those found in the Mpox case samples. However, distinct mutations were also observed, suggesting a potential silent spread of the virus among individuals who did not seek medical attention. These results underscore the importance of sewage monitoring for enhancing infectious disease surveillance.

This study attempted to comprehensively incorporate publicly available sequencing data on indigenous Mpox in China. However, the included sequences covered only parts of the provinces and cities, which may have affected the results of the fine-scale molecular tracing analysis. Due to limitations, such as sampling strategies and difficulties in obtaining epidemiological information, this study did not sample close contacts of patients and the environment. Therefore, it is not possible to validate the transmission relationships between various transmission clusters divided by genomic sequencing based on epidemiological investigation results. Additionally, there is a limited understanding of the variations in immune status, clinical manifestations, and disease outcomes among patients from different transmission clusters, as well as their potential association with viral genomic mutations. Further research is needed to investigate whether MPXV can be transmitted to other animals through humans, because monkeypox has a wide range of natural hosts.

This study analyzed viral genome sequencing data from indigenous Mpox cases in Sichuan Province. These results indicate that these cases stem primarily from multiple distinct introductory events. The haplotype network and phylogenetic tree revealed at least six distinct local transmission clusters. Furthermore, three full-length MPXV genomes were successfully isolated from sewage samples collected from local communities. These sewage-derived MPXV genomes belong to the C.1.1 lineage, share all predominant mutations with viral strains detected in clinical cases, and exhibit a limited number of unique mutations. This finding suggests that sewage-based MPXV surveillance may serve as a valuable complementary approach to the existing monitoring strategies. In summary, this study investigated the local transmission dynamics of Mpox in Sichuan Province. By integrating sequencing data from other provinces, this study provides a comprehensive overview of the epidemiology, transmission dynamics, and genomic variation trends of the endemic monkeypox virus in China, offering critical insights into evidence-based control strategies.

Conflicts of interest: No conflicts of interests

Ethical statement: Approved by the Sichuan CDC (approval no. SCCDCIRB 2024-014). All the patients were informed in advance and authorized to use their clinical samples for this study.

Funding: Supported by the Sichuan Science and Technology Program (2023YFS0501), the Health Commission of Sichuan Province Medical Science and Technology Program (24QNMP064), the Science Foundation of Sichuan Center for Disease Control and Prevention (ZX202404), the Youth Science Foundation of the Chinese Center for Disease Control and Prevention (2024A103), and the Beijing Natural Science Foundation (7254390).

doi: 10.46234/ccdcw2025.198

[#] Corresponding authors: Changcheng Wu, wucc@ivdc.chinacdc.cn; Li Zhang, Zhanglilyscdc@163.com; Wenjie Tan, tanwj@ivdc.chinacdc.cn.

[1] Sichuan Center for Disease Control and Prevention, Chendu City, Sichuan Province, China; [2] Sichuan International Travel Healthcare Center (Chengdu Customs Port Clinic), Chendu City, Sichuan Province, China; [3] Jinjiang Center for Disease Control and Prevention, Chendu City, Sichuan Province, China; [4] National Key Laboratory of Intelligent Tracking and Forecasting for Infectious Diseases, National Institute for Viral Disease Control and Prevention, Chinese Center for Disease Control and Prevention, Beijing, China.

Submitted: March 24, 2025
Accepted: September 01, 2025
Issued: September 12, 2025

REFERENCES

1. Lu JJ, Xing H, Wang CH, Tang MJ, Wu CC, Ye F, et al. Mpox (formerly monkeypox): pathogenesis, prevention and treatment. Signal Transduct Target Ther 2023;8(1):458. https://doi.org/10.1038/s41392-023-01675-2.
2. Ladnyj ID, Ziegler P, Kima E. A human infection caused by monkeypox virus in Basankusu Territory, Democratic Republic of the Congo. Bull World Health Organ 1972;46(5):593-7. https://pubmed.ncbi.nlm.nih.gov/4340218.
3. Isidro J, Borges V, Pinto M, Sobral D, Santos JD, Nunes A, et al. Phylogenomic characterization and signs of microevolution in the 2022

multi-country outbreak of monkeypox virus. Nat Med 2022;28(8):1569 – 72. https://doi.org/10.1038/s41591-022-01907-y.
4. Gigante CM, Korber B, Seabolt MH, Wilkins K, Davidson W, Rao AK, et al. Multiple lineages of monkeypox virus detected in the United States, 2021-2022. Science 2022;378(6619):560 – 5. https://doi.org/10.1126/science.add4153.
5. Otieno JR, Ruis C, Onoja AB, Kuppalli K, Hoxha A, Nitsche A, et al. Global genomic surveillance of monkeypox virus. Nat Med 2025;31(1):342 – 50. https://doi.org/10.1038/s41591-024-03370-3.
6. Zhao H, Wang WL, Zhao L, Ye S, Song JD, Lu RJ, et al. The first imported case of monkeypox in the mainland of China — Chongqing municipality, China, September 16, 2022. China CDC Wkly 2022;4(38):853 – 4. https://doi.org/10.46234/ccdcw2022.175.
7. Wu CC, Ruhan A, Ye S, Ye F, Huo WB, Lu RJ, et al. Rapid identification of full-length genome and tracing variations of monkeypox virus in clinical specimens based on mNGS and amplicon sequencing. Virol Sin 2024;39(1):134 – 43. https://doi.org/10.1016/j.virs.2023.12.002.
8. Yu JH, Zhang X, Liu JJ, Xiang LL, Huang S, Xie XT, et al. Phylogeny and molecular evolution of the first local monkeypox virus cluster in Guangdong Province, China. Nat Commun 2023;14(1):8241. https://doi.org/10.1038/s41467-023-44092-3.
9. Wu CC, Cui LB, Pan Y, Lv ZQ, Yao MX, Wang WL, et al. Characterization of whole genomes from recently emerging Mpox cases in several regions of China, 2023. Sci China Life Sci 2024;67(5):1079 – 81. https://doi.org/10.1007/s11427-023-2485-8.
10. Ren RQ, Li C, Bai WQ, Wang YL, Li D, Ding F, et al. The epidemiological characteristics of mpox cases - China, 2023. China CDC Wkly 2024;6(26):619 – 23. https://doi.org/10.46234/ccdcw2024.118.
11. Shan KJ, Wu CC, Tang XL, Lu RJ, Hu YL, Tan WJ, et al. Molecular evolution of protein sequences and codon usage in monkeypox viruses. Genomics Proteomics Bioinf 2024;22(1):qzad003. https://doi.org/10.1093/gpbjnl/qzad003.
12. Hatmal MM, Al-Hatamleh MAI, Olaimat AN, Ahmad S, Hasan H, Ahmad Suhaimi NA, et al. Comprehensive literature review of monkeypox. Emerg Microbes Infect 2022;11(1):2600 – 31. https://doi.org/10.1080/22221751.2022.2132882.
13. Chen YD, Wu CC, Ruhan A, Zhao L, Zhang ZX, Tan WJ. Perspective on the application of genome sequencing for monkeypox virus surveillance. Virol Sin 2023;38(2):327 – 33. https://doi.org/10.1016/j.virs.2023.03.006.
14. Chen SF, Zhou YQ, Chen YR, Gu J. fastp: an ultra-fast all-in-one FASTQ preprocessor. Bioinformatics 2018;34(17):i884 – 90. https://doi.org/10.1093/bioinformatics/bty560.
15. Li H. New strategies to improve minimap2 alignment accuracy. Bioinformatics 2021;37(23):4572 – 4. https://doi.org/10.1093/bioinformatics/btab705.
16. Garrison E, Marth G. Haplotype-based variant detection from short-read sequencing. arXiv:1207.3907 [Preprint] 2012. https://doi.org/10.48550/arXiv.1207.3907.
17. Danecek P, Bonfield JK, Liddle J, Marshall J, Ohan V, Pollard MO, et al. Twelve years of SAMtools and BCFtools. Gigascience 2021;10(2):giab008. https://doi.org/10.1093/gigascience/giab008.
18. Aksamentov I, Roemer C, Hodcroft EB, Neher RA. Nextclade: clade assignment, mutation calling and quality control for viral genomes. J Open Source Softw 2021;6(67):3773. https://doi.org/10.21105/joss.03773.
19. Minh BQ, Schmidt HA, Chernomor O, Schrempf D, Woodhams MD, von Haeseler A, et al. IQ-TREE 2: new models and efficient methods for phylogenetic inference in the genomic era. Mol Biol Evol 2020;37(5):1530 – 4. https://doi.org/10.1093/molbev/msaa015.
20. Sagulenko P, Puller V, Neher RA. TreeTime: maximum-likelihood phylodynamic analysis. Virus Evol 2018;4(1):vex042. https://doi.org/10.1093/ve/vex042.
21. Chi LJ, Zhang XL, Xue YB, Chen H. fastHaN: a fast and scalable program for constructing haplotype network for large-sample sequences. Mol Ecol Resour 2025;25(5):e13829. https://doi.org/10.1111/1755-0998.13829.
22. Tang XL, Wu CC, Li X, Song YH, Yao XM, Wu XK, et al. On the origin and continuing evolution of SARS-CoV-2. Natl Sci Rev 2020;7(6):1012 – 23. https://doi.org/10.1093/nsr/nwaa036.
23. Xu J, Liu C, Zhang Q, Zhu HN, Cui F, Zhao ZQ, et al. The first detection of mpox virus DNA from wastewater in China. Sci Total Environ 2024;932:172742. https://doi.org/10.1016/j.scitotenv.2024.172742.
24. Zhang SJ, Wang FX, Peng Y, Gong XH, Fan GH, Lin YL, et al. Evolutionary trajectory and characteristics of Mpox virus in 2023 based on a large-scale genomic surveillance in Shenzhen, China. Nat Commun 2024;15(1):7452. https://doi.org/10.1038/s41467-024-51737-4.
25. Vakaniaki EH, Kacita C, Kinganda-Lusamaki E, O'Toole Á, Wawina-Bokalanga T, Mukadi-Bamuleka D, et al. Sustained human outbreak of a new MPXV clade I lineage in eastern Democratic Republic of the Congo. Nat Med 2024;30(10):2791-5. http://dx.doi.org/10.1038/s41591-024-03130-3.
26. de Araujo JC, Carvalho APA, Leal CD, Natividade M, Borin M, Guerra A, et al. Detection of multiple human viruses, including mpox, using a wastewater surveillance approach in brazil. Pathogens 2024;13(7):589. https://doi.org/10.3390/pathogens13070589.
27. Tiwari A, Adhikari S, Kaya D, Islam MA, Malla B, Sherchan SP, et al. Monkeypox outbreak: wastewater and environmental surveillance perspective. Sci Total Environ 2023;856(Pt 2):159166. http://dx.doi.org/10.1016/j.scitotenv.2022.159166.
28. WHO. Considerations for wastewater and environmental surveillance for monkeypox virus: Interim guidance. 2024. https://www.who.int/publications/i/item/B09178. [2025-7-4].

SUPPLEMENTARY MATERIAL

SUPPLEMENTARY TABLE S1. The meta information of Mpox cases and wastewater samples.

Sequence ID	Sex/Sample type	Age	Collection_date	Region	Genotype	qc.overallStatus	Coverage (%)	Genebase accession number	Quality
SCHD-001	Male	38	2023/6/29	Chengdu, China	undetermined	/	/	/	
SCHD-004	Male	25	2023/6/30	Chengdu, China	C.1.1	good	99.78	C_AA103404.1	high
SCHD-005	Male	40	2023/6/30	Chengdu, China	C.1.1	bad	87.43	C_AA103405.1	low
SCHD-006	Male	52	2023/6/30	Chengdu, China	/	bad	30.37	C_AA103406.1	
SCHD-007	Male	34	2023/7/1	Chengdu, China	C.1.1	good	99.37	C_AA103407.1	high
SCHD-008	Male	34	2023/7/3	Chengdu, China	C.1.1	good	99.78	C_AA103408.1	high
SCHD-009	Male	38	2023/7/3	Chengdu, China	C.1.1	good	99.61	C_AA103409.1	high
SCHD-010	Male	30	2023/7/3	Chengdu, China	C.1.1	good	99.48	C_AA103410.1	high
SCHD-015	Male	31	2023/7/5	Chengdu, China	undetermined	/	/	/	
SCHD-016	Male	27	2023/7/6	Chengdu, China	C.1.1	good	98.78	C_AA103411.1	high
SCHD-017	Male	25	2023/7/6	Chengdu, China	C.1.1	good	99.02	C_AA103412.1	high
SCHD-018	Male	31	2023/7/6	Chengdu, China	C.1.1	good	96.93	C_AA103413.1	high
SCHD-019	Male	25	2023/7/6	Chengdu, China	C.1.1	mediocre	94.70	C_AA103414.1	high
SCHD-020	Male	29	2023/7/6	Chengdu, China	C.1	good	98.94	C_AA103415.1	high
SCHD-021	Male	27	2023/7/7	Chengdu, China	C.1.1	bad	82.42	C_AA103416.1	low
SCHD-022	Male	31	2023/7/8	Chengdu, China	C.1.1	bad	95.43	C_AA103417.1	low
SCHD-025	Male	32	2023/7/10	Chengdu, China	C.1.1	bad	90.43	C_AA103418.1	low
SCHD-026	Male	19	2023/7/11	Chengdu, China	undetermined	/	/	/	
SCHD-027	Male	30	2023/7/12	Chengdu, China	undetermined	/	/	/	
SCHD-028	Male	32	2023/7/13	Chengdu, China	undetermined	/	/	/	
SCHD-029	Male	32	2023/7/13	Chengdu, China	C.1.1	good	99.80	C_AA103419.1	high
SCHD-030	Male	39	2023/7/18	Chengdu, China	/	bad	23.20	C_AA103420.1	
SCHD-031	Male	38	2023/7/12	Chengdu, China	undetermined	/	/	/	
SCHD-032	Male	39	2023/7/18	Chengdu, China	undetermined	/	/	/	
SCHD-033	Male	39	2023/7/18	Chengdu, China	undetermined	/	/	/	
SCHD-034	Male	36	2023/7/19	Chengdu, China	C.1	good	99.70	C_AA103421.1	high
SCHD-035	Male	29	2023/7/19	Chengdu, China	C.1.1	good	99.83	C_AA103422.1	high
SCHD-036	Male	32	2023/7/20	Chengdu, China	C.1.1	good	95.06	C_AA103423.1	high
SCHD-037	Male	35	2023/7/26	Chengdu, China	C.1.1	good	99.89	C_AA103424.1	high
SCHD-038	Male	21	2023/7/27	Chengdu, China	C.1.1	good	99.95	C_AA103425.1	high
SCHD-039	Male	36	2023/7/27	Chengdu, China	undetermined	/	/	/	
SCHD-040	Male	25	2023/7/24	Chengdu, China	C.1.1	bad	83.14	C_AA103426.1	low
SCHD-041	Male	23	2023/7/21	Chengdu, China	C.1.1	good	99.78	C_AA103427.1	high
SCHD-042	Male	32	2023/7/21	Chengdu, China	C.1.1	good	99.94	C_AA103428.1	high
SCHD-043	Male	36	2023/7/21	Chengdu, China	C.1.1	good	99.72	C_AA103429.1	high
SCHD-044	Male	30	2023/7/24	Chengdu, China	C.1.1	good	99.91	C_AA103430.1	high
SCHD-045	Male	42	2023/7/22	Chengdu, China	C.1	good	99.94	C_AA103431.1	high
SCHD-046	Male	24	2023/7/22	Chengdu, China	undetermined	/	/	/	
SCHD-047	Male	35	2023/7/22	Chengdu, China	undetermined	/	/	/	

Continued

Sequence ID	Sex/Sample type	Age	Collection_date	Region	Genotype	qc.overallStatus	Coverage (%)	Genebase accession number	Quality
SCHD-048	Male	34	2023/7/29	Chengdu, China	undetermined	/	/	/	
SCHD-049	Male	30	2023/7/26	Chengdu, China	C.1.1	good	98.96	C_AA103432.1	high
SCHD-050	Male	27	2023/7/30	Chengdu, China	undetermined	/	/	/	
SCHD-051	Male	45	2023/7/31	Yibin, China	C.1.1	bad	70.11	C_AA103433.1	low
SCHD-052	Male	36	2023/8/2	Chengdu, China	C.1.1	good	99.77	C_AA103434.1	high
SCHD-053	Male	33	2023/8/4	Mianyang, China	C.1.1	bad	86.27	C_AA103435.1	low
SCHD-054	Male	51	2023/8/4	Chengdu, China	C.1.1	good	99.96	C_AA103436.1	high
SCHD-055	Male			Chengdu, China	C.1.1	good	99.91	C_AA103437.1	high
SCHD-056	Male	28	2023/8/6	Chengdu, China	C.1.1	good	99.90	C_AA103438.1	high
SCHD-057	Male	28	2023/8/6	Chengdu, China	undetermined	/	/	/	
SCHD-058	Male	29	2023/8/5	Chengdu, China	undetermined	/	/	/	
SCHD-059	Male	34	2023/8/1	Chengdu, China	undetermined	/	/	/	
SCHD-060	Male	35	2023/8/1	Chengdu, China	undetermined	/	/	/	
SCHD-061	Male	27	2023/7/31	Chengdu, China	undetermined	/	/	/	
SCHD-062	Male	32	2023/7/31	Chengdu, China	undetermined	/	/	/	
SCHD-063	Male	23	2023/8/4	Chengdu, China	undetermined	/	/	/	
SCHD-064	Male	39	2023/8/4	Chengdu, China	undetermined	/	/	/	
SCHD-065	Male	46	2023/8/9	Chengdu, China	C.1.1	good	97.79	C_AA103439.1	high
SCHD-066	Male	28	2023/8/3	Chengdu, China	undetermined	/	/	/	
SCHD-067	Male	31	2023/8/4	Chengdu, China	undetermined	/	/	/	
SCHD-068	Male	25	2023/8/4	Chengdu, China	undetermined	/	/	/	
SCHD-069	Male	29	2023/8/8	Chengdu, China	undetermined	/	/	/	
SCHD-070	Male	20	2023/8/10	Chengdu, China	C.1.1	good	99.80	C_AA103440.1	high
SCHD-071	Male	42	2023/8/17	Chengdu, China	C.1.1	good	99.27	C_AA103441.1	high
SCHD-072	Male	29	2023/8/20	Chengdu, China	C.1.1	bad	74.63	C_AA103442.1	low
SCHD-073	Male	28	2023/8/18	Chengdu, China	C.1.1	good	99.80	C_AA103443.1	high
SCHD-074	Male	37	2023/8/27	Chengdu, China	undetermined	/	/	/	
SCHD-075	Male	34	2023/8/25	Chengdu, China	undetermined	/	/	/	
SCHD-076	Male	24	2023/8/22	Chengdu, China	undetermined	/	/	/	
SCHD-077	Male	38	2023/8/22	Chengdu, China	undetermined	/	/	/	
SCHD-078	Male	47	2023/8/22	Chengdu, China	undetermined	/	/	/	
SCHD-079	Male	16	2023/8/23	Chengdu, China	undetermined	/	/	/	
SCHD-080	Male	42	2023/8/19	Chengdu, China	undetermined	/	/	/	
SCHD-081	Male	34	2023/8/19	Chengdu, China	undetermined	/	/	/	
SCHD-082	Male	39	2023/8/20	Chengdu, China	undetermined	/	/	/	
SCHD-084	Male	30	2023/8/25	Chengdu, China	undetermined	/	/	/	
SCHD-085	Male	23	2023/8/31	Chengdu, China	C.1.1	good	99.82	C_AA103444.1	high
SCHD-086	Male	37	2023/9/1	Chengdu, China	C.1.1	good	98.17	C_AA103445.1	high
SCHD-087	Male	37	2023/8/31	Chengdu, China	undetermined	/	/	/	
SCHD-088	Male	29	2023/8/30	Chengdu, China	C.1.1	good	99.85	C_AA103446.1	high
SCHD-089	Male	34	2023/8/29	Chengdu, China	C.1.1	bad	64.14	C_AA103447.1	low

Continued

Sequence ID	Sex/Sample type	Age	Collection_date	Region	Genotype	qc.overallStatus	Coverage (%)	Genebase accession number	Quality
SCHD-090	Male	31	2023/8/29	Chengdu, China	C.1.1	good	99.28	C_AA103448.1	high
SCHD-091	Male	38	2023/8/28	Chengdu, China	undetermined	/	/	/	
SCHD-092	Male	24	2023/9/9	Chengdu, China	C.1.1	mediocre	93.74	C_AA103449.1	high
SCHD-093	Male	36	2023/9/9	Chengdu, China	C.1.1	good	99.65	C_AA103450.1	high
SCHD-094	Male	18	2023/8/29	Chengdu, China	C.1.1	good	98.04	C_AA103451.1	high
SCHD-095	Male	29	2023/9/12	Chengdu, China	C.1.1	good	99.06	C_AA103452.1	high
SCHD-096	Male	32	2023/9/22	Chengdu, China	C.1.1	good	99.65	C_AA103453.1	high
SCHD-097	Male	29	2023/9/14	Chengdu, China	C.1.1	good	99.16	C_AA103454.1	high
SCHD-098	Male	37	2023/9/18	Chengdu, China	C.1.1	good	99.77	C_AA103455.1	high
SCHD-099	Male	29	2023/10/4	Chengdu, China	C.1.1	good	99.75	C_AA103456.1	high
SCHD-100	Male	29	2023/10/5	Chengdu, China	C.1.1	good	99.78	C_AA103457.1	high
SCHD-101	Male	31	2023/9/30	Chengdu, China	C.1.1	good	99.46	C_AA103458.1	high
SCHD-102	Male	28	2023/10/8	Chengdu, China	C.1.1	good	99.37	C_AA103459.1	high
SCHD-103	Male	34	2023/10/11	Chengdu, China	/	bad	55.78	C_AA103460.1	
SCHD-104	Male	35	2023/10/11	Chengdu, China	C.1.1	good	99.71	C_AA103461.1	high
SCHD-105	Male	31	2023/10/12	Chengdu, China	/	bad	52.46	C_AA103462.1	
HD1	Sewage	/	2023/7/24	Chengdu, China	C.1.1	mediocre	92.92	C_AA103396.1	high
HD2	Sewage	/	2023/7/31	Chengdu, China	/	bad	2.61	C_AA103397.1	
HD3	Sewage	/	2023/8/7	Chengdu, China	/	bad	4.40	C_AA103398.1	
HD4	Sewage	/	2023/8/10	Chengdu, China	/	bad	28.98	C_AA103399.1	
HD5	Sewage	/	2023/8/17	Chengdu, China	/	bad	5.90	C_AA103400.1	
HD6	Sewage	/	2023/8/24	Chengdu, China	C.1.1	good	94.72	C_AA103401.1	high
HD7	Sewage	/	2023/9/4	Chengdu, China	/	bad	43.52	C_AA103402.1	
HD8	Sewage	/	2023/9/14	Chengdu, China	C.1.1	good	95.37	C_AA103403.1	high

Abbreviation: Mpox=monkeypox.

SUPPLEMENTARY TABLE S2. The meta information of the sequences included in constructing the haplotype network

Name	Country	Province	Collection date	Sources	Revised collection date for treetime	Revised month
hMPXV/China/SCHD-004/2023-6-29	China	Sichuan	2023/6/29	This_study	2023-06-29	2023-06
hMPXV/China/SCHD-007/2023-7-1	China	Sichuan	2023/7/1	This_study	2023-07-01	2023-07
hMPXV/China/SCHD-009/2023-7-3	China	Sichuan	2023/7/3	This_study	2023-07-03	2023-07
hMPXV/China/SCHD-017/2023-7-6	China	Sichuan	2023/7/6	This_study	2023-07-06	2023-07
hMPXV/China/SCHD-008/2023-7-3	China	Sichuan	2023/7/3	This_study	2023-07-03	2023-07
hMPXV/China/SCHD-020/2023-7-6	China	Sichuan	2023/7/6	This_study	2023-07-06	2023-07
hMPXV/China/SCHD-010/2023-7-3	China	Sichuan	2023/7/3	This_study	2023-07-03	2023-07
hMPXV/China/SCHD-016/2023-7-6	China	Sichuan	2023/7/6	This_study	2023-07-06	2023-07
hMPXV/China/SCHD-038/2023-7-27	China	Sichuan	2023/7/27	This_study	2023-07-27	2023-07
hMPXV/China/SCHD-018/2023-7-6	China	Sichuan	2023/7/6	This_study	2023-07-06	2023-07
hMPXV/China/SCHD-041/2023-7-21	China	Sichuan	2023/7/21	This_study	2023-07-21	2023-07
hMPXV/China/SCHD-037/2023-7-26	China	Sichuan	2023/7/26	This_study	2023-07-26	2023-07
hMPXV/China/SCHD-034/2023-7-19	China	Sichuan	2023/7/19	This_study	2023-07-19	2023-07

Continued

Name	Country	Province	Collection date	Sources	Revised collection date for treetime	Revised month
hMPXV/China/SCHD-035/2023-7-19	China	Sichuan	2023/7/19	This_study	2023-07-19	2023-07
hMPXV/China/SCHD-029/2023-7-13	China	Sichuan	2023/7/13	This_study	2023-07-13	2023-07
hMPXV/China/SCHD-044/2023-7-24	China	Sichuan	2023/7/24	This_study	2023-07-24	2023-07
hMPXV/China/SCHD-036/2023-7-20	China	Sichuan	2023/7/20	This_study	2023-07-20	2023-07
hMPXV/China/SCHD-042/2023-7-21	China	Sichuan	2023/7/21	This_study	2023-07-21	2023-07
hMPXV/China/SCHD-045/2023-7-22	China	Sichuan	2023/7/22	This_study	2023-07-22	2023-07
hMPXV/China/SCHD-049/2023-7-26	China	Sichuan	2023/7/26	This_study	2023-07-26	2023-07
hMPXV/China/SCHD-043/2023-7-21	China	Sichuan	2023/7/21	This_study	2023-07-21	2023-07
hMPXV/China/SCHD-088/2023-8-30	China	Sichuan	2023/8/30	This_study	2023-08-30	2023-08
hMPXV/China/SCHD-054/2023-8-4	China	Sichuan	2023/8/4	This_study	2023-08-04	2023-08
hMPXV/China/SCHD-056/2023-8-6	China	Sichuan	2023/8/6	This_study	2023-08-06	2023-08
hMPXV/China/SCHD-100/2023-10-5	China	Sichuan	2023/10/5	This_study	2023-10-05	2023-10
hMPXV/China/SCHD-055/2023/8/1	China	Sichuan	2023/8/1	This_study	2023-08-01	2023-08
hMPXV/China/SCHD-065/2023-8-9	China	Sichuan	2023/8/9	This_study	2023-08-09	2023-08
hMPXV/China/SCHD-086/2023-9-1	China	Sichuan	2023/9/1	This_study	2023-09-01	2023-09
hMPXV/China/SCHD-070/2023-8-10	China	Sichuan	2023/8/10	This_study	2023-08-10	2023-08
hMPXV/China/SCHD-104/2023-10-11	China	Sichuan	2023/10/11	This_study	2023-10-11	2023-10
hMPXV/China/SCHD-095/2023-9-12	China	Sichuan	2023/9/12	This_study	2023-09-12	2023-09
hMPXV/China/SCHD-096/2023-9-22	China	Sichuan	2023/9/22	This_study	2023-09-22	2023-09
hMPXV/China/SCHD-052/2023-8-2	China	Sichuan	2023/8/2	This_study	2023-08-02	2023-08
hMPXV/China/SCHD-085/2023-9-1	China	Sichuan	2023/9/1	This_study	2023-09-01	2023-09
hMPXV/China/SCHD-097/2023-9-14	China	Sichuan	2023/9/14	This_study	2023-09-14	2023-09
hMPXV/China/SCHD-073/2023-8-18	China	Sichuan	2023/8/18	This_study	2023-08-18	2023-08
hMPXV/China/SCHD-071/2023-8-17	China	Sichuan	2023/8/17	This_study	2023-08-17	2023-08
hMPXV/Portugal/INSA-PT0649/2023	Portugal		2023-07-10	GISAID	2023-07-10	2023-07
hMPXV/China/SCHD-099/2023-10-4	China	Sichuan	2023/10/4	This_study	2023-10-04	2023-10
hMPXV/China/SCHD-102/2023-10-8	China	Sichuan	2023/10/8	This_study	2023-10-08	2023-10
hMPXV/China/SCHD-094/2023-8-29	China	Sichuan	2023/8/29	This_study	2023-08-29	2023-08
hMPXV/China/SZ-SZTH42/2023	China	Guangdong	2023-06-24	GISAID	2023-06-24	2023-06
hMPXV/China/SCHD-101/2023-9-30	China	Sichuan	2023/9/30	This_study	2023-09-30	2023-09
hMPXV/China/SCHD-098/2023-9-18	China	Sichuan	2023/9/18	This_study	2023-09-18	2023-09
hMPXV/Portugal/INSA-PT0671/2023	Portugal		2023-08-02	GISAID	2023-08-02	2023-08
hMPXV/China/YN-CDC-0002/2023	China	Yunnan	2023-06-28	GISAID	2023-06-28	2023-06
hMPXV/China/SCHD-093/2023-9-9	China	Sichuan	2023/9/9	This_study	2023-09-09	2023-09
hMPXV/China/SCHD-090/2023-8-29	China	Sichuan	2023/8/29	This_study	2023-08-29	2023-08
hMPXV/China/YN-CDC-0001/2023	China	Yunnan	2023-06-27	GISAID	2023-06-27	2023-06
hMPXV/Portugal/INSA-PT0645/2023	Portugal		2023-07-07	GISAID	2023-07-07	2023-07
hMPXV/Portugal/INSA-PT0791/2023	Portugal		2023-11-08	GISAID	2023-11-08	2023-11
hMPXV/China/YN-CDC-0003/2023	China	Yunnan	2023-07-03	GISAID	2023-07-03	2023-07
hMPXV/Portugal/INSA-PT0660/2023	Portugal		2023-07-26	GISAID	2023-07-26	2023-07
hMPXV/China/SZ-SZTH45/2023	China	Guangdong	2023-6-16	GISAID	2023-06-16	2023-06
hMPXV/Portugal/INSA-PT0656/2023	Portugal		2023-07-21	GISAID	2023-07-21	2023-07

Continued

Name	Country	Province	Collection date	Sources	Revised collection date for treetime	Revised month
hMPXV/Portugal/INSA-PT0733/2023	Portugal		2023-09-19	GISAID	2023-09-19	2023-09
hMPXV/Portugal/INSA-PT0629/2023	Portugal		2023-06-20	GISAID	2023-06-20	2023-06
hMPXV/Portugal/INSA-PT0713/2023	Portugal		2023-08-21	GISAID	2023-08-21	2023-08
hMPXV/Netherlands/un-EMC-NL089/2023	Netherlands		2023-10-15	GISAID	2023-10-15	2023-10
hMPXV/Portugal/INSA-PT0748/2023	Portugal		2023-09-29	GISAID	2023-09-29	2023-09
hMPXV/Portugal/INSA-PT0666/2023	Portugal		2023-08-01	GISAID	2023-08-01	2023-08
hMPXV/Portugal/INSA-PT0727/2023	Portugal		2023-09-12	GISAID	2023-09-12	2023-09
hMPXV/Brazil/RJ-FIOCRUZ-10491/2024	Brazil		2024-04-18	GISAID	2024-04-18	2024-04
hMPXV/Portugal/INSA-PT0775/2023	Portugal		2023-10-19	GISAID	2023-10-19	2023-10
hMPXV/Portugal/INSA-PT0711/2023	Portugal		2023-08-21	GISAID	2023-08-21	2023-08
hMPXV/Germany/BY-IMB-2541/2023	Germany		2023-11-22	GISAID	2023-11-22	2023-11
hMPXV/Portugal/INSA-PT0694/2023	Portugal		2023-07-18	GISAID	2023-07-18	2023-07
hMPXV/Portugal/INSA-PT0736/2023	Portugal		2023-09-19	GISAID	2023-09-19	2023-09
hMPXV/Portugal/INSA-PT0778/2023	Portugal		2023-10-27	GISAID	2023-10-27	2023-10
hMPXV/Portugal/INSA-PT0661/2023	Portugal		2023-07-26	GISAID	2023-07-26	2023-07
hMPXV/China/SZ-SZTH41/2023	China	Guangdong	2023-06-19	GISAID	2023-06-19	2023-06
hMPXV/USA/CA-UW-301960/2024	USA		2024-02-14	GISAID	2024-02-14	2024-02
hMPXV/Portugal/INSA-PT0744/2023	Portugal		2023-09-26	GISAID	2023-09-26	2023-09
hMPXV/USA/CA-CDPH-1M1000432/2023	USA		2023-10-14	GISAID	2023-10-14	2023-10
hMPXV/Portugal/INSA-PT0739/2023	Portugal		2023-09-24	GISAID	2023-09-24	2023-09
hMPXV/Portugal/INSA-PT0724/2023	Portugal		2023-09-08	GISAID	2023-09-08	2023-09
hMPXV/Ireland/un-NVRL-Z22IRL00908/2023	Ireland		2023-08-18	GISAID	2023-08-18	2023-08
hMPXV/Portugal/INSA-PT0799/2023	Portugal		2023-11-20	GISAID	2023-11-20	2023-11
hMPXV/Portugal/INSA-PT0750/2023	Portugal		2023-10-02	GISAID	2023-10-02	2023-10
hMPXV/Ireland/un-NVRL-Z22IRL00909/2023	Ireland		2023-08-31	GISAID	2023-08-31	2023-08
hMPXV/Portugal/INSA-PT0756/2023	Portugal		2023-10-06	GISAID	2023-10-06	2023-10
hMPXV/Portugal/INSA-PT0740/2023	Portugal		2023-09-22	GISAID	2023-09-22	2023-09
hMPXV/Portugal/INSA-PT0738/2023	Portugal		2023-09-22	GISAID	2023-09-22	2023-09
hMPXV/Portugal/INSA-PT0783/2023	Portugal		2023-10-29	GISAID	2023-10-29	2023-10
hMPXV/Portugal/INSA-PT0780/2023	Portugal		2023-10-29	GISAID	2023-10-29	2023-10
hMPXV/Portugal/INSA-PT0771/2023	Portugal		2023-10-12	GISAID	2023-10-12	2023-10
hMPXV/Portugal/INSA-PT0701/2023	Portugal		2023-08-07	GISAID	2023-08-07	2023-08
hMPXV/Portugal/INSA-PT0708/2023	Portugal		2023-08-10	GISAID	2023-08-10	2023-08
hMPXV/Portugal/INSA-PT0784/2023	Portugal		2023-11-01	GISAID	2023-11-01	2023-11
hMPXV/Portugal/INSA-PT0793/2023	Portugal		2023-11-07	GISAID	2023-11-07	2023-11
hMPXV/Portugal/INSA-PT0800/2023	Portugal		2023-11-18	GISAID	2023-11-18	2023-11
hMPXV/Netherlands/un-EMC-NL090/2023	Netherlands		2023-11-07	GISAID	2023-11-07	2023-11
hMPXV/Portugal/INSA-PT0741/2023	Portugal		2023-09-25	GISAID	2023-09-25	2023-09
hMPXV/Ireland/un-NVRL-G23IRL50393/2023	Ireland		2023-08-16	GISAID	2023-08-16	2023-08
hMPXV/Germany/un-IMB-2541/2023	Germany		2023-11-22	GISAID	2023-11-22	2023-11
hMPXV/Ireland/un-NVRL-Z22IRL00910/2023	Ireland		2023-08-28	GISAID	2023-08-28	2023-08
hMPXV/Portugal/INSA-PT0772/2023	Portugal		2023-10-12	GISAID	2023-10-12	2023-10

Continued

Name	Country	Province	Collection date	Sources	Revised collection date for treetime	Revised month
hMPXV/Portugal/INSA-PT0787/2023	Portugal		2023-11-02	GISAID	2023-11-02	2023-11
hMPXV/Portugal/INSA-PT0768/2023	Portugal		2023-10-12	GISAID	2023-10-12	2023-10
hMPXV/Portugal/INSA-PT0767/2023	Portugal		2023-10-13	GISAID	2023-10-13	2023-10
hMPXV/Portugal/INSA-PT0757/2023	Portugal		2023-10-04	GISAID	2023-10-04	2023-10
hMPXV/Portugal/INSA-PT0734/2023	Portugal		2023-09-19	GISAID	2023-09-19	2023-09
hMPXV/Portugal/INSA-PT0806/2023	Portugal		2023-11-30	GISAID	2023-11-30	2023-11
hMPXV/Portugal/INSA-PT0759/2023	Portugal		2023-10-10	GISAID	2023-10-10	2023-10
hMPXV/Netherlands/un-EMC-NL092/2023	Netherlands		2023-12-18	GISAID	2023-12-18	2023-12
hMPXV/Portugal/INSA-PT0785/2023	Portugal		2023-10-31	GISAID	2023-10-31	2023-10
hMPXV/Portugal/INSA-PT0652/2023	Portugal		2023-07-19	GISAID	2023-07-19	2023-07
hMPXV/Netherlands/un-EMC-NL088/2023	Netherlands		2023-08-29	GISAID	2023-08-29	2023-08
hMPXV/Italy/PIE-OAS-59215348/2022	Italy		2022-09-05	GISAID	2022-09-05	2022-09
hMPXV/Netherlands/un-EMC-NL093/2023	Netherlands		2023-12-19	GISAID	2023-12-19	2023-12
hMPXV/Portugal/INSA-PT0794/2023	Portugal		2023-11-09	GISAID	2023-11-09	2023-11
hMPXV/Portugal/INSA-PT0809/2023	Portugal		2023-12-21	GISAID	2023-12-21	2023-12
hMPXV/Netherlands/un-EMC-NL098/2023	Netherlands		2023-12-19	GISAID	2023-12-19	2023-12
hMPXV/Italy/PIE-OAS-02591782/2022	Italy		2022-07-19	GISAID	2022-07-19	2022-07
hMPXV/Brazil/RS-CEVS-378/2023	Brazil		2023-11-08	GISAID	2023-11-08	2023-11
hMPXV/Brazil/SP-IAL-357531658/2024	Brazil		2024-02-28	GISAID	2024-02-28	2024-02
hMPXV/England/CDC_P3/2018	England		2018-09	GISAID	2018-09	2018-09
hMPXV/England/CDC_P2/2018	England		2018-09	GISAID	2018-09	2018-09
hMPXV/England/CDC_P1/2018	England		2018-09	GISAID	2018-09	2018-09
hMPXV/Nigeria/CBR-003/2019	Nigeria		2019-01-16	GISAID	2019-01-16	2019-01
hMPXV/Nigeria/CBR-053/2019	Nigeria		2019-07-01	GISAID	2019-07-01	2019-07
hMPXV/Singapore/CDC-01/2019	Singapore		2019	GISAID	2019	2019
hMPXV/Nigeria/CBR-052/2019	Nigeria		2019-06-08	GISAID	2019-06-08	2019-06
hMPXV/Israel/IIBR-01/2018	Israel		2018-10-04	GISAID	2018-10-04	2018-10
hMPXV/Brazil/SP-IAL-357514864/2024	Brazil		2024-02-22	GISAID	2024-02-22	2024-02
hMPXV/Nigeria/CBR-042/2019	Nigeria		2019-04-29	GISAID	2019-04-29	2019-04
hMPXV/Brazil/RJ-FIOCRUZ-10501/2024	Brazil		2024-05-14	GISAID	2024-05-14	2024-05
hMPXV/Hungary/NBL_63/2024	Hungary		2024-06-20	GISAID	2024-06-20	2024-06
hMPXV/Nigeria/CBR-040/2019	Nigeria		2019-04-29	GISAID	2019-04-29	2019-04
hMPXV/Brazil/PR-FIOCRUZ-10548/2024	Brazil		2024-07-19	GISAID	2024-07-19	2024-07
hMPXV/Brazil/RJ-FIOCRUZ-09217/2024	Brazil		2024-03-29	GISAID	2024-03-29	2024-03
hMPXV/United_Kingdom/UKHSA-0MZd8B_9000260/2022	United_Kingdom		2022-08	GISAID	2022-08	2022-08
hMPXV/Brazil/RJ-FIOCRUZ-10527/2024	Brazil		2024-08-16	GISAID	2024-08-16	2024-08
hMPXV/Brazil/RJ-FIOCRUZ-09216/2024	Brazil		2024-03-31	GISAID	2024-03-31	2024-03
hMPXV/Brazil/RJ-FIOCRUZ-09219/2024	Brazil		2024-04-08	GISAID	2024-04-08	2024-04
hMPXV/USA/IL-RIPHL-004-0142/2024	USA		2024-02-07	GISAID	2024-02-07	2024-02
hMPXV/Portugal/INSA-PT0815/2024	Portugal		2024-01-13	GISAID	2024-01-13	2024-01
hMPXV/Brazil/SP-IAL-357496487/2024	Brazil		2024-02-16	GISAID	2024-02-16	2024-02
hMPXV/Nigeria/CBR-039/2019	Nigeria		2019-04-29	GISAID	2019-04-29	2019-04

Continued

Name	Country	Province	Collection date	Sources	Revised collection date for treetime	Revised month
hMPXV/China/HZCDC-0001/2023	China	Zhejiang	2023-06-15	GISAID	2023-06-15	2023-06
hMPXV/Portugal/INSA-PT0814/2024	Portugal		2024-01-15	GISAID	2024-01-15	2024-01
hMPXV/Brazil/RJ-FIOCRUZ-09215/2024	Brazil		2024-03-29	GISAID	2024-03-29	2024-03
hMPXV/Japan/TMIPH-0260/2023	Japan		2023-09-16	GISAID	2023-09-16	2023-09
hMPXV/Portugal/INSA-PT0752/2023	Portugal		2023-10-03	GISAID	2023-10-03	2023-10
hMPXV/Brazil/SP-IAL-357531200/2024	Brazil		2024-02-27	GISAID	2024-02-27	2024-02
hMPXV/Portugal/INSA-PT0807/2023	Portugal		2023-12-27	GISAID	2023-12-27	2023-12
hMPXV/Portugal/INSA-PT0776/2023	Portugal		2023-10-20	GISAID	2023-10-20	2023-10
hMPXV/Portugal/INSA-PT0781/2023	Portugal		2023-10-26	GISAID	2023-10-26	2023-10
hMPXV/Brazil/SP-IAL-357983351/2024	Brazil		2024-10-08	GISAID	2024-10-08	2024-10
hMPXV/Brazil/SP-IAL-357911339/2024	Brazil		2024-08-23	GISAID	2024-08-23	2024-08
hMPXV/Portugal/INSA-PT0774/2023	Portugal		2023-10-18	GISAID	2023-10-18	2023-10
hMPXV/Brazil/BA-LACEN-293860175/2024	Brazil		2024-08-07	GISAID	2024-08-07	2024-08
hMPXV/Portugal/INSA-PT0691/2023	Portugal		2023-07-15	GISAID	2023-07-15	2023-07
hMPXV/Ireland/D-NVRL-Z22IRL00925/2023	Ireland		2023-10	GISAID	2023-10	2023-10
hMPXV/Ireland/D-NVRL-Z22IRL00922/2023	Ireland		2023-10	GISAID	2023-10	2023-10
hMPXV/Brazil/SP-IAL-357975925/2024	Brazil		2024-10-02	GISAID	2024-10-02	2024-10
hMPXV/Portugal/INSA-PT0773/2023	Portugal		2023-10-17	GISAID	2023-10-17	2023-10
hMPXV/Japan/TMIPH-0353/2024	Japan		2024-01-25	GISAID	2024-01-25	2024-01
hMPXV/Portugal/INSA-PT0747/2023	Portugal		2023-09-26	GISAID	2023-09-26	2023-09
hMPXV/Brazil/SP-IAL-357897692/2024	Brazil		2024-08-14	GISAID	2024-08-14	2024-08
hMPXV/Portugal/INSA-PT0655/2023	Portugal		2023-07-21	GISAID	2023-07-21	2023-07
hMPXV/Brazil/SP-IAL-357640019/2024	Brazil		2024-04-03	GISAID	2024-04-03	2024-04
hMPXV/Brazil/SP-IAL-357886830/2024	Brazil		2024-08-06	GISAID	2024-08-06	2024-08
hMPXV/Portugal/INSA-PT0702/2023	Portugal		2023-08-08	GISAID	2023-08-08	2023-08
hMPXV/Portugal/INSA-PT0703/2023	Portugal		2023-08-10	GISAID	2023-08-10	2023-08
hMPXV/Brazil/RJ-UG_UFRJ_0572/2024	Brazil		2024-08-27	GISAID	2024-08-27	2024-08
hMPXV/Brazil/SP-IAL-357821026/2024	Brazil		2024-06-18	GISAID	2024-06-18	2024-06
hMPXV/Portugal/INSA-PT0685/2023	Portugal		2023-07-13	GISAID	2023-07-13	2023-07
hMPXV/Brazil/RJ-FIOCRUZ-10490/2024	Brazil		2024-04-10	GISAID	2024-04-10	2024-04
hMPXV/Brazil/SP-IAL-357899878/2024	Brazil		2024-08-15	GISAID	2024-08-15	2024-08
hMPXV/Brazil/SP-IAL-357979688/2024	Brazil		2024-10-06	GISAID	2024-10-06	2024-10
hMPXV/Brazil/SP-IAL-357904928/2024	Brazil		2024-08-19	GISAID	2024-08-19	2024-08
hMPXV/Brazil/SP-IAL-357941922/2024	Brazil		2024-09-11	GISAID	2024-09-11	2024-09
hMPXV/Brazil/SP-IAL-357921858/2024	Brazil		2024-09-01	GISAID	2024-09-01	2024-09
hMPXV/Thailand/KCMH-459/2023	Thailand		2023-12-12	GISAID	2023-12-12	2023-12
hMPXV/Brazil/SP-IAL-357882670/2024	Brazil		2024-08-02	GISAID	2024-08-02	2024-08
hMPXV/Brazil/SP-IAL-357981172/2024	Brazil		2024-10-04	GISAID	2024-10-04	2024-10
hMPXV/Brazil/SP-IAL-357903818/2024	Brazil		2024-08-19	GISAID	2024-08-19	2024-08
hMPXV/Brazil/RJ-UG_UFRJ_0568/2024	Brazil		2024-08-15	GISAID	2024-08-15	2024-08
hMPXV/Australia/VIC-VIDRL-6948/2024	Australia		2024-05-06	GISAID	2024-05-06	2024-05
hMPXV/Brazil/PR-FIOCRUZ-10549/2024	Brazil		2024-07-20	GISAID	2024-07-20	2024-07

Continued

Name	Country	Province	Collection date	Sources	Revised collection date for treetime	Revised month
hMPXV/Thailand/KCMH-455/2023	Thailand		2023-12-01	GISAID	2023-12-01	2023-12
hMPXV/Brazil/SP-IAL-357802143/2024	Brazil		2024-06-06	GISAID	2024-06-06	2024-06
hMPXV/Brazil/SP-IAL-357792329/2024	Brazil		2024-06-02	GISAID	2024-06-02	2024-06
hMPXV/Cambodia/NPHL1211017/2023	Cambodia		2023-12-11	GISAID	2023-12-11	2023-12
hMPXV/USA/WA-UW-092809/2023	USA		2023-09	GISAID	2023-09	2023-09
hMPXV/South_Korea/KDCA-P019/2023	South_Korea		2023-04-19	GISAID	2023-04-19	2023-04
hMPXV/Brazil/SP-IAL-357798278/2024	Brazil		2024-06-04	GISAID	2024-06-04	2024-06
hMPXV/Brazil/SP-IAL-357899716/2024	Brazil		2024-08-15	GISAID	2024-08-15	2024-08
hMPXV/Portugal/INSA-PT0754/2023	Portugal		2023-10-04	GISAID	2023-10-04	2023-10
hMPXV/Brazil/RJ-UG_UFRJ_0554/2024	Brazil		2024-08-21	GISAID	2024-08-21	2024-08
hMPXV/Japan/TMIPH-0255/2024	Japan		2023-09-11	GISAID	2023-09-11	2023-09
hMPXV/Portugal/INSA-PT0751/2023	Portugal		2023-10-03	GISAID	2023-10-03	2023-10
hMPXV/USA/CA-LACPHL-MA00658/2024	USA		2024-07-24	GISAID	2024-07-24	2024-07
hMPXV/Brazil/SP-IAL-357944650/2024	Brazil		2024-09-15	GISAID	2024-09-15	2024-09
hMPXV/Brazil/SP-IAL-357933783/2024	Brazil		2024-09-08	GISAID	2024-09-08	2024-09
hMPXV/Brazil/SP-IAL-357914556/2024	Brazil		2024-08-26	GISAID	2024-08-26	2024-08
hMPXV/Brazil/SP-IAL-357994370/2024	Brazil		2024-10-16	GISAID	2024-10-16	2024-10
hMPXV/Portugal/INSA-PT0653/2023	Portugal		2023-07-21	GISAID	2023-07-21	2023-07
hMPXV/Brazil/SP-IAL-357949045/2024	Brazil		2024-09-17	GISAID	2024-09-17	2024-09
hMPXV/Brazil/SP-IAL-357929674/2024	Brazil		2024-09-04	GISAID	2024-09-04	2024-09
hMPXV/Brazil/RJ-FIOCRUZ-10502/2024	Brazil		2024-05-15	GISAID	2024-05-15	2024-05
hMPXV/Netherlands/un-EMC-NL110/2024	Netherlands		2024-08-07	GISAID	2024-08-07	2024-08
hMPXV/Brazil/SP-IAL-357928627/2024	Brazil		2024-09-04	GISAID	2024-09-04	2024-09
hMPXV/South_Korea/KDCA-P022/2023	South_Korea		2023-04-21	GISAID	2023-04-21	2023-04
hMPXV/Brazil/SP-IAL-357897410/2024	Brazil		2024-08-13	GISAID	2024-08-13	2024-08
hMPXV/Brazil/SP-IAL-357899889/2024	Brazil		2024-08-15	GISAID	2024-08-15	2024-08
hMPXV/Portugal/INSA-PT0716/2023	Portugal		2023-08-31	GISAID	2023-08-31	2023-08
hMPXV/Brazil/RJ-FIOCRUZ-10495/2024	Brazil		2024-05-02	GISAID	2024-05-02	2024-05
hMPXV/Brazil/SP-IAL-357909240/2024	Brazil		2024-08-21	GISAID	2024-08-21	2024-08
hMPXV/Brazil/RJ-UG_UFRJ_0553/2024	Brazil		2024-08-19	GISAID	2024-08-19	2024-08
hMPXV/Brazil/SP-IAL-357985080/2024	Brazil		2024-10-09	GISAID	2024-10-09	2024-10
hMPXV/Brazil/SP-IAL-357903632/2024	Brazil		2024-08-19	GISAID	2024-08-19	2024-08
hMPXV/Japan/TMIPH-220516/2023	Japan		2023-03-29	GISAID	2023-03-29	2023-03
hMPXV/Brazil/SP-IAL-357901450/2024	Brazil		2024-08-18	GISAID	2024-08-18	2024-08
hMPXV/Brazil/SP-IAL-357896065/2024	Brazil		2024-08-13	GISAID	2024-08-13	2024-08
hMPXV/South_Korea/KDCA-P006/2023	South_Korea		2023-04-06	GISAID	2023-04-06	2023-04
hMPXV/Japan/TMIPH-0318/2022	Japan		2023-01-25	GISAID	2023-01-25	2023-01
hMPXV/South_Korea/KDCA-P020/2023	South_Korea		2023-04-19	GISAID	2023-04-19	2023-04
hMPXV/Japan/TMIPH-220524/2023	Japan		2023-03-30	GISAID	2023-03-30	2023-03
hMPXV/South_Korea/KDCA-P010/2023	South_Korea		2023-04-13	GISAID	2023-04-13	2023-04
hMPXV/Brazil/SP-IAL-357903502/2024	Brazil		2024-08-19	GISAID	2024-08-19	2024-08
hMPXV/South_Korea/KDCA-P008/2023	South_Korea		2023-04-11	GISAID	2023-04-11	2023-04

Continued

Name	Country	Province	Collection date	Sources	Revised collection date for treetime	Revised month
hMPXV/South_Korea/KDCA-P032/2023	South_Korea		2023-04-25	GISAID	2023-04-25	2023-04
hMPXV/Japan/TMIPH-0019/2023	Japan		2023-04-11	GISAID	2023-04-11	2023-04
hMPXV/Japan/TMIPH-0047/2023	Japan		2023-04-19	GISAID	2023-04-19	2023-04
hMPXV/Japan/TMIPH-0076/2023	Japan		2023-04-28	GISAID	2023-04-28	2023-04
hMPXV/South_Korea/KDCA-P013/2023	South_Korea		2023-04-15	GISAID	2023-04-15	2023-04
hMPXV/Japan/TMIPH-0310/2022	Japan		2023-01-25	GISAID	2023-01-25	2023-01
hMPXV/Brazil/SP-IAL-357718239/2024	Brazil		2024-04-30	GISAID	2024-04-30	2024-04
hMPXV/South_Korea/KDCA-P029/2023	South_Korea		2023-04-23	GISAID	2023-04-23	2023-04
hMPXV/Japan/TMIPH-0342/2022	Japan		2023-02-09	GISAID	2023-02-09	2023-02
hMPXV/Japan/FKTMIPH-220343/2023	Japan		2023-02-13	GISAID	2023-02-13	2023-02
hMPXV/South_Korea/KDCA-P012/2023	South_Korea		2023-04-15	GISAID	2023-04-15	2023-04
hMPXV/Japan/TMIPH-230002/2023	Japan		2023-03-31	GISAID	2023-03-31	2023-03
hMPXV/Portugal/INSA-PT0633/2023	Portugal		2023-06-25	GISAID	2023-06-25	2023-06
hMPXV/Japan/TMIPH-0126/2023	Japan		2023-05-15	GISAID	2023-05-15	2023-05
hMPXV/Thailand/KCMH-465/2023	Thailand		2023-12-28	GISAID	2023-12-28	2023-12
hMPXV/South_Korea/KDCA-P030/2023	South_Korea		2023-04-23	GISAID	2023-04-23	2023-04
hMPXV/Japan/TMIPH-0325/2022	Japan		2023-01-30	GISAID	2023-01-30	2023-01
hMPXV/South_Korea/KDCA-P007/2023	South_Korea		2023-04-10	GISAID	2023-04-10	2023-04
hMPXV/South_Korea/KDCA-P034/2023	South_Korea		2023-04-25	GISAID	2023-04-25	2023-04
hMPXV/South_Korea/KDCA-P016/2023	South_Korea		2023-04-18	GISAID	2023-04-18	2023-04
hMPXV/South_Korea/NMC-P003/2023	South_Korea		2023-05-03	GISAID	2023-05-03	2023-05
hMPXV/Thailand/KCMH-296/2023	Thailand		2023-07-03	GISAID	2023-07-03	2023-07
hMPXV/South_Korea/KDCA-P027/2023	South_Korea		2023-04-22	GISAID	2023-04-22	2023-04
hMPXV/South_Korea/KDCA-P028/2023	South_Korea		2023-04-22	GISAID	2023-04-22	2023-04
hMPXV/South_Korea/KDCA-P021/2023	South_Korea		2023-04-21	GISAID	2023-04-21	2023-04
hMPXV/Indonesia/JK-NIHRD-MP044/2023	Indonesia		2023-10-25	GISAID	2023-10-25	2023-10
hMPXV/Japan/FKTMIPH-220304/2023	Japan		2023-01-23	GISAID	2023-01-23	2023-01
hMPXV/South_Korea/KDCA-P009/2023	South_Korea		2023-04-12	GISAID	2023-04-12	2023-04
hMPXV/Japan/TMIPH-0162/2023	Japan		2023-06-02	GISAID	2023-06-02	2023-06
hMPXV/Japan/TMIPH-220512/2023	Japan		2023-03-28	GISAID	2023-03-28	2023-03
hMPXV/Japan/TMIPH-220323/2023	Japan		2023-01-30	GISAID	2023-01-30	2023-01
hMPXV/South_Korea/KDCA-P011/2023	South_Korea		2023-04-14	GISAID	2023-04-14	2023-04
hMPXV/Japan/TMIPH-220357/2023	Japan		2023-02-20	GISAID	2023-02-20	2023-02
hMPXV/South_Korea/KDCA-P024/2023	South_Korea		2023-04-21	GISAID	2023-04-21	2023-04
hMPXV/Japan/TMIPH-0129/2023	Japan		2023-05-17	GISAID	2023-05-17	2023-05
hMPXV/South_Korea/KDCA-P018/2023	South_Korea		2023-04-18	GISAID	2023-04-18	2023-04
hMPXV/South_Korea/KDCA-P005/2023	South_Korea		2023-03-13	GISAID	2023-03-13	2023-03
hMPXV/USA/WA-UW-066957/2023	USA		2023-06	GISAID	2023-06	2023-06
hMPXV/Japan/TMIPH-0072/2023	Japan		2023-04-28	GISAID	2023-04-28	2023-04
hMPXV/Japan/TMIPH-0085/2023	Japan		2023-05-01	GISAID	2023-05-01	2023-05
hMPXV/Japan/TMIPH-220510/2023	Japan		2023-03-28	GISAID	2023-03-28	2023-03
hMPXV/Indonesia/JK-NIHRD-MP010/2023	Indonesia		2023-10-20	GISAID	2023-10-20	2023-10

Continued

Name	Country	Province	Collection date	Sources	Revised collection date for treetime	Revised month
hMPXV/Japan/TMIPH-0288/2023	Japan		2023-10-11	GISAID	2023-10-11	2023-10
hMPXV/Japan/TMIPH-0171/2023	Japan		2023-06-06	GISAID	2023-06-06	2023-06
hMPXV/South_Korea/KDCA-P015/2023	South_Korea		2023-04-18	GISAID	2023-04-18	2023-04
hMPXV/Japan/TMIPH-0082/2023	Japan		2023-05-01	GISAID	2023-05-01	2023-05
hMPXV/Japan/TMIPH-220531/2023	Japan		2023-03-31	GISAID	2023-03-31	2023-03
hMPXV/Thailand/KCMH-295/2023	Thailand		2023-07-03	GISAID	2023-07-03	2023-07
hMPXV/Japan/TMIPH-0112/2023	Japan		2023-05-11	GISAID	2023-05-11	2023-05
hMPXV/Japan/TMIPH-0144/2023	Japan		2023-05-20	GISAID	2023-05-20	2023-05
hMPXV/Japan/TMIPH-0017/2023	Japan		2023-04-06	GISAID	2023-04-06	2023-04
hMPXV/Brazil/SP-IAL-357981364/2024	Brazil		2024-10-07	GISAID	2024-10-07	2024-10
hMPXV/Japan/TMIPH-0267/2023	Japan		2023-09-22	GISAID	2023-09-22	2023-09
hMPXV/Thailand/KCMH-026/2023	Thailand		2023-05-12	GISAID	2023-05-12	2023-05
hMPXV/Brazil/SP-IAL-357934564/2024	Brazil		2024-09-09	GISAID	2024-09-09	2024-09
hMPXV/Philippines/RITM-007/2023	Philippines		2023-12-05	GISAID	2023-12-05	2023-12
hMPXV/Japan/TMIPH-0223/2023	Japan		2023-07-07	GISAID	2023-07-07	2023-07
hMPXV/India/DL-ICMR-MCL-174-40451050/2024	India		2024-09-09	GISAID	2024-09-09	2024-09
hMPXV/Brazil/RJ-UG_UFRJ_0552/2024	Brazil		2024-08-15	GISAID	2024-08-15	2024-08
hMPXV/South_Korea/KDCA-P017/2023	South_Korea		2023-04-18	GISAID	2023-04-18	2023-04
hMPXV/Japan/TMIPH-0100/2023	Japan		2023-05-06	GISAID	2023-05-06	2023-05
hMPXV/Brazil/SP-IAL-357909129/2024	Brazil		2024-08-19	GISAID	2024-08-19	2024-08
hMPXV/Netherlands/un-EMC-NL106/2024	Netherlands		2024-08-13	GISAID	2024-08-13	2024-08
hMPXV/Japan/TMIPH-0012/2023	Japan		2023-04-04	GISAID	2023-04-04	2023-04
hMPXV/Japan/TMIPH-0029/2023	Japan		2023-04-17	GISAID	2023-04-17	2023-04
hMPXV/Brazil/SP-IAL-357980969/2024	Brazil		2024-09-30	GISAID	2024-09-30	2024-09
hMPXV/Japan/TMIPH-0204/2023	Japan		2023-06-26	GISAID	2023-06-26	2023-06
hMPXV/Japan/TMIPH-0113/2023	Japan		2023-05-12	GISAID	2023-05-12	2023-05
hMPXV/Japan/TMIPH-0109/2023	Japan		2023-05-11	GISAID	2023-05-11	2023-05
hMPXV/Brazil/SP-IAL-357981061/2024	Brazil		2024-10-06	GISAID	2024-10-06	2024-10
hMPXV/China/GDCDC_GZ_M23050/2023	China	Guangdong	2023/6/16	GenBase	2023-06-16	2023-06
hMPXV/China/GDCDC_GZ_M23011/2023	China	Guangdong	2023/6/7	GenBase	2023-06-07	2023-06
hMPXV/China/SKLID_ZJU-10/2023	China	Guangdong	2023	GenBase	2023	2023
hMPXV/Brazil/SP-IAL-357938508/2024	Brazil		2024-09-10	GISAID	2024-09-10	2024-09
hMPXV/Brazil/SP-IAL-357890330/2024	Brazil		2024-08-07	GISAID	2024-08-07	2024-08
hMPXV/Brazil/RJ-FIOCRUZ-10505/2024	Brazil		2024-05-16	GISAID	2024-05-16	2024-05
hMPXV/Portugal/INSA-PT0803/2023	Portugal		2023-11-28	GISAID	2023-11-28	2023-11
hMPXV/Brazil/RJ-UG_UFRJ_0551/2024	Brazil		2024-08-09	GISAID	2024-08-09	2024-08
hMPXV/China/GDCDC_FS_M23108/2023	China	Guangdong	2023/6/22	GenBase	2023-06-22	2023-06
hMPXV/China/SZPMI-041/2023	China	Guangdong	2023/7/13	GenBase	2023-07-13	2023-07
hMPXV/Brazil/SP-IAL-357911479/2024	Brazil		2024-08-24	GISAID	2024-08-24	2024-08
hMPXV/Brazil/SP-IAL-357996884/2024	Brazil		2024-10-18	GISAID	2024-10-18	2024-10
hMPXV/China/SZPMI-038/2023	China	Guangdong	2023/7/7	GenBase	2023-07-07	2023-07
hMPXV/China/SZPMI-016/2023	China	Guangdong	2023/6/21	GenBase	2023-06-21	2023-06

Continued

Name	Country	Province	Collection date	Sources	Revised collection date for treetime	Revised month
hMPXV/Portugal/INSA-PT0764/2023	Portugal		2023-10-13	GISAID	2023-10-13	2023-10
hMPXV/China/SZPMI-048/2023	China	Guangdong	2023/7/16	GenBase	2023-07-16	2023-07
hMPXV/China/Guangdong01-BS/2023	China	Guangdong	2023/6/1	GenBase	2023-06-01	2023-06
hMPXV/Portugal/INSA-PT0770/2023	Portugal		2023-10-12	GISAID	2023-10-12	2023-10
hMPXV/China/SZPMI-056/2023	China	Guangdong	2023/7/25	GenBase	2023-07-25	2023-07
hMPXV/China/SZPMI-076/2023	China	Guangdong	2023/8/14	GenBase	2023-08-14	2023-08
hMPXV/China/SZPMI-049/2023	China	Guangdong	2023/7/12	GenBase	2023-07-12	2023-07
hMPXV/China/SZPMI-043/2023	China	Guangdong	2023/7/14	GenBase	2023-07-14	2023-07
hMPXV/China/GDCDC_GZ_M23008/2023	China	Guangdong	2023/6/8	GenBase	2023-06-08	2023-06
hMPXV/China/SZPMI-024/2023	China	Guangdong	2023/7/2	GenBase	2023-07-02	2023-07
hMPXV/China/SZPMI-069/2023	China	Guangdong	2023/8/4	GenBase	2023-08-04	2023-08
hMPXV/China/SZPMI-032/2023	China	Guangdong	2023/7/2	GenBase	2023-07-02	2023-07
hMPXV/China/SKLID_ZJU-04/2023	China	Zhejiang	2023/7/28	GenBase	2023-07-28	2023-07
hMPXV/China/SZPMI-021/2023	China	Guangdong	2023/7/2	GenBase	2023-07-02	2023-07
hMPXV/China/SZPMI-004/2023	China	Guangdong	2023/6/16	GenBase	2023-06-16	2023-06
hMPXV/China/SKLID_ZJU-01/2023	China	Zhejiang	2023/7/17	GenBase	2023-07-17	2023-07
hMPXV/China/SZPMI-051/2023	China	Guangdong	2023/7/19	GenBase	2023-07-19	2023-07
hMPXV/China/SKLID_ZJU-09/2023	China	Guangdong	2023	GenBase	2023	2023
hMPXV/China/SZPMI-026/2023	China	Guangdong	2023/7/1	GenBase	2023-07-01	2023-07
hMPXV/China/SZPMI-035/2023	China	Guangdong	2023/7/5	GenBase	2023-07-05	2023-07
hMPXV/China/SZPMI-085/2023	China	Guangdong	2023/8/29	GenBase	2023-08-29	2023-08
hMPXV/China/SZPMI-008/2023	China	Guangdong	2023/6/13	GenBase	2023-06-13	2023-06
hMPXV/China/SZPMI-023/2023	China	Guangdong	2023/7/10	GenBase	2023-07-10	2023-07
hMPXV/China/SZPMI-005/2023	China	Guangdong	2023/6/16	GenBase	2023-06-16	2023-06
hMPXV/China/SZPMI-045/2023	China	Guangdong	2023/7/15	GenBase	2023-07-15	2023-07
hMPXV/China/SKLID_ZJU-03/2023	China	Zhejiang	2023/7/25	GenBase	2023-07-25	2023-07
hMPXV/China/SZPMI-028/2023	China	Guangdong	2023/6/29	GenBase	2023-06-29	2023-06
hMPXV/China/SZPMI-018/2023	China	Guangdong	2023/6/27	GenBase	2023-06-27	2023-06
hMPXV/China/SZPMI-039/2023	China	Guangdong	2023/7/11	GenBase	2023-07-11	2023-07
hMPXV/China/SZPMI-017/2023	China	Guangdong	2023/6/26	GenBase	2023-06-26	2023-06
hMPXV/China/SZPMI-066/2023	China	Guangdong	2023/7/31	GenBase	2023-07-31	2023-07
hMPXV/China/SZPMI-059/2023	China	Guangdong	2023/7/24	GenBase	2023-07-24	2023-07
hMPXV/China/SZPMI-033/2023	China	Guangdong	2023/6/30	GenBase	2023-06-30	2023-06
hMPXV/China/SZPMI-025/2023	China	Guangdong	2023/6/29	GenBase	2023-06-29	2023-06
hMPXV/China/SZPMI-029/2023	China	Guangdong	2023/6/30	GenBase	2023-06-30	2023-06
hMPXV/China/SZPMI-036/2023	China	Guangdong	2023/6/30	GenBase	2023-06-30	2023-06
hMPXV/China/SZPMI-015/2023	China	Guangdong	2023/6/21	GenBase	2023-06-21	2023-06
hMPXV/China/SZPMI-060/2023	China	Guangdong	2023/7/28	GenBase	2023-07-28	2023-07
hMPXV/China/SZPMI-040/2023	China	Guangdong	2023/7/16	GenBase	2023-07-16	2023-07
hMPXV/China/SZPMI-078/2023	China	Guangdong	2023/8/20	GenBase	2023-08-20	2023-08
hMPXV/China/SZPMI-072/2023	China	Guangdong	2023/8/14	GenBase	2023-08-14	2023-08
hMPXV/China/SZPMI-057/2023	China	Guangdong	2023/7/31	GenBase	2023-07-31	2023-07

Continued

Name	Country	Province	Collection date	Sources	Revised collection date for treetime	Revised month
hMPXV/China/SZPMI-013/2023	China	Guangdong	2023/6/19	GenBase	2023-06-19	2023-06
hMPXV/China/SZPMI-065/2023	China	Guangdong	2023/8/5	GenBase	2023-08-05	2023-08
hMPXV/China/SZPMI-031/2023	China	Guangdong	2023/6/30	GenBase	2023-06-30	2023-06
hMPXV/China/SZPMI-022/2023	China	Guangdong	2023/7/2	GenBase	2023-07-02	2023-07
hMPXV/China/SZPMI-006/2023	China	Guangdong	2023/6/14	GenBase	2023-06-14	2023-06
hMPXV/China/SZPMI-037/2023	China	Guangdong	2023/7/1	GenBase	2023-07-01	2023-07
hMPXV/China/SZPMI-073/2023	China	Guangdong	2023/8/12	GenBase	2023-08-12	2023-08
hMPXV/China/SZPMI-030/2023	China	Guangdong	2023/6/30	GenBase	2023-06-30	2023-06
hMPXV/China/SZPMI-058/2023	China	Guangdong	2023/7/24	GenBase	2023-07-24	2023-07
hMPXV/China/SZPMI-077/2023	China	Guangdong	2023/8/14	GenBase	2023-08-14	2023-08
hMPXV/China/SZPMI-095/2023	China	Guangdong	2023/10/14	GenBase	2023-10-14	2023-10
hMPXV/China/SZPMI-061/2023	China	Guangdong	2023/7/29	GenBase	2023-07-29	2023-07
hMPXV/China/SZPMI-009/2023	China	Guangdong	2023/6/21	GenBase	2023-06-21	2023-06
hMPXV/China/SZPMI-050/2023	China	Guangdong	2023/7/13	GenBase	2023-07-13	2023-07
hMPXV/China/SZPMI-074/2023	China	Guangdong	2023/10/10	GenBase	2023-10-10	2023-10
hMPXV/China/SZPMI-027/2023	China	Guangdong	2023/6/30	GenBase	2023-06-30	2023-06
hMPXV/China/SZPMI-088/2023	China	Guangdong	2023/9/12	GenBase	2023-09-12	2023-09
hMPXV/China/SZPMI-054/2023	China	Guangdong	2023/7/24	GenBase	2023-07-24	2023-07
hMPXV/China/SKLID_ZJU-05/2023	China	Zhejiang	2023/7/31	GenBase	2023-07-31	2023-07
hMPXV/China/SZPMI-071/2023	China	Guangdong	2023/8/4	GenBase	2023-08-04	2023-08
hMPXV/China/SZPMI-007/2023	China	Guangdong	2023/6/10	GenBase	2023-06-10	2023-06
hMPXV/China/SZPMI-083/2023	China	Guangdong	2023/8/27	GenBase	2023-08-27	2023-08
hMPXV/China/SKLID_ZJU-07/2023	China	Guangdong	2023	GenBase	2023	2023
hMPXV/China/SZPMI-020/2023	China	Guangdong	2023/6/27	GenBase	2023-06-27	2023-06
hMPXV/China/Beijing01-OS/2023	China	Beijing	2023/6/1	GenBase	2023-06-01	2023-06
hMPXV/China/SKLID_ZJU-08/2023	China	Guangdong	2023	GenBase	2023	2023
hMPXV/China/SZPMI-063/2023	China	Guangdong	2023/8/1	GenBase	2023-08-01	2023-08
hMPXV/China/Beijing01-BS/2023	China	Beijing	2023/6/1	GenBase	2023-06-01	2023-06
hMPXV/China/SZPMI-067/2023	China	Guangdong	2023/7/29	GenBase	2023-07-29	2023-07
hMPXV/China/SZPMI-019/2023	China	Guangdong	2023/6/27	GenBase	2023-06-27	2023-06
hMPXV/China/SZPMI-034/2023	China	Guangdong	2023/7/2	GenBase	2023-07-02	2023-07
hMPXV/China/SZPMI-092/2023	China	Guangdong	2023/10/7	GenBase	2023-10-07	2023-10
hMPXV/China/SZPMI-047/2023	China	Guangdong	2023/7/14	GenBase	2023-07-14	2023-07
hMPXV/China/SKLID_ZJU-06/2023	China	Guangdong	2023	GenBase	2023	2023
hMPXV/China/SKLID_ZJU-02/2023	China	Zhejiang	2023/7/25	GenBase	2023-07-25	2023-07
hMPXV/China/SZPMI-046/2023	China	Guangdong	2023/7/12	GenBase	2023-07-12	2023-07
hMPXV/China/SZPMI-052/2023	China	Guangdong	2023/7/19	GenBase	2023-07-19	2023-07
hMPXV/China/SZPMI-094/2023	China	Guangdong	2023/10/10	GenBase	2023-10-10	2023-10
hMPXV/China/SZPMI-062/2023	China	Guangdong	2023/7/29	GenBase	2023-07-29	2023-07
hMPXV/China/SZPMI-080/2023	China	Guangdong	2023/8/30	GenBase	2023-08-30	2023-08
hMPXV/China/SZPMI-053/2023	China	Guangdong	2023/7/19	GenBase	2023-07-19	2023-07
hMPXV/China/SZPMI-002/2023	China	Guangdong	2023/6/12	GenBase	2023-06-12	2023-06

Continued

Name	Country	Province	Collection date	Sources	Revised collection date for treetime	Revised month
hMPXV/China/SZPMI-011/2023	China	Guangdong	2023/6/17	GenBase	2023-06-17	2023-06
hMPXV/China/GDCDC_FS_M23028/2023	China	Guangdong	2023/6/13	GenBase	2023-06-13	2023-06
hMPXV/China/SZPMI-075/2023	China	Guangdong	2023/8/17	GenBase	2023-08-17	2023-08
hMPXV/China/SZPMI-012/2023	China	Guangdong	2023/6/18	GenBase	2023-06-18	2023-06

Preplanned Studies

Cost-effectiveness Assessment of A Smart Health Education Pillbox for Canine Echinococcosis Control During A Cluster-Randomized Trial — Western China, 2023–2024

Shijie Yang[1]; Chenqing Sun[1]; Ning Xiao[1]; Shuai Han[1]; Liying Wang[1]; Ying Wang[1]; Jiangshan Zhao[2]; Shanglin Wu[3]; Xiao Ma[4]; Yu Feng[5]; Benfu Li[6]; Tongmin Wang[7]; Yuhua Li[8]; Yuancheng Yang[8]; Kaisaier Tuerxunjiang[2]; Zonglin Shen[8]; Xiao-nong Zhou[1,#]

Summary

What is already known about this topic?

Echinococcosis remains a significant zoonotic threat in western China, with canines serving as the primary reservoir for *Echinococcus* transmission. Despite monthly praziquantel (PZQ) deworming programs, challenges in compliance persist in remote pastoral regions due to logistical constraints.

What is added by this report?

The smart health education pillbox (SHEP) demonstrated a 22.62% reduction in the overall cost of dog deworming, an increase of 52.59% in the proportion of dogs receiving the recommended annual deworming frequency of 9–12 times, a 35.45% decrease in the risk of *Echinococcus* infection, and a 1.55-fold higher protective efficacy against canine echinococcosis transmission compared to conventional manual deworming (CMD) approaches.

What are the implications for public health practice?

These results indicate that SHEP reduces labor costs and mitigates echinococcosis transmission risk, highlighting its potential as a valuable tool for disease control.

ABSTRACT

Introduction: Echinococcosis is a zoonotic parasitic disease that necessitates regular deworming of canines. The efficacy of the conventional manual deworming (CMD) is impeded by geography, the workforce, and severe weather conditions. This study evaluated the effectiveness and cost-effectiveness of the smart health education pillbox (SHEP) compared to CMD in canine echinococcosis control.

Methods: A 12-month cluster randomized trial was conducted across nine endemic Chinese counties, where townships were randomly assigned to either the SHEP or CMD group. The primary outcomes included *Echinococcus* antigen positivity rates in dog feces, deworming frequency, and cost components. Data analysis was conducted using SPSS 27.0, employing Generalized Estimating Equations (GEE), odds ratios (*OR*), relative risk (*RR*), relative risk reduction (*RRR*), and protective efficacy (1/*RR*).

Results: SHEP implementation significantly reduced *Echinococcus* infection risk by 35.45% and demonstrated 1.55-fold higher protective efficacy than CMD. The total deworming costs decreased by 22.62%, with substantial savings in personnel (53.15%), transportation (79.48%), and operational time requirements (30.13%). The proportion of dogs that achieved the target annual deworming frequency (9–12 times) increased from 51.89% to 91.38%, representing a relative improvement of 52.59%.

Conclusion: SHEP, which integrates automated reminders of praziquantel (PZQ) tablet delivery, is a promising tool for diminishing resource utilization and mitigating *Echinococcus* transmission in endemic areas.

Echinococcosis, a zoonotic parasitic disease designated by the World Health Organization as a neglected tropical disease, manifests predominantly in cystic (CE) and alveolar (AE) forms, caused by *Echinococcus granulosus sensu lato* and *E. multilocularis*, respectively. Both forms impose substantial public health burdens, with dogs serving as the definitive hosts for transmission. Despite the nationwide monthly praziquantel (PZQ) deworming initiative for dogs implemented in China in 2006, which led to a decrease in canine fecal antigen prevalence from 4.25% to 0.50% (*1–2*), persistent operational obstacles such as veterinary workforce shortages, logistical barriers, and

financial constraints in remote regions persistently impede consistent deworming coverage and frequency. Surveys have revealed suboptimal deworming frequency (ranging from 21.7%–68.9%) (*3*–*6*) as a key factor contributing to sustained high rates of canine infection (ranging from 0.15%–1.60%) (*2*). These fluctuations in infection rates contribute to ongoing environmental transmission risks. Therefore, there is a need to explore novel approaches to enhance adherence to canine deworming regimens and mitigate environmental contamination.

From 2023 to 2024, a 12-month cluster randomized trial was conducted across nine endemic counties: Xiji County, Ningxia Hui Autonomous Region, Yushu City, Qinghai Province; Emin County, Hejing County, Artux City, Qapqal Xibe Autonomous County, Xinjiang Uygur Autonomous Region; Shangri-La City, Yunnan Province; Tianzhu Xizang Autonomous County, Gansu Province; and Fourth Division, Xinjiang Production and Construction Corps. Within each county, two townships were randomly assigned to interventions: one to the smart health education pillbox (SHEP) group and the other to the conventional manual deworming (CMD) group, with 150 eligible households with dogs randomly selected as study participants in each group. The SHEP group received an automated SHEP reminder and dog owner deworming scheme, where each targeted household received a pre-programmed SHEP and a deworming schedule (e.g., monthly deworming on the 5th day of each month, totaling 12 times annually). On designated deworming days, the SHEP delivered five sequential one-minute reminders combining auditory prompts ("Owner, please administer deworming PZQ chewable tablet to your dog") and visual cues (flashing red indicator light). Successful completion of all five steps — 1) opening the SHEP lid, 2) removing the PZQ chewable tablets, 3) administering them to the dog, 4) returning unused tablets to the compartment, and 5) closing the lid — is necessary to activate the green light and receive an auditory acknowledgment ("Congratulations! The deworming work has been successfully completed"). Failure to execute all five steps within the scheduled day (e.g., due to dog owner absence) would activate persistent reminders for three consecutive days. In the CMD group, conventional manual deworming procedures were followed in which health workers (veterinarians) from the township or village visited households on scheduled deworming dates to administer door-to-door PZQ chewable tablets. Additionally, stratified training, including canine fecal testing and questionnaire administration, was conducted for all participants across both the SHEP and CMD cohorts.

The primary indicators included the *Echinococcus* antigen-positive rate in dog feces, deworming frequency, and cost components. Data analysis was conducted using SPSS (version 27.0, IBM Corp., NY, USA), employing Generalized Estimating Equations (GEE), odds ratios (*OR*), relative risk (*RR*), relative risk reduction (*RRR*), and protective efficacy (1/*RR*). The distribution of deworming frequencies between groups was assessed using the Cochran-Armitage test, employing two-tailed testing, with statistical significance set at $P<0.05$.

Dog fecal samples were collected twice from each enrolled dog in both groups: at baseline in 2023 and at a 12-month follow-up in 2024. Copro-ELISA was performed at 9 county CDC locations. Baseline fecal testing of 2,643 samples (SHEP group: 1,310; CMD group: 1,333) revealed no significant intergroup variance in *Echinococcus* antigen positivity (*OR*=0.86, [95% confidence interval (*CI*): 0.30, 2.48, *P*=0.78]. At the 12-month follow-up (2,270 samples: SHEP group, 1,169; CMD group: 1,101), no significant efficacy difference was observed between the two groups (*OR*=0.74, 95% *CI*: 0.18, 3.04, *P*=0.68). Both groups demonstrated significant risk reduction compared to the baseline (SHEP group: *OR*=0.273, 95% *CI*: 0.04, 0.96, *P*=0.048; CMD group: *OR*=0.30, 95% *CI*: 0.11, 0.80, *P*=0.016). GEE accounting for repeated measures and cluster effects (9 counties) indicated that the SHEP group yielded a 35.45% greater risk reduction than the CMD group (*RRR*=35.45%, 95% *CI*: –63.78%, –15.21%), with a protective efficacy ratio (1/*RR*) of 1.55-fold (95% *CI*: 0.75, 0.97, *P*=0.046) (Table 1).

At the 12-month follow-up, the deworming frequency in the SHEP group was assessed by enumerating residual PZQ chewable tablets in the SHEP compartments, while in the CMD group, cross-verification of township/village health worker (veterinarian) deworming logs against dog owner interview records was performed. Furthermore, SHEP functionality was monitored, and the annual 12 PZQ tablets were replenished in the SHEP group (each SHEP had a three-year service period). Statistical analysis using the Cochran–Armitage test revealed a significantly higher deworming frequency in the SHEP group than in the CMD group ($Z=16.78$, $P<0.001$). All frequency bands showed significant differences

TABLE 1. *OR* for *Echinococcus* antigen in fecal samples between SHEP and CMD groups at baseline and 12-month follow-up in nine endemic counties, 2023–2024.

Site of fecal collection	Function of sample	Date of collection	SHEP automated reminder + dog owner deworming		Door-to-door deworming by township/village health workers		*OR*	95% *CI*	*P*
			Number tested	Positive rate, % (positive number)	Number tested	Positive rate, % (positive number)			
The Fourth Division	Baseline	2023-10	138	0	150	0 (0)			
	Follow-up	2024-11	113	0	124	0			
Xiji County	Baseline	2023-10	150	0	150	0			
	Follow-up	2024-12	113	0	110	0			
Hejing County	Baseline	2023-11	150	0	150	0			
	Follow-up	2024-12	150	0.67 (1)	150	0.67 (1)			
Qapqal Xibe Autonomous County	Baseline	2023-11	150	1.33 (2)	150	2.00 (3)			
	Follow-up	2024-12	118	0	111	0.90 (1)			
Emin County	Baseline	2023-11	150	0	150	0			
	Follow-up	2024-12	131	0	85	0			
Artux City	Baseline	2023-11	150	0	138	0			
	Follow-up	2024-12	124	0	84	0			
Shangri-La City	Baseline	2023-11	132	0.76 (1)	150	0			
	Follow-up	2024-12	132	0	150	0			
Yushu City	Baseline	2023-09	140	1.43 (2)	145	1.38 (2)			
	Follow-up	2024-10	140	0	144	0			
Tianzhu Xizang Autonomous County	Baseline	2023-10	150	2.00 (3)	150	1.33 (2)			
	Follow-up	2024-10	148	0	143	0			
Total	Baseline	2023	1,310	0.61(8)	1,333	0.53 (7)	0.86	0.30, 2.48	0.78
	Follow-up	2024	1,169	0.09(1)	1,101	0.18 (2)	0.74	0.18, 3.04	0.68

Abbreviations: *OR*=odds ratio; *CI*=confidence interval; SHEP=Smart Health Education Pillbox; CMD=conventional manual deworming.

TABLE 2. *OR*, *RR*, and *RRR* of deworming frequency distribution between SHEP and CMD groups for PZQ chewable tablet delivery in nine endemic counties, 2023–2024.

Residual PZQ chewable tablets (tab)	Deworming frequency (times/year)	SHEP automated reminder +dog owner deworming (%, *n*)	Door-to-door deworming by township/village health workers (%, *n*)	*OR*	95% *CI*	*P*	*RR*	*RRR* (%)
0−3	9−12	91.38 (933/1,021)	59.89 (557/930)	6.61	5.41, 8.08	<0.001	1.526	−52.59
4−8	4−8	7.44 (76/1,021)	16.88 (157/930)	0.40	0.31, 0.52	<0.001	0.441	55.87
9−12	0−3	1.08 (11/1,021)	23.23 (216/930)	0.04	0.02, 0.07	<0.001	0.046	95.35

Note: Each SHEP contained 12 PZQ chewable tablets, and the compulsory deworming frequency was once a month, 12 times a year.
Abbreviation: OR=odds ratio; RR=relative risk; RRR=relative risk reduction; *CI*=confidence interval; SHEP=smart health education pillbox; CMD=conventional manual deworming; PZQ=praziquantel.

(*P*<0.001), with SHEP achieving a 52.59% increase in high-frequency adherence (9–12 times/year; *OR*=6.61, 95% *CI*: 5.41, 8.08) and a 95.35% reduction in low-frequency risk (≤3 times/year, *OR*=0.036, 95% *CI*: 0.02, 0.07) (Table 2).

Throughout the study, expenses related to materials, personnel, transportation, and time allocation for the delivery of PZQ chewable tablets were meticulously documented. The SHEP yielded a 22.62% reduction in the overall cost of dog deworming, resulting in annual savings of 53.15% in labor costs, 79.48% in transportation costs, 30.13% in time costs and the commuting efficiency increased by 83.33% (Table 3).

DISCUSSION

The persistence of canine echinococcosis, despite China's nationwide monthly deworming program

TABLE 3. Expenditures on PZQ chewable tablets delivered for SHEP and CMD groups in nine endemic counties, 2023–2024.

Groups	Delivery methods	SHEP (CNY/year)*	PZQ chewable tablets (CNY/year) †	Manpower (CNY/year) §	Transportation (CNY/year) ¶	Total cost (CNY, dog /year) **	Cost per deworming (CNY, time/dog) ††	Total time (hour, dog/year) §§	Time per deworming (hours, dog /time) ††	Total commuting times per year	Saved commuting times per year
SHEP group	SHEP automated reminder + dog owner deworming	38.33	11.4	17.54	10.64	77.91	6.49	1.09	0.09	2	10
CMD group	Door-to-door deworming by township/village health workers	0	11.4	37.44	51.84	100.68	8.39	1.56	0.13	12	0

Abbreviation: CNY=Chinese Yuan; SHEP=smart health education pillbox; CMD=conventional manual deworming; PZQ=praziquantel.

* According to the market price, each SHEP is priced at 115 yuan, with a service life of three years and 12 deworming reminders per year (once a month); the annual depreciation cost is 38.33 yuan.

† According to the market bidding price, each commercially available PZQ chewable tablet costs 0.95 yuan, and each dog requires 12 tablets annually.

§ Based on the 2024 statistical yearbooks of nine counties, the average wages of health and veterinary personnel and residents' incomes were estimated, including the labor cost of township doctors and village deworming personnel, who worked 22 days a month for 8 hours each day.

¶ Estimated according to the average depreciation cost of vehicles and fuel expenses in these nine counties at the end of 2024, including the number of visits to rural areas and households.

** This includes the cost of SHEP and PZQ chewable tablets, manpower, and transportation.

†† Compulsory deworming frequency was once a month, 12 times a year.

§§ The time cost includes the commuting time of township doctors and village deworming personnel.

initiated in 2006, highlights systemic challenges. While the prevalence of antigens in dogs has decreased from 4.25% (*1*) to 0.50% (*2*), achieving the WHO's advocated dog infection rate targets (<0.01%) remains a formidable task (*7*). Conventional manual door-to-door deworming efforts by township/village health workers encounter persistent obstacles, such as geographic isolation, severe weather conditions, and shortages of veterinary professionals in endemic regions such as Xinjiang and Qinghai. Deworming frequency adherence — ranging from 21.7% to 47.5% (*3*,*6*) (12 times per year) — and deworming coverage in individual townships, varying from 24% to 84% in Ningxia (*4*), illustrate the challenges faced. Moreover, cultural customs (e.g., non-harm principles), strong human-dog relationships, and limited health literacy impede compliance, while issues such as overreported deworming records by health workers (veterinarians) lead to data inaccuracies. These factors contribute to sustained environmental egg contamination, with canine infection rates persistently fluctuating between 0.15% and 1.60% across the endemic provincial-level administrative divisions (PLADs) (*2*).

The SHEP addresses these gaps using a multifaceted approach. Its automated reminder system, featuring monthly light and voice alerts that persist for three days if unacknowledged, mitigates forgetfulness and seasonal mobility (e.g., pastoral transhumance). The dedicated compartment prevents PZQ chewable tablet loss, which is a critical failure point in dog-owner-administered programs. Additionally, daily health broadcasts enhance dog owners' awareness and facilitate the transition from mere knowledge of control measures to the adoption of healthy behaviors, countering cultural resistance by emphasizing the link between deworming and the reduction of zoonotic risks. This integrated design aligns with the One Health principle, concurrently targeting behavioral, logistical, and educational obstacles.

This trial highlights the superior efficacy of SHEP on both fronts. SHEP reduced canine *Echinococcus* antigen positivity to 0.09% (compared to 0.18% in conventional delivery; *OR*=0.273, 95% *CI*: 0.040–0.960), achieving near-elimination levels. This significant reduction in infected dogs was presumed to decrease environmental egg contamination by approximately 2.1 million eggs/dog annually, considering that each infected dog sheds approximately 40,000 eggs daily during peak transmission seasons (*8*–*9*). The resulting decline in soil egg burdens reduced human exposure risk, driving the basic

reproduction number (R_0) below 1.0 when canine prevalence falls below 0.1%. SHEP interrupts sustained transmission cycles and aligns with the WHO elimination objectives through source-level decontamination. From an economic standpoint, SHEP significantly improved the deworming frequency distribution, achieving a high adherence rate of 91.38% (9–12 times/year), compared to 59.89% with door-to-door manual delivery. The 6.6-fold increase in the odds of optimal adherence indicated that automated reminders effectively addressed habitual noncompliance, leading to a 95.35% reduction in low-frequency deworming risks. These improvements were realized alongside an 83.33% increase in commuting efficiency, and notable reductions of 53.15%, 79.48%, and 30.13% in labor, transportation, and time costs, respectively. These advancements are particularly crucial for regions with limited personnel and resources, such as highland pastoral areas. The 22.6% cost savings achieved by SHEP facilitate its scalable deployment in hyper-endemic areas, such as Qinghai and Sichuan. The adherence efficacy of SHEP aligns with the WHO's emphasis on sustaining deworming frequency and effectively supports the control objectives outlined in the "National Implementation Plan for Comprehensive Prevention and Control of Echinococcosis and Other Key Parasitic Diseases (2024–2030)" (*10*).

This study had several limitations. First, the assumed 3-year device lifespan requires field validation. Additionally, corrosion or damage in extreme environments may increase long-term costs. Second, the deworming frequency adherence in the CMD group relied on unverified self-reporting. Finally, factors, such as county variability, dog attrition within the target population, and limited temporal sampling, may have introduced bias into the estimates. Future iterations should focus on product optimization, integration of deworming strategies, and implementation of spatiotemporal covariance structures through stratified models and multiple imputations to address these limitations and enhance canine echinococcosis control measures.

In conclusion, the SHEP effectively addresses the fundamental challenges associated with conventional deworming practices by promoting verifiable and cost-efficient adherence. By targeting the crucial dog-human-animal interface, SHEP directly interrupts the transmission cycle, providing a scalable solution to attain a sub-0.01% canine infection target. This is recommended as the preferred intervention to improve dog deworming adherence. The integration of SHEP into national programs has the potential to optimize resource utilization and expedite efforts towards the elimination of echinococcosis.

Conflicts of interest: No conflicts of interest.

Acknowledgements: The Shangri-La CDC, Xiji County CDC, Emin County CDC, Hejing County CDC, Artux City CDC, Yushu Xizang Autonomous Prefecture CDC, Qapqal Xibe Autonomous County CDC, and the Disease Control and Prevention Center of the Fourth Division of Xinjiang Production and Construction Corps for distributing the Smart Health Education Pillboxes and facilitating on-site dog fecal collection and testing. We also thank all the participants for contributing their time and support to this study.

Ethical statement: Approval by the National Institute of Parasitic Diseases, China CDC (Ethical Review Committee No. 2021019)

Funding: Supported by National Key Research and Development Program of China [grant numbers 2021YFC2300800 and 2021YFC2300804].

doi: 10.46234/ccdcw2025.199

Corresponding author: Xiaonong Zhou, zhouxn1@chinacdc.cn.

[1] National Institute of Parasitic Diseases, Chinese Center for Disease Control and Prevention (Chinese Center for Tropical Diseases Research), National Key Laboratory of Intelligent Tracking and Forecasting for Infectious Diseases, National Health Commission Key Laboratory on Parasite and Vector Biology, WHO Centre for Tropical Diseases, National Center for International Research on Tropical Diseases, Ministry of Science and Technology, Shanghai, China; [2] Xinjiang Uygur Autonomous Region Center for Disease Control and Prevention, Urumqi City, Xinjiang Uygur Autonomous Region, China; [3] Ningxia Hui Autonomous Region Center for Disease Control and Prevention, Yinchuan City, Ningxia Hui Autonomous Region, China; [4] Qinghai Institute for Endemic Disease Prevention and Control, Xining City, Qinghai Province, China; [5] Department of Parasitic Diseases, Gansu Center for Disease Control and Prevention, Lanzhou City, Gansu Province, China; [6] Yunnan Institute of Parasitic Diseases, Kunming City, Yunnan Province, China; [7] Center for Disease Control and Prevention of Xinjiang Production and Construction Corps, Urumqi City, Xinjiang Uygur Autonomous Region, China; [8] Tianzhu Tibetan Autonomous County Center for Disease Control and Prevention, Wuwei City, Gansu Province, China.

Submitted: July 22, 2025
Accepted: September 08, 2025
Issued: September 12, 2025

REFERENCES

1. Wu WP, Wang H, Wang Q, Zhou XN, Wang LY, Zheng CJ, et al. A

nationwide sampling survey on echinococcosis in China during 2012-2016. Chin J Parasitol Parasit Dis 2018;36(1):1-14. https://link.cnki.net/urlid/31.1248.R.20180227.1951.002. (In Chinese).
2. Liu BX, Kui Y, Xue CZ, Wang X, Wang Y, Wang LY, et al. Progress of the national echinococcosis control programme in China, 2023. Chin J Parasitol Parasit Dis 2025;43(1):6 – 13. https://doi.org/10.12140/j.issn.1000-7423.2025.01.002.
3. van Kesteren F, Qi XW, Tao J, Feng XH, Mastin A, Craig PS, et al. Independent evaluation of a canine Echinococcosis Control Programme in Hobukesar County, Xinjiang, China. Acta Trop 2015;145:1 – 7. https://doi.org/10.1016/j.actatropica.2015.01.009.
4. Liu CN, Xu YY, Cadavid-Restrepo AM, Lou ZZ, Yan HB, Li L, et al. Estimating the prevalence of *Echinococcus* in domestic dogs in highly endemic for echinococcosis. Infect Dis Poverty 2018;7(1):77. https://doi.org/10.1186/s40249-018-0458-8.
5. Liu ZJ, Xiao N, Zhang LJ, Feng Y, Ge PF, Li F, et al. A survey of deworming with praziquantel in domestic dogs infected with *Echinococcus* in Huanxian, Gansu. Dis Surveill 2018;33(9):766-9. . (In Chinese).
6. Cui XY, Gong WC, Han S, Xue CZ, Wang X, Ma X, et al. The state of and risk factors for an Echinococcus infection in domestic dogs in Maqin County, Qinghai Province. J Pathog Biol 2020;15(6):692-7. . (In Chinese).
7. WHO. Report of the WHO Informal Working Group on cystic and alveolar echinococcosis surveillance, prevention and control. Geneva: WHO; 2011. https://www.who.int/publications/i/item/9789241502924.
8. Kapel CMO, Torgerson PR, Thompson RCA, Deplazes P. Reproductive potential of *Echinococcus multilocularis* in experimentally infected foxes, dogs, raccoon dogs and cats. Int J Parasitol 2006;36(1):79 – 86. https://doi.org/10.1016/j.ijpara.2005.08.012.
9. Thompson RCA. Chapter Two - Biology and systematics of *Echinococcus*. Adv Parasitol 2017;95:65 – 109. https://doi.org/10.1016/bs.apar.2016.07.001.
10. Han S, Li SZ. Echinococcosis in China: current status and future disease control priorities. Chin J Parasitol Parasit Dis 2025;43(1):1 – 5. https://doi.org/10.12140/j.issn.1000-7423.2025.01.001.

Preplanned Studies

Analysis on Cross-Species Transmission of Human–Suidae Zoonotic Viruses — Global, 1882–2022

Mingchen Zhao[1,2]; Xuechun Wang[3]; Erri Du[4]; Qiang Wang[5]; Tao Li[6]; Lifeng Zhang[7]; Zhongwei Jia[7,#]

Summary

What is already known about this topic?

Zoonotic diseases, particularly those caused by viruses capable of cross-species transmission, represent a significant threat to global public health security. Suidae have been recognized as critical intermediate hosts in numerous zoonotic virus transmission pathways. However, previous research has predominantly concentrated on individual viruses or isolated outbreaks, thereby constraining our comprehensive understanding of broader cross-species transmission patterns and risk factors.

What is added by this report?

This study systematically investigates cross-species transmission patterns of Suidae-related zoonotic viruses using comprehensive data from public databases, including the National Center for Biotechnology Information (NCBI). Through the integration of viral characteristics, host factors, environmental variables, and anthropogenic influences, we constructed predictive models to identify transmission hotspots and assess potential cross-species events. The research provides a comprehensive, data-driven framework for understanding zoonotic virus dynamics on a global scale.

What are the implications for public health practice?

These findings provide robust theoretical foundations and practical tools for early warning systems and targeted prevention strategies for zoonotic diseases, particularly those involving Suidae as intermediate hosts. This research advances the One Health approach by elucidating the interconnected roles of humans, animals, and environmental factors in viral transmission dynamics, thereby informing evidence-based global surveillance and response strategies for pandemic preparedness.

ABSTRACT

Introduction: Suidae-associated zoonotic viruses represent a significant global public health threat through cross-species transmission events. Current research remains limited to localized outbreak investigations and lacks comprehensive, systematic global analysis.

Methods: We collected human–Suidae virus data from the National Center for Biotechnology Information (NCBI) Virus Database, integrating viral characteristics, host information, and environmental and anthropogenic factors. Boosted Regression Trees (BRT) models were employed to evaluate cross-species transmission risk and identify key predictive factors.

Results: A total of 43 human-Suidae zoonotic viruses reported durng 1882–2022 were evaluated. The Boosted Regression Trees (BRT) model achieved area under the curve (AUC) values of 0.924 (training) and 0.804 (testing). Host–human phylogenetic distance and viral genome size emerged as the primary predictors. Porcine circovirus 3 (PCV3) demonstrated the highest predicted risk (>0.9).

Conclusions: This study establishes a data-driven framework for assessing cross-species transmission risk, supporting early warning systems and targeted prevention strategies. The findings underscore the critical importance of One Health approaches and recommend enhanced surveillance and biosecurity measures for high-risk viruses such as PCV3.

Zoonotic diseases represent a major threat to global public health, accounting for nearly 60% of recognized human diseases and approximately 75% of emerging infectious diseases in recent decades (*1*). Among animal reservoirs, Suidae (pig family) are of particular concern due to their widespread distribution, intensive farming practices, and close contact with humans, which establish them as critical intermediate hosts facilitating viral spillover events (*2*).

Although substantial progress has been achieved in understanding transmission mechanisms of individual viruses such as influenza and Japanese encephalitis,

most existing studies remain fragmented — focusing on single pathogens, geographically restricted regions, or lacking comprehensive integration across viral, host, and environmental dimensions (*3*–*4*). Consequently, the key drivers and spatiotemporal dynamics of zoonotic spillovers remain inadequately quantified.

To address these knowledge gaps, this study systematically analyzes globally reported human–Suidae zoonotic viruses using the National Center for Biotechnology Information (NCBI) Virus Database. By integrating viral genomic characteristics, host phylogenetic relationships, and environmental data, we developed a predictive model to identify the relative importance of risk factors and characterize high-risk viral species. These findings aim to provide an evidence-based framework for early warning systems and targeted interventions under the One Health approach, with particular relevance for major pork-producing countries such as China and the United States.

We retrieved spatiotemporal data on human-Suidae viruses and their hosts from the NCBI Virus Database (last accessed July 2025), including the 2025 data update, which verified that the initial sampling dates for all identified viruses remained consistent, defined cross-species transmission (CST) events, and integrated external datasets to explore potential influencing factors and their relative importance in shaping these transmission patterns (Supplementary Figure S1, available athttps://weekly.chinacdc.cn/).

After removing duplicates and incomplete entries, 813,809 entries were retained, from which we identified 43 viruses infecting both humans and Suidae, yielding 188,302 records. These zoonotic viruses were standardized using the International Committee on Taxonomy of Viruses (ICTV) Master Species List (2022.v1). Viral attributes were annotated using the ViralZone database, including genome type, strandedness, segmentation, replication site, envelope presence, and genome size. Host taxonomy was verified through the Animal Diversity Web and NCBI Taxonomy, with evolutionary divergence times between host families and humans or Suidae estimated using TimeTree as a proxy for genetic distance. Environmental and anthropogenic factors were compiled from WorldClim and FAOSTAT databases, including long-term climate indicators (temperature and precipitation), artificial surface area (representing human environmental modification such as roads, buildings, and other impervious infrastructure), urban/rural population densities, and World Bank income classifications. Cross-species transmission events were defined following the host-association framework established by Olival et al. (*5*), whereby viruses empirically detected in both humans and Suidae were classified as zoonotic, reflecting their biological capacity to cross host barriers regardless of confirmed transmission directionality.

Predictive modeling was performed to evaluate CST risk by integrating viral, host, and environmental attributes. We tested logistic regression and machine learning models, selecting the Boosted Regression Tree (BRT) as the primary approach (Table1) (*6*). Hyperparameters were optimized through grid search and 10-fold cross-validation. The final model employed a learning rate of 0.01, tree complexity (interaction depth) of 3, and Bernoulli deviance loss function appropriate for binary classification. We allowed up to 10,000 trees with early stopping based on minimum cross-validation deviance. A bag fraction of 0.5 was applied to introduce stochasticity and reduce overfitting. Model performance was monitored across folds, and variable importance was assessed based on relative influence of each predictor across all fitted trees. Model performance was evaluated using a stratified 7:3 training–testing split, with metrics including sensitivity, specificity, accuracy, balanced accuracy, and the area under the receiver operating characteristic curve (AUC). Variable importance was quantified by relative influence across fitted trees, with predictors considered statistically significant if $P< 0.05$ and *95% confidence intervals* excluded zero. All statistical analyses were performed using R statistical software (version 4.1.0, The R Foundation for Statistical Computing, Vienna, Austria).

Among the evaluated models, the BRT demonstrated superior performance, achieving an AUC of 0.924 for the training dataset and 0.804 for the test dataset (Figure 1). These evaluations were based on 43 human–Suidae viruses reported during 1882–2022, indicating robust predictive capability with minimal overfitting, and confirming the model's suitability for assessing CST risk among human-Suidae viruses.

The BRT analysis revealed eleven predictors with measurable contributions, with the top five demonstrating the greatest influence: host–human divergence time (28.50%), viral genome size (18.55%), rural human population density (11.29%), annual precipitation (9.72%), and artificial surface coverage (9.65%). These findings emphasize the critical importance of host phylogenetic proximity and viral genomic characteristics, alongside environmental and

TABLE 1. Comparison of performance metrics across multiple methods for predicting cross-species transmission risk.

Model	Sensitivity	Specificity	Accuracy	Balanced accuracy	AUC
LR	0.681	0.717	0.716	0.699	0.699
BRT	0.653	0.807	0.803	0.730	0.804
DT	0.702	0.744	0.743	0.723	0.723
RF	0.319	0.960	0.946	0.640	0.640
SVM	0.722	0.747	0.747	0.735	0.735

Abbreviation: LR=Logistic Regression, BRT=Boosted Regression Trees, DT=Decision Tree, RF=Random Forest, SVM=Support Vector Machine, AUC=area under the curve.

anthropogenic factors, in determining zoonotic transmission risk (Figure 2).

Specifically, viruses originating from hosts with closer genetic relationships to humans demonstrated higher propensity for crossing species barriers, while viruses with larger genomes exhibited enhanced adaptive capacity for novel host environments. Rural population density and precipitation patterns reflected increased opportunities for human–animal interactions and favorable conditions for viral persistence, while land-use modifications indicated ecological disruptions that promote spillover events.

To extend the model's application to Suidae viruses not yet documented in humans, we evaluated six common livestock viruses with the highest number of Suidae host records from the NCBI Virus database: Porcine reproductive and respiratory syndrome virus, African swine fever virus, Pestivirus C (classical swine fever virus), Foot-and-mouth disease virus, Porcine epidemic diarrhea virus, and Porcine circovirus 3.

Notably, Porcine circovirus 3 exhibited the highest predicted transmission risk, with probabilities exceeding 0.9 (Table 2). A predicted risk value >0.9 indicates that samples within this interval were assigned a probability exceeding 90% for cross-species transmission, reflecting high model confidence that these instances are associated with elevated spillover risk.

Given its exceptionally high predicted zoonotic potential, we strongly recommend implementing enhanced surveillance protocols and strengthened biosecurity measures specifically targeting PCV3 to effectively mitigate potential spillover threats to human populations.

This study highlights that cross-species transmission of Suidae-associated viruses is jointly shaped by host genetic relatedness, viral genome features, and environmental factors. The BRT model demonstrated strong predictive performance and identified PCV3 as a virus with particularly high spillover risk. These findings provide a quantitative basis for early warning and surveillance prioritization and reinforce the importance of the One Health approach to prevent future zoonotic emergence.

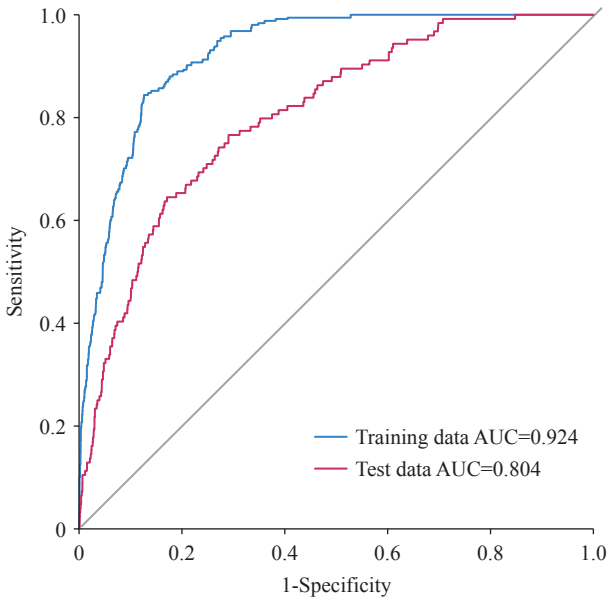

FIGURE 1. ROC curves for training and test datasets using the BRT model.
Abbreviation: ROC=receiver operating characteristic; BRT=Boosted Regression Tree; AUC=area under the curve.

DISCUSSION

Understanding and predicting cross-species transmission remains fundamental to pandemic preparedness. This study employed a BRT model to integrate viral, host, environmental, and anthropogenic variables for assessing spillover risk in human-Suidae zoonotic viruses. Our findings illuminate critical ecological and evolutionary drivers of zoonotic risk while establishing a data-driven framework for early warning and surveillance prioritization. Recent investigations have validated machine learning approaches for pathogen risk assessment (*7*–*8*), and our methodology advances this field by specifically

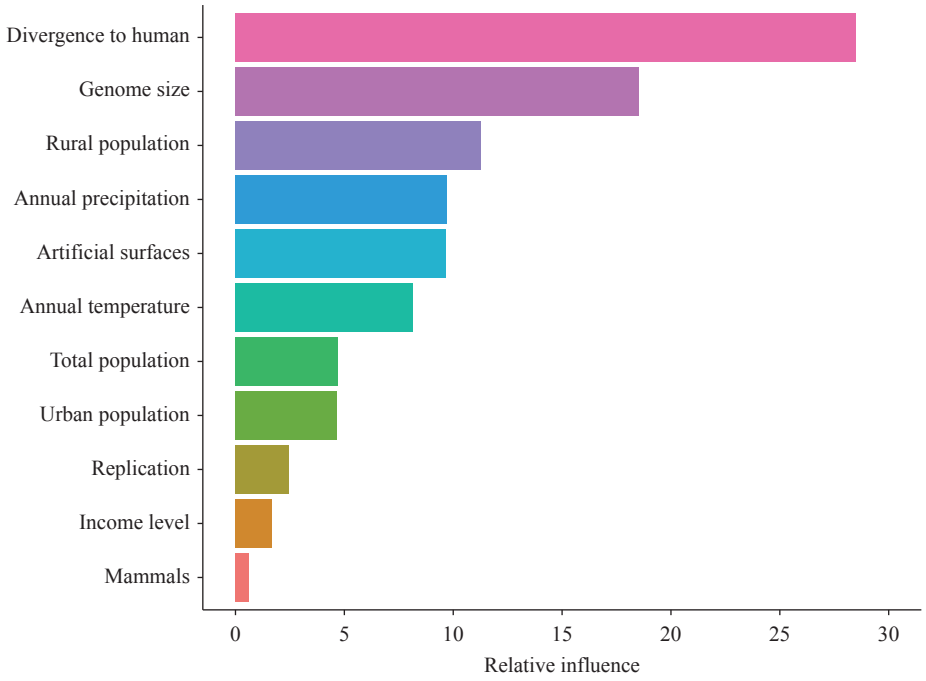

FIGURE 2. Feature importance ranking in the BRT model.
Abbreviation: BRT=Boosted Regression Tree.

targeting the human–Suidae transmission interface.

Host–human divergence time emerged as the most influential predictor in our analysis. This finding reinforces the principle that viruses demonstrate greater propensity for cross-species transmission between phylogenetically related species due to conserved receptor mechanisms and immunological similarities (*5*,*9*). Phylogenetic proximity facilitates viral entry, replication efficiency, and immune evasion strategies in novel hosts, thereby substantially increasing the likelihood of successful spillover events. Consequently, host evolutionary relationships should constitute a fundamental component of zoonotic risk assessment frameworks, particularly in biodiverse regions characterized by frequent human–animal interactions.

Viral genome size emerged as a strong predictor of spillover potential, consistent with previous studies demonstrating that larger genomes confer greater adaptive capacity and evolutionary flexibility (*8*). Environmental and anthropogenic factors — including rural human population density, precipitation patterns, and artificial surface coverage — proved significant predictors, reflecting both increased exposure opportunities and ecological disruptions that facilitate viral emergence. These findings underscore that zoonotic risk arises from complex interactions among viral characteristics, host biology, and human-mediated environmental changes (*7*).

TABLE 2. Predicted cross-species transmission risk levels and corresponding observed event probabilities for human–Suidae viruses.

Predicted risk level (%)	Event Probabilities(%)	No. of samples	95% *CI*
0–15	0.5	1,796	(0.002, 0.009)
15–30	1.4	1,112	(0.008, 0.023)
30–45	2.3	565	(0.012, 0.039)
45–60	3.6	552	(0.022, 0.055)
60–75	8.4	407	(0.058, 0.115)
75–90	14.1	199	(0.096, 0.197)
90–100	28.6	14	(0.084, 0.581)

Abbreviation: *CI*= confidence interval.

Applying the BRT model to viruses not yet reported in humans highlighted Porcine circovirus 3 as a high-risk candidate, due to its stability, recombination capacity, and widespread distribution (*10*). Although no human infections have been reported, proactive surveillance of PCV3 and similar viruses is warranted, especially in regions with intensive Suidae farming and limited biosecurity. These results echo calls by Grange et al. (*8*) and Carlson et al. (*7*) for proactive identification of high-risk viruses before they emerge. We recommend that health authorities integrate such model outputs into zoonotic surveillance systems, prioritizing high-risk viruses like PCV3 for serological

testing, metagenomic screening, and field investigations in both animal reservoirs and sentinel human populations. This predictive approach can help shift from reactive outbreak response to proactive early warning.

While these findings highlight the value of the BRT model for proactive surveillance, it is important to consider its limitations. First, the model depends on publicly available data, which may be geographically biased or incomplete. Sampling gaps, especially in low-resource or biodiverse regions, may affect model reliability (*11*). Second, spillover involves complex ecological and socio-behavioral processes not fully captured here. Nevertheless, the BRT framework is robust and could be integrated into zoonotic surveillance pipelines to guide evidence-based prioritization of high-risk viruses (*12*).

Our findings reinforce the fundamental One Health principle by demonstrating that viral characteristics, host biology, and environmental conditions collectively determine spillover risk rather than operating in isolation.

The integration of predictive modeling frameworks with comprehensive ecological and epidemiological surveillance systems can facilitate a paradigm shift from reactive outbreak response toward proactive risk management strategies, thereby enhancing global pandemic preparedness capabilities.

Conflicts of Interest: No conflicts of interest.

doi: 10.46234/ccdcw2025.200

[#] Corresponding author: Zhongwei Jia, jiazw@bjmu.edu.cn.

[1] Department of Epidemiology and Biostatistics, School of Public Health, Peking University, Beijing, China; [2] Beijing Center for Disease Prevention and Control, Beijing, China; [3] Graduate School of Chinese PLA General Hospital, Beijing, China; [4] SILC Business School, Shanghai University, Shanghai, China; [5] Goodwill Hessian Health Technology Co., Ltd., Beijing, China; [6] National Center for Tuberculosis Control and Prevention, Chinese Center for Disease Control and Prevention, Beijing, China; [7] Department of Global Health, School of Public Health, Peking University, Beijing, China.

Submitted: April 21, 2025
Accepted: September 08, 2025
Issued: September 12, 2025

REFERENCES

1. Taylor LH, Latham SM, Woolhouse MEJ. Risk factors for human disease emergence. Philos Trans Roy Soc B 2001;356(1411):983 – 9. https://doi.org/10.1098/rstb.2001.0888.
2. Ma WJ, Kahn RE, Richt JA. The pig as a mixing vessel for influenza viruses: human and veterinary implications. J Mol Genet Med 2008;3 (1):158-66. https://pubmed.ncbi.nlm.nih.gov/19565018/.
3. Smith GJD, Vijaykrishna D, Bahl J, Lycett SJ, Worobey M, Pybus OG, et al. Origins and evolutionary genomics of the 2009 swine-origin H1N1 influenza A epidemic. Nature 2009;459(7250):1122 – 5. https://doi.org/10.1038/nature08182.
4. Zhao MC, Chen JY, Wang Q, Lu ZH, Jia ZW. A landscape analysis on virus: based on NCBI database. China CDC Wkly 2022;4(7):120 – 5. https://doi.org/10.46234/ccdcw2022.019.
5. Olival KJ, Hosseini PR, Zambrana-Torrelio C, Ross N, Bogich TL, Daszak P. Host and viral traits predict zoonotic spillover from mammals. Nature 2017;546(7660):646 – 50. https://doi.org/10.1038/nature22975.
6. Ridgeway G. Generalized boosted models: a guide to the gbm package. 2007;1(1):2007.
7. Carlson CJ, Albery GF, Merow C, Trisos CH, Zipfel CM, Eskew EA, et al. Climate change increases cross-species viral transmission risk. Nature 2022;607(7919):555 – 62. https://doi.org/10.1038/s41586-022-04788-w.
8. Grange ZL, Goldstein T, Johnson CK, Anthony S, Gilardi K, Daszak P, et al. Ranking the risk of animal-to-human spillover for newly discovered viruses. Proc Natl Acad Sci USA 2021;118(15): e2002324118. https://doi.org/10.1073/pnas.2002324118.
9. Mollentze N, Streicker DG. Viral zoonotic risk is homogenous among taxonomic orders of mammalian and avian reservoir hosts. Proc Natl Acad Sci USA 2020;117(17):9423 – 30. https://doi.org/10.1073/pnas.1919176117.
10. Chen Y, Xu QM, Chen H, Luo X, Wu Q, Tan C, et al. Evolution and genetic diversity of porcine circovirus 3 in China. Viruses 2019;11(9): 786. https://doi.org/10.3390/v11090786.
11. Becker DJ, Albery GF, Sjodin AR, Poisot T, Bergner LM, Chen BQ, et al. Optimising predictive models to prioritise viral discovery in zoonotic reservoirs. Lancet Microbe 2022;3(8):E625 – 37. https://doi.org/10.1016/S2666-5247(21)00245-7.
12. Elith J, Leathwick JR, Hastie T. A working guide to boosted regression trees. J Anim Ecol 2008;77(4):802 – 13. https://doi.org/10.1111/j.1365-2656.2008.01390.x.

SUPPLEMENTARY MATERIAL

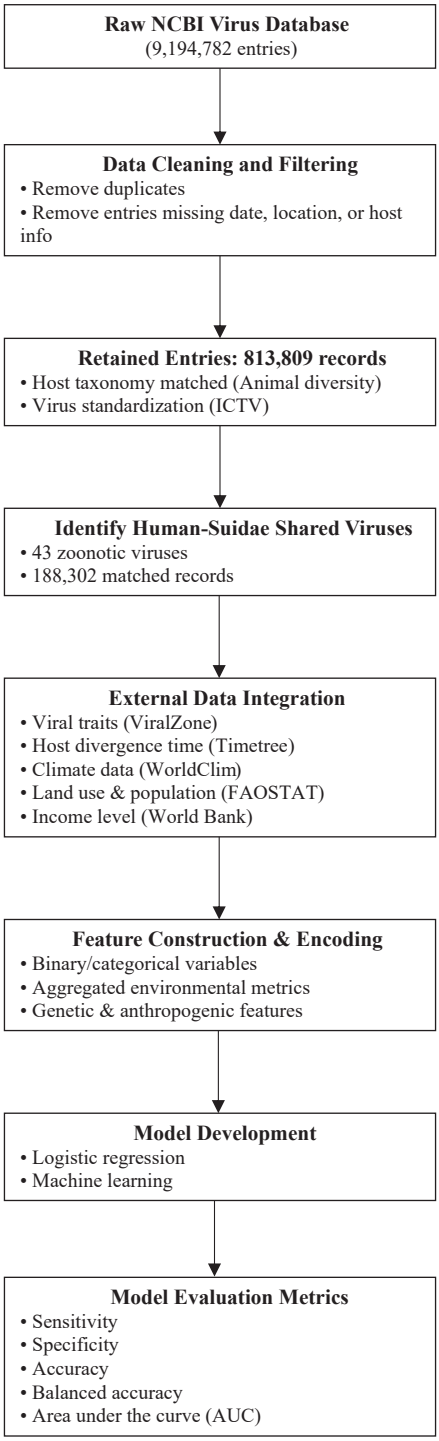

SUPPLEMENTARY FIGURE S1. Workflow of data preprocessing and integration for modeling CST of zoonotic viruses shared between humans and Suidae.
Note: Raw sequence metadata from the NCBI Virus Database were systematically cleaned, standardized, and matched to external databases to generate relevant predictors for model input.
Abbreviation: CST=cross-species transmission.

Outbreak Reports

Identification of A Novel Human Adenovirus Type 114 Associated with An Acute Respiratory Disease Outbreak at An Elementary School — Beijing, China, September 2024

Xiuxia Wei[1]; Min Li[1]; Yi Wang[1]; Yanna Yang[1]; Ruoran Lyu[1]; Guilan Lu[2,#]; Zhen Zhu[3,#]

Summary

What is already known about this topic?

Recent years have witnessed increasing reports of acute respiratory outbreaks caused by novel recombinant human adenovirus (HAdV). In November 2023, researchers at the Medical University of Hannover in Germany identified HAdV-B114.

What is added by this report?

The six strains of HAdV isolated in this outbreak were 100% homologous and also had the highest homology with the GenBank reference OR853835 for HAdV-B114 at 99.9%, 100%, and 99.8% in penton base gene hexon gene, and fiber gene. This is the first documented outbreak in China associated with HAdV-B114.

What are the implications for public health practice?

Given that genetically recombined HAdVs can pose serious threats to human health and trigger emerging infectious disease outbreaks, continuous monitoring — particularly of novel recombinant types based onpenton base gene, hexon gene, and fiber gene sequences — should be prioritized to enable early detection and effective public health response.

ABSTRACT

Introduction: On September 11, 2024, a school in the Beijing Economic and Technological Development Area (Jingkai area) reported multiple cases of fever. Public health professionals from the local CDC promptly initiated an on-site epidemiological investigation.

Methods: We conducted an initial epidemiological assessment and rapidly identified the index case. Simultaneously, we performed active case finding throughout the school. Throat swab samples were collected from symptomatic individuals and submitted to the laboratory for pathogen testing. Real-time RT-PCR was used to screen for a comprehensive panel of respiratory pathogens. We established viral cultures and performed PCR to amplify target gene sequences. Molecular characterization was conducted using gene homology analysis and phylogenetic reconstruction.

Results: Active case finding identified 15 fever cases (37.8 °C–39.9 °C), all from two adjacent classes in the school. Case onset was concentrated between September 9 and 11, with 6 males and 9 females, all aged 6 years. Fourteen throat swab samples were collected, with 10 testing positive for HAdV genes. Six viral strains were successfully isolated through cell culture. Sequence analysis revealed 100% gene homology in the hexon Loop2 region, consistent with HAdV-B3. Furthermore, the penton base gene, hexon gene, and fiber gene of all 6 strains exhibited 100% homology. The penton base gene showed 99.2% homology with the HAdV-B7 reference strain, while the hexon and fiber genes demonstrated 99% and 96.8% homology, respectively, with the HAdV-B3 reference strain. The genotype of all 6 strains was P7H3F3, consistent with the HAdV-B114 (P7H3F3) genotype, confirming their identification as HAdV-B114.

Conclusions: This outbreak was caused by a novel recombinant human adenovirus, HAdV-B114. Given the potential for such emerging HAdV strains to trigger infectious disease outbreaks, enhanced surveillance systems and comprehensive molecular characterization are essential for early detection and effective public health response.

Human adenovirus (HAdV) represents a significant viral pathogen capable of infecting multiple vital organ systems, including the respiratory tract, ocular tissues, and gastrointestinal tract (*1*). HAdV belongs to the genus *Mastadenovirus* within the family *Adenoviridae* and is characterized as a non-enveloped virus

containing linear double-stranded DNA. The viral genome spans approximately 36 kb and encodes roughly 40 proteins, among which the most critical structural components are the penton base, hexon, and fiber proteins (*1*–*2*). The penton base protein facilitates viral endocytosis and promotes cellular infection (*1*–*2*). The hexon protein contains two highly variable loop domains, Loop1 and Loop2, which are associated with serotype-specific antigenic differences and host immune responses, making them valuable tools for preliminary HAdV strain identification (*1*–*2*). The fiber protein mediates viral attachment by binding to specific host-cell receptors.

HAdV classification is based on biological characteristics and genetic homology, resulting in seven distinct subgenera (A–G). The genes encoding the penton base, hexon, and fiber proteins are particularly susceptible to homologous recombination events. According to the Human Adenovirus Working Group guidelines, accurate genotyping requires analysis of the complete sequences of these three critical genes (http://hadvwg.gmu.edu).

In September 2024, an acute respiratory outbreak occurred at an elementary school in the Beijing Economic and Technological Development Area. Local CDC professionals responded by conducting comprehensive epidemiological investigations and collecting throat swab samples from affected individuals. Laboratory analysis confirmed adenoviral infection, prompting immediate implementation of prevention and control measures. Subsequent molecular characterization and phylogenetic analysis revealed that the outbreak was caused by a novel recombinant HAdV-B114, which emerged through genetic recombination between HAdV-B3 and HAdV-B7.

INVESTIGATION AND RESULTS

On September 11, 2024, two classes at an elementary school in the Jingkai area reported multiple fever cases. Public health professionals from the local CDC immediately conducted an on-site epidemiological investigation. The school housed 189 classes with 7,368 students and 739 faculty and staff members. Overall sanitary conditions were satisfactory, and full-time school physicians were available onsite. All reported cases occurred exclusively among students; no teachers or staff members were affected. The two affected classes were situated on the east side of the same floor within the same building, positioned adjacent to the girls' restroom where ventilation was observed to be inadequate.

Epidemiological investigation revealed that the index case developed symptoms on September 9, including fever (reaching 38.6 °C), body aches, and nasal congestion. Between September 9 and 11, a total of 15 students from the 2 classes developed fever, with maximum recorded temperatures reaching 39.9 °C. Among these cases, 4 students experienced headache, fatigue, and other systemic symptoms; 3 reported cough and sore throat; 2 had muscle aches; 1 presented with nasal congestion; and 5 exhibited only fever. No hospitalizations, severe cases, or fatalities occurred. The temporal distribution of cases demonstrated a concentrated pattern: 5 cases on September 9, 6 cases on September 10, and 4 cases on September 11. Of the 15 affected individuals, 6 were male and 9 were female, with all students being 6 years old.

A total of 14 throat swab samples were collected from the identified cases. Total viral nucleic acid was extracted using a nucleic acid extraction and purification kit (DA0623, Da'an, Guangzhou) with a nucleic acid extractor (Smart32, Da'an, Guangzhou). Comprehensive screening for respiratory pathogens was performed using a nucleic acid detection kit targeting 22 respiratory pathogens (Beijing Kangrun Gino) in combination with a PCR amplification instrument (TianLong Gentier 96R, Xi'an Tianlong). The screening panel included Severe Acute Respiratory Syndrome Coronavirus 2 (SARS-CoV-2), influenza A (H1N1) pdm09 and A(H3N2), influenza B viruses, human respiratory syncytial virus, HAdV, human metapneumovirus, human rhinovirus, human parainfluenza virus (HPIV I-IV), human coronavirus (HCoV-NL63, -229E, -OC43, and -HKU1), human bocavirus, human enterovirus, *Mycoplasma pneumoniae*, *Streptococcus pneumoniae*, group A streptococcus, *Bordetella pertussis*, *Haemophilus influenzae*, *Klebsiella pneumoniae*, *Legionella pneumoniae*, *Aspergillus*, *Chlamydia pneumoniae*, *Chlamydia psittaci*, *Cryptococcus*, and *Pneumocystis*. HAdV-specific genes were detected in 10 of the 14 samples, while no other pathogens were identified, establishing HAdV as the causative agent of the outbreak.

Six viral isolates were successfully obtained by inoculating the human epidermoid larynx carcinoma cell line (HEp-2 cells) with HAdV-positive samples. Cytopathic effects were monitored daily, and viral material was harvested when greater than 75% of the HEp-2 cells exhibited cytopathic changes. The six viral

isolates were subsequently stored at −70 °C for further analysis.

For preliminary genotyping, we amplified and sequenced the Loop2 region of the hexon gene from all six viral strains following national CDC protocols (*3*) (Table 1). For definitive genotyping, we amplified and sequenced the complete penton base gene (1,635 bp), hexon gene (2,935 bp), and fiber gene (960 bp) (*4*) (Table 1). All PCR products underwent bidirectional sequencing to ensure accuracy and reliability. We assembled and processed sequence data using Sequencher v5.0 software (Genecode, USA). Phylogenetic trees were constructed using both Neighbor-Joining and Maximum Likelihood (ML) methods in MEGA12, with bootstrap values set to 1,000 replicates for statistical validation. Reference sequences were obtained from the GenBank database.

Sequence analysis of the hexon Loop2 region revealed 100% identity among the six viral strains, all clustering with the HAdV-B3 genotype. Further analysis of the complete penton base gene, hexon gene, and fiber gene demonstrated 100% sequence identity among the six isolates. Phylogenetic analysis indicated that the penton base gene was closely related to HAdV-B7 (Figure 1), while the hexon gene and fiber gene were closely related to HAdV-B3 (Figure 1). According to the International Adenovirus Working Group guidelines for HAdV genotype identification (http://hadvwg.gmu.edu), this recombinant profile (P7H3F3) corresponds to the genotype HAdV-B114.

Further analysis of amino acid sequence differences between the six HAdV-B114 strains revealed that the penton base demonstrated 99.2% amino acid homology with the HAdV-B7 reference strain, the hexon showed 99% amino acid homology with the HAdV-B3 reference strain, and the fiber exhibited 96.8% amino acid homology with the HAdV-B3 reference strain (Table 2). BLAST analysis further confirmed that the penton base gene, hexon gene, and fiber gene of the six HAdV strains exhibited the highest homology with the GenBank reference OR853835 for HAdV-B114 — at 99.9%, 100% and 99.8%, respectively. Therefore, the causative agent of this outbreak was conclusively identified as the novel recombinant HAdV type HAdV-B114.

PUBLIC HEALTH RESPONESE

According to the *Prevention and Control Technical Guide for Respiratory Infections with Human Adenovirus* (2019 Edition), in order to better and faster control the epidemic, CDC professionals suggest that schools regularly take temperature screenings, identify absent cases due to respiratory infection, prompt report respiratory infections in students and faculty and staff members, isolate symptomatic infected individuals, and ensure treatment in time. Meanwhile, schools should increase ventilation and disinfection in activity areas, such as classrooms, and provide health education on the prevention of respiratory infectious diseases to students, teachers, and parents. All large gatherings are prohibited under the outbreak of epidemic.

DISCUSSION

Human adenovirus represents a globally prevalent pathogen and constitutes one of the primary etiological agents of acute respiratory infections (ARI) (*1–2*). Recent years have witnessed multiple reports

TABLE 1. Primers used to amplify the target genome.

Primer	Primer sequence (5'–3')	The length of the PCR Products (bp)	Specificity	Reference
ad1	TTCCCCATGGCICAYAACAC	482	Loop2	(*3*)
ad2	CCCTGGTAKCCRATRTTGTA			
HAdV3-Fiber-F	CTTCCTACCAGCAGCACCTC	1,210	Fiber	(*4*)
HAdV3-Fiber-R	CGTGGGGAGAGATTGGTGTA			
HAdV3-Hexon-1F	AGTACTCTGAACAGCATCGT	1,621	Hexon-1	(*4*)
HAdV3-Hexon-1R	TAGGTGGCGTGTACTTGTAA			
HAdV3-Hexon-2F	ACCGATGACGCTAATGGATG	1,739	Hexon-2	(*4*)
HAdV3-Hexon-2R	TATGGCGCAGGCGAGCTTGT			
HAdV3-Penton-F	AGGACTCTGCCGATGAYAGC	1,846	Penton base	(*4*)
HAdV3-Penton-R	GATGTAGGCGCAGTAGGAGT			

Abbreviation: PCR=polymerase chain reaction; HAdV=human adenovirus.

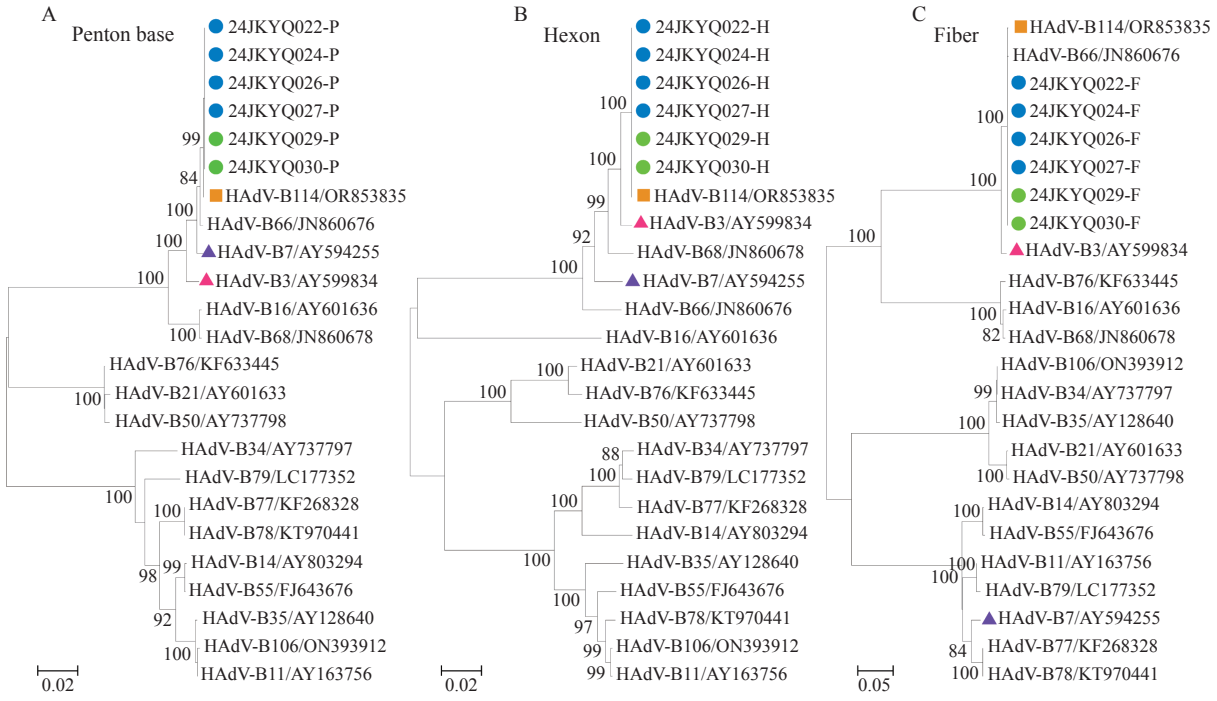

FIGURE 1. Phylogenetic tree of HAdV final genotyping based on the penton base gene, hexon gene, and fiber gene.
Note: ●Representative HAdV strains isolated from one class; ●Representative HAdV strains isolated from another class; ■Prototype strains of representative types HAdV-B114; ▲Prototype strains of representative types HAdV-B7; ▲Prototype strains of representative types HAdV-B3.
Abbreviation: HAdV=human adenovirus.

TABLE 2. Variations in amino acids of human adenovirus type 114 (HAdV-114) strains.

Strain name	Penton base gene				Hexon gene									Fiber gene								
	11	32	159	462	141	299	302	411	418	429	439	440	445	22	23	150	207	215	222	223	246	272	316
HAdV-B3/AY599834	–	–	–	–	G	E	N	N	T	T	A	P	T	S	S	Q	S	E	A	D	H	M	R
HAdV-B7/AY594255	M	I	V	A	–	–	–	–	–	–	–	–	–	–	–	–	–	–	–	–	–	–	–
24JKYQ022-P	V	L	A	T	R	G	D	D	R	A	D	T	A	N	L	E	L	Q	T	H	D	T	T
24JKYQ024-P	V	L	A	T	R	G	D	D	R	A	D	T	A	N	L	E	L	Q	T	H	D	T	T
24JKYQ026-P	V	L	A	T	R	G	D	D	R	A	D	T	A	N	L	E	L	Q	T	H	D	T	T
24JKYQ027-P	V	L	A	T	R	G	D	D	R	A	D	T	A	N	L	E	L	Q	T	H	D	T	T
24JKYQ029-P	V	L	A	T	R	G	D	D	R	A	D	T	A	N	L	E	L	Q	T	H	D	T	T
24JKYQ030-P	V	L	A	T	R	G	D	D	R	A	D	T	A	N	L	E	L	Q	T	H	D	T	T

Note: "–" means Amino acid site not provided.
Abbreviation: HAdV=human adenovirus.

documenting acute respiratory outbreaks attributed to HAdV (*5*–*7*). In September 2024, an acute respiratory outbreak emerged at an elementary school in the Jingkai area. The predominant clinical manifestation among infected children was fever, while other typical respiratory symptoms remained notably absent or mild. The rapid progression from the index case to clustered onset presented diagnostic challenges, making pathogen identification through epidemiological investigation alone insufficient. Laboratory analysis utilizing genetic screening and pathogen identification definitively established that this outbreak was caused by a novel recombinant HAdV-B114 with genotype P7H3F3, representing an evolutionary product of genetic recombination between HAdV-B3 and HAdV-B7.

Domestic and international research demonstrates that HAdV-B3 and HAdV-B7 represent the most prevalent HAdV types causing acute respiratory infections. The six HAdV-B114 strains identified in

this study exhibited 100% nucleotide homology across the penton base, hexon, and fiber genes, suggesting that this novel recombinant HAdV-B114 possesses distinct evolutionary advantages and may demonstrate epidemic potential in Beijing. During the 2022–2023 acute respiratory outbreak in Bangladesh, India (*7*), three HAdV strains with the P7H3F3 genotype were identified, further indicating the widespread prevalence of HAdV-B114. Currently, domestic HAdV surveillance protocols only conduct genotype screening based on the Loop2 region of the hexon gene. Whether HAdV-B114 has achieved widespread circulation in Beijing or throughout China requires retrospective genotype confirmation based on complete penton base, hexon, and fiber gene sequences. This outbreak reinforces the critical importance of comprehensive genotyping based on full-length sequences of these three key genes.

This study's comparative gene analysis revealed that HAdV-B114 exhibits multiple sequence variations at both the nucleotide and amino acid levels compared to HAdV-B3 and HAdV-B7 across the penton base, hexon, and fiber genes. Given the critical roles these proteins play in viral adsorption, cellular infection, and host immune response modulation, further investigation is warranted to determine how genetic recombination has altered the infectivity and pathogenicity profiles of this novel HAdV-B114 strain. Additionally, the HAdV-B114 isolates obtained in this study demonstrate high nucleotide and amino acid homology with existing reference sequences, indicating that the HAdV-B114 strain identified in Beijing remains within the same evolutionary lineage as the 2023 German isolate.

In recent years, HAdV outbreaks have increased in frequency, accompanied by continuous genetic evolution through recombination (*7*–*8*). These evolutionary changes have altered viral tissue tropism and immune evasion profiles, resulting in the emergence of novel strains with enhanced pathogenicity and transmissibility. This phenomenon poses significant challenges to public health systems worldwide. There is an urgent need to establish a comprehensive HAdV surveillance network in China that incorporates genotyping based on complete sequences of the penton base, hexon, and fiber genes. Such enhanced surveillance would strengthen our capacity to identify emerging strains, trace outbreak origins, and improve preparedness for future HAdV-related epidemics.

doi: 10.46234/ccdcw2025.201

Corresponding authors: Guilan Lu, luguilan@bjcdc.org; Zhen Zhu, zhuzhen@ivdc.chinacdc.cn.

[1] Beijing Economic-Technological Development Area Center for Disease Prevention and Control, Beijing, China; [2] Beijing Center for Disease Control and Prevention, Beijing, China; [3] World Health Organization Regional Office for the Western Pacific Regional Reference Poliovirus Laboratory, State Key Laboratory of Molecular Virology & Genetic Engineering, National Institute for Viral Disease Control and Prevention, Chinese Center for Disease Control and Prevention, Beijing, China.

Submitted: June 30, 2025
Accepted: September 04, 2025
Issued: September 12, 2025

REFERENCES

1. Mao NY, Zhu Z, Zhang Y, Xu WB. Current status of human adenovirus infection in China. World J Pediatr 2022;18(8):533 – 7. https://doi.org/10.1007/s12519-022-00568-8.
2. Usman N, Suarez M. Adenoviruses. Treasure Island: StatPearls Publishing. 2025. https://pubmed.ncbi.nlm.nih.gov/32644498/.
3. Expert Writing Group of Technical Guidelines for Prevention and Control of Human Adenovirus Respiratory Infection. Technical guidelines for prevention and control of human adenovirus respiratory infection (2019 edition). Chin J Prev Med 2019;53(11):1088 – 93. https://doi.org/10.3760/cma.j.issn.0253-9624.2019.11.003.
4. Technical plan for sentinel surveillance of acute respiratory infectious diseases in China (trial draft). https://wenku.baidu.com/view/10e3550dc2c708a1284ac850ad02de80d5d8060e.html?_wkts_=1756960486565&needWelcomeRecommand=1&unResetStore=1. (In Chinese).
5. Guo ZY, Tong LB, Xu S, Li B, Wang Z, Liu YD. Epidemiological analysis of an outbreak of an adenovirus type 7 infection in a boot camp in China. PLoS One 2020;15(6):e0232948. https://doi.org/10.1371/journal.pone.0232948.
6. Liu WK, Qiu SY, Zhang L, Wu HK, Tian XG, Li X, et al. Analysis of severe human adenovirus infection outbreak in Guangdong Province, southern China in 2019. Virol Sin 2022;37(3):331 – 40. https://doi.org/10.1016/j.virs.2022.01.010.
7. Chatterjee A, Bhattacharjee U, Gupta R, Debnath A, Majumdar A, Saha R, et al. Genomic expedition: deciphering human adenovirus strains from the 2023 outbreak in west Bengal, India: insights into viral evolution and molecular epidemiology. Viruses 2024;16(1):159. https://doi.org/10.3390/v16010159.
8. Zhou ML, Chen WJ, Zhang D, Ma SC, Liu MG, Ren LL, et al. Identification and characterization of a novel human adenovirus type HAdV-D116. Front Microbiol 2025;16:1566316. https://doi.org/10.3389/fmicb.2025.1566316.

Youth Editorial Board

Indexed by Science Citation Index Expanded (SCIE), Social Sciences Citation Index (SSCI), PubMed Central (PMC), Scopus, Chinese Scientific and Technical Papers and Citations, and Chinese Science Citation Database (CSCD)

The inauguration of *China CDC Weekly* is in part supported by Project for Enhancing International Impact of China STM Journals Category D (PIIJ2-D-04-(2018)) of China Association for Science and Technology (CAST).

CCDC weekly

Vol. 7 No. 37 Sept. 12, 2025

Responsible Authority
National Disease Control and Prevention Administration

Sponsor
Chinese Center for Disease Control and Prevention

Editing and Publishing
China CDC Weekly Editorial Office
No.155 Changbai Road, Changping District, Beijing, China
Tel: 86-10-63150501, 63150701
Email: weekly@chinacdc.cn

CSSN
ISSN 2096-7071 (Print)
ISSN 2096-3101 (Online)
CN 10-1629/R1